UCRL-CR-143772
B344836

Seismic Characterization of Coal-Mining Seismicity in Utah for CTBT Monitoring

W. J. Arabasz, J. C. Pechmann

March 1, 2001

U.S. Department of Energy

Lawrence
Livermore
National
Laboratory

This work was performed under the auspices of the U. S. Department of Energy by the University of California, Lawrence Livermore National Laboratory under Contract No. W-7405-Eng-48.

FINAL REPORT
LLNL Research Agreement No. B344836

Seismic Characterization of Coal-Mining Seismicity in Utah for CTBT Monitoring

Prepared for
Lawrence Livermore National Laboratory
University of California
Livermore, California

Prepared by
Walter J. Arabasz [1] and James C. Pechmann [1]

with contributions from Michael K. McCarter [2] and
Jefferson D. McKenzie [2]

March 1, 2001

1 University of Utah Seismograph Stations
Department of Geology and Geophysics
University of Utah
135 South 1460 East, Room 705 WBB
Salt Lake City, Utah 84112

2 Department of Mining Engineering
University of Utah
135 South 1460 East, Room 313 WBB
Salt Lake City, Utah 84112

DISCLAIMER

TABLE OF CONTENTS

TABLE OF CONTENTS (cont)

LIST OF TABLES

TABLE OF CONTENTS (cont)

LIST OF FIGURES

TABLE OF CONTENTS (cont)

TABLE OF CONTENTS (cont)

APPENDICES

EXECUTIVE SUMMARY

Underground coal mining (down to ~0.75 km depth) in the contiguous Wasatch Plateau (WP) and Book Cliffs (BC) mining districts of east-central Utah induces abundant seismicity that is monitored by the University of Utah regional seismic network. This report presents the results of a systematic characterization of mining seismicity (magnitude ≤ 4.2) in the WP-BC region from January 1978 to June 2000—together with an evaluation of three seismic events (magnitude ≤ 4.3) associated with underground trona mining in southwestern Wyoming during January-August 2000. (Unless specified otherwise, magnitude implies Richter local magnitude, M_L.)

The University of Utah Seismograph Stations (UUSS) undertook this cooperative project to assist the University of California Lawrence Livermore National Laboratory (LLNL) in research and development relating to monitoring the Comprehensive Test Ban Treaty (CTBT). The project, which formally began February 28, 1998, and ended September 1, 2000, had three basic objectives:

1. Strategically install a three-component broadband digital seismic station in the WP-BC region to ensure the continuous recording of high-quality waveform data to meet the long-term needs of LLNL, UUSS, and other interested parties, including the international CTBT community.

2. Determine source mechanisms—to the extent that available source data and resources allowed—for comparative seismic characterization of stress release in mines versus earthquakes in the WP-BC study region.

3. Gather and report to LLNL local information on mine operations and associated seismicity, including "ground truth" for significant events.

Following guidance from LLNL's Technical Representative, the focus of Objective 2 was changed slightly to place emphasis on three mining-related events that occurred in and near the study area after the original work plan had been made, thus posing new targets of opportunity. These included: a magnitude 3.8 shock that occurred close to the Willow Creek coal mine in the Book Cliffs area on February 5, 1998 (UTC date), just prior to the start of this project; a magnitude 4.2 shock on March 7, 2000 (UTC date), in the same area as the February 5 event; and a magnitude 4.3 shock that occurred on January 30, 2000 (UTC and local date), associated with a panel collapse at the Solvay trona mine in southwestern Wyoming. This is the same mine in which an earlier collapse event of magnitude 5.2 occurred in February 1995, attracting considerable attention from the CTBT community.

Objective 1

Objective 1 was successfully met with the completed installation (described in detail in section 2) of a high-quality, three-component, broadband digitally telemetered seismograph station in the San Rafael Swell, Utah (SRU) on September 9, 1998. Station SRU (39° 6.65′ N, 110° 31.43′ W, 1804 m elevation) is located at a roughly uniform distance of 70 ± 20 km from the active mines in the arcuate WP-BC coal-mining region. This distance enables good recordings of larger mine tremors (magnitude ≥ 3.0), which are of primary interest, with minimal interference from more frequent smaller-magnitude events (hundreds per day) that occur in the coal fields.

Seismographic equipment at station SRU includes a Guralp CMG-3T broadband seismometer, with a flat velocity response from .01 to 50 Hz, and a 24-bit REF TEK 72A-07 data logger. The signal from the seismometer is digitized at 100 samples/sec and is continuously transmitted to the UUSS central recording laboratory in Salt Lake City where data are recorded using an Earthworm data-acquisition system. Instrumental response to ground motion was carefully calibrated, and calibration details are described in section 2.

Waveform data from station SRU are made publicly available in two ways. First, the UUSS Earthworm system routinely exports triggered 40 sample/sec waveform data from station SRU and other selected stations via an Internet link to the U.S. National Seismograph Network (USNSN) data center in Golden, Colorado. These data are available from the data center via the USNSN AutoDRM system. Second, since June 19, 2000, continuous data files from station SRU and other selected UUSS stations have been converted to SEED format and sent daily via FTP to the IRIS Data Management Center in Seattle, Washington, where the data are permanently archived and made available to all interested users.

Objective 3 (Background for Objective 2)

Information on seismic monitoring and mining seismicity in the WP-BC region is presented in section 3. We extend and update information earlier summarized by Arabasz et al. (1997) in order to provide a useful reference for LLNL researchers as well as other interested parties. We describe the University of Utah's current monitoring capabilities and summarize incident reports communicated to LLNL during the course of this project. These reports concerned seven seismic events of magnitude 3 or larger that occurred between February 1998 and August 2000.

In section 3 we also describe our methodology for creating a catalog of mining seismicity in the WP-BC region for the period January 1, 1978-June 30, 2000 with revised, homogeneous magnitudes. A complete listing of all seismic events (N=148) of magnitude 2.5 or larger in this catalog is presented in Appendix A. Using the refined catalog (6851 events; 95 percent ≥ magnitude 1.3) together with updated information on coal production (summarized in Appendix B), we present numerous plots and briefly discuss the spatial and temporal association of seismicity with mining in the WP-BC area. Figures include annual epicenter maps from 1992 through mid-2000 and composite time-series plots for 12 local areas where clustered seismicity coincides with sites of active mining. For each sample area, the time-history plots show quarterly coal production, quarterly counts of seismic events above a threshold magnitude, and the magnitudes of individual events.

A magnitude 4.2 shock that occurred in the BC district on March 7, 2000 (more below) is the largest seismic event to have originated in the WP-BC mining region since at least mid-1962, when instrumental seismic monitoring began. Mining-related seismic events in the magnitude 3 range have occurred throughout most of the WP-BC mining region, associated with sites of both longwall and room-and-pillar mining.

There is an evident spatial association of clustered epicenters with sites of active mining in the WP-BC area. Epicentral clustering in the WP mining district is generally tighter and more intense than in the BC district, due to better epicentral control and higher extraction rates at mines in the WP district during the sample period. Seismic events located in the WP-BC area by the University of Utah's regional seismic network have poorly constrained focal depths because of the relatively large station spacing. Nevertheless, combined evidence from (a) an analysis of focal-depth resolution, (b) data from local studies, and (c) the spatial and temporal association of seismicity with active mining allows and suggests that the vast majority (> 95 percent) of the observed seismicity in the WP-BC coal fields is shallow, probably occurs either at or within hundreds of meters above or below mine level, and is mining-related.

Temporal variations in observed seismic activity in the WP-BC area correlate simply in some cases with the start or completion of mining. In other cases, where extraction was relatively continuous over several years, seismic activity has occurred in distinct episodes—indicating the influence of other mine-specific factors, such as local geology and depth of cover. In the WP-BC area, longwall mining results in higher extraction rates and generally tends to be accompanied by higher rates of mining seismicity than room-and-pillar mining. But time series of longwall production and seismicity do not always correlate simply. Again, other mine-specific variables besides extraction rate appear to influence the generation of seismicity in the size range recorded by the regional seismic network.

Information on "ground truth"—what actually happened in or near a mine at the time of a discrete event that produced observable seismic signals—was gathered with the help of Dr. M. K. McCarter of the University of Utah's Department of Mining Engineering. Ground-truth information was successfully acquired for eight seismic events, for which observational data summaries and mine sketches are provided in Appendix C. These include (a) seven events of magnitude 3.1 to 4.2 related to underground coal mining in the WP-BC area between 1981 and 2000 and (b) a trona-mining-related event of magnitude 4.3 in southwestern Wyoming in January 2000. Multiple pillar failures are documented for four of the WP-BC events, and a roof collapse involving three room-and-pillar sections is documented for the trona-mining-related event.

Objective 2

Results of our investigations of source mechanisms of mining seismicity in the WP-BC region, as well as of three seismic events in the trona-mining region of southwest Wyoming, are presented in section 4. For the WP-BC mining region, we systematically investigated the 18 largest events ($3.0 \leq$ magnitude ≤ 4.2) since 1978. Because of the early dates and (or) relatively small size of most of the events (14 have magnitudes < 3.5), broadband waveform data at regional distances are either sparse or of marginal signal-to-noise quality. In this study we carefully refined local velocity models and then analyzed P-wave first motions for focal-mechanism information. Companion ground-truth information was successfully recovered for seven of the 18 events.

Contrary to some published interpretations and our expectation, mechanisms for only three of the 18 events are unambiguously of a shear-slip type: (1) a shallow (~0.6 km), predominantly reverse-faulting event of magnitude 4.2 near the Willow Creek Mine in the BC district on March, 7, 2000; (2) a magnitude 3.8 event on February 5, 1998, in nearly the same location as event (1) and with first motions compatible with the same mechanism; and (3) a tectonic normal-faulting earthquake (11 km deep) of magnitude 3.0 on June 2, 1996, beneath the WP district. For events (1) and (2), observations in the Willow Creek Mine (< 1 km distance) indicate isolated roof falls, interpreted for each event to be the result of shaking caused by nearby shear-slip and not as the seismic source.

For 13 of the other 15 events, coincident with sites of both longwall and room-and-pillar mining throughout the WP-BC region, only dilatational first motions were recorded by the University of Utah's regional seismic network (209 total observations). For the remaining two of the 18 events, first-motions are obscured by small preceding events. Collapses or partial closures of mine openings are documented for four of the events with all dilatational first motions. Based on varied evidence presented in section 4, including size considerations, we consider it highly likely that these four events were collapse-type events with implosional mechanisms. We also consider it plausible that the other events with only dilatational first motions had similar source mechanisms, with variable likelihood depending on available data.

Available evidence favors the working hypothesis that the predominant mechanism of larger (magnitude ≥ 3.0) mining-induced seismic events in the WP-BC region is implosional and caused by sudden roof-floor closure, either partial or total, due to loss of pillar support. The shallow shear-slip earthquakes of magnitude 4.2 and 3.8 near the Willow Creek Mine in March 2000 and January 1998, respectively, are notable exceptions.

Finally, we investigated the source mechanisms of three seismic events that occurred in the trona-mining district of southwestern Wyoming between January and August 2000. A seismic event of magnitude 4.3 on January 30, which coincided with a major roof fall at the Solvay Minerals trona mine, had an implosional collapse-type mechanism. We were unable to find any ground-truth information for shocks of magnitude 3.0 on July 16 and magnitude 3.1 on August 17. P-wave first-motion data and regional broadband waveforms indicate that the July 16 event was a shear-slip earthquake and suggest that the August 17 event was a collapse-type event.

ACKNOWLEDGMENTS

We thank William Walter, Technical Representative of Lawrence Livermore National Laboratory (LLNL), for facilitating this project. We also offer special thanks to staff of the University of Utah Seismograph Stations for varied assistance in completing the project tasks. In particular, we thank Sue Nava for help with project management; Erwin McPherson for the engineering and field installation of the broadband station SRU; Dave Drobeck, Ken Whipp, and Paul Onstott for field assistance; and Julie Bernier, Jeff Fotheringham, Matt Jensen, Ali Moeinvaziri, Lorraine Nelms and Julie Bernier for technical help with data analysis, computing, and graphics.

Kim McCarter and Jeff McKenzie of the University of Utah's Department of Mining Engineering provided many useful insights from their mining engineering experience, and their contributions of Appendices B and C to this report are greatfully acknowledged. Several individuals kindly provided key information that advanced our understanding of specific seismic events within or near active mines in the Utah and southwestern Wyoming regions. For their gracious cooperation, we thank Pete Swanson of the National Institute for Occupational Safety and Health; Larry Refsdal of Solvay Minerals, Inc.; Rodger Fry of Interwest Mining Company; Tom Hurst, John Mercier, and Andy Schissler, all presently or formerly with RAG American Holding, Inc.; and Jim Case of the Wyoming Geological Survey.

This project was funded by LLNL Research Agreement No. B344836. Cooperative funding was provided by the state of Utah under a line-item appropriation to the University of Utah Seismograph Stations. Operational support for the University of Utah Regional Seismic Network, which supplied essential data for this project, was provided chiefly by the U.S. Geological Survey, the State of Utah, and the U.S. Bureau of Reclamation.

1.0 INTRODUCTION

Mining operations and practices have important implications for monitoring the Comprehensive Test Ban Treaty (CTBT). Seismic signals from legitimate mining operations can have the ambiguous appearance of being caused by small clandestine nuclear explosions, so confidence-building measures are needed for international treaty monitoring (Taylor, 1994; Walter et al., 1996; Richards, 1997; Committee on Seismic Signals from Mining Activities, National Research Council, 1998). There are distinct challenges, however, to understanding the causes, and discriminating the mechanisms, of seismic energy release in mining environments in the western U.S. and elsewhere. Problematic events include, for example, panel collapses in the Solvay trona mine in southwestern Wyoming in February 1995, which was associated with an M_L 5.2 seismic event (Pechmann et al., 1995; Swanson and Boler, 1995), and underground failures in coal mines in Utah in 1981 (Taylor, 1994) and 1993 (Boler et al., 1997) that produced seismic events in the magnitude (M_L) 3 range.

Mining seismicity is a prominent feature of seismic activity in the Utah region. Besides blasting at surface mines, intense seismic activity is associated with areas of extensive underground coal mining along the arcuate crescent of the Wasatch Plateau (WP) and Book Cliffs (BC) coal fields (Figures 1-1 and 1-2; see also review by Arabasz et al., 1997). The WP-BC region is notable as one of two areas in the western U.S. (the other, the Coeur d'Alene metal mining district of northern Idaho) where mining-induced seismicity is well documented (Wong, 1993). For international monitoring, seismic signals from rockbursts, coal bumps, and mine collapses are more likely to be ambiguous than those from surface blasting (Committee on Seismic Signals from Mining Activities, National Research Council, 1998). Rockbursts and mining tremors of magnitude (M_L) $\leq$ 4.2 have been instrumentally recorded in the WP-BC region since the 1960s. About 27 million short tons of coal are produced annually from this region, with longwall-mining methods accounting for 75 percent of the total production (Jahanbani, 1999).

Given the significant level of seismic activity associated with active underground coal mining in the WP-BC region, seismic monitoring and the characterization of seismic events in this region are of interest both to the University of Utah Seismograph Stations (UUSS), for earthquake research and mine safety, and to Lawrence Livermore National Lab (LLNL), for research and development relating to the Comprehensive Test Ban Treaty. This cooperative project was undertaken to assist LLNL researchers in the latter role.

1.1 OBJECTIVES AND SCOPE OF WORK

This study had three basic objectives:

1. Strategically install a 3-component broadband digital seismic station in the WP-BC region to ensure the continuous recording of high-quality waveform data. The aim was to meet the long-term needs of various interested parties—including LLNL, UUSS, mine operators and others in the state of Utah, and the international CTBT community at large.

2. Determine source mechanisms—to the extent that available source data and resources allowed—for comparative seismic characterization of stress release in mines versus earthquakes in the study region.

3. Gather and report to LLNL local information on mine operations and associated seismicity, including "ground truth" for significant events.

The time period for this project was originally set for a 12-month period beginning February 28, 1998. Due to unexpected health problems affecting one of the principal investigators (JCP), no-cost extensions were agreed upon which ultimately changed the ending date of the project to September 1, 2000.

Funding for Objective 1 accounted for 60 percent of the total budget; funding for Objectives 2 and 3 accounted for approximately 25 percent and 15 percent, respectively. In addition to the awarded amount of $58,960 for this study, UUSS to date has contributed more than $20,000 to this project. LLNL provided funds for more than 90 percent of the equipment costs; UUSS provided the remainder together with engineering and technical personnel for installing and operating the broadband digital seismic station as well as funds to meet ongoing costs for telemetry, maintenance, and operation of the broadband station. Thus, this project truly has been a cooperative one between LLNL and UUSS.

The scope of work to meet Objective 1 involved all aspects of achieving what might be referred to as an "end-to-end" seismographic system—variously involving: (1) engineering, site construction, and equipment installation at the field site; (2) completion of a continuous telemetry connection from the field site to the UUSS central recording laboratory in Salt Lake City, 216 km away; (3) calibration of the complete broadband station system; and (4) continuous recording, processing, and archiving of the digital data. Significant effort on the part of the Principal Investigators was required to oversee each of the above and to perform the system calibration, described in section 2.2.

Following guidance from LLNL's Technical Representative for this contract, William Walter, the focus of Objective 2 was changed slightly to place emphasis on three mining-related events that occurred in and near the study area after the original work plan had been made, thus posing new targets of opportunity. These included a magnitude (M_L) 3.8 shock that occurred on February 5, 1998 (UTC date) just prior to the start of this project, and a magnitude (M_L) 4.2 shock that occurred on March 7, 2000 (UTC date). Both these events originated close to active mine workings in the Book Cliffs area. The M_L 4.2 event was the largest mining-related seismic event instrumentally recorded in the WP-BC area since monitoring began in 1962. The third seismic event of special interest was a magnitude (M_L) 4.3 shock that occurred on January 30, 2000 (UTC and local date), associated with a panel collapse at the Solvay trona mine in southwestern Wyoming—the same mine in which a larger and earlier collapse event in February 1995 attracted considerable attention from the CTBT community, prompting joint study by UUSS and LLNL seismologists (Pechmann et al., 1995).

Also following guidance from William Walter, emphasis on Objective 3 was placed on providing LLNL with information on mining seismicity in the study area that would extend and update the information published by Arabasz et al. (1997). The latter study included seismicity data through March 1996 and comparisons of seismic data with levels of coal production for the period January 1978 through December 1994.

We proceed to describe results relating to the three basic objectives of this study in the following order. First, in section 2, we address Objective 1 (installation of a 3-component broadband digital seismic station. Next, in section 3, we describe results for Objective 3 (information on mine operations and associated seismicity) in order to present necessary background information before addressing Objective 2 (source mechanisms of significant seismic events) in section 4.

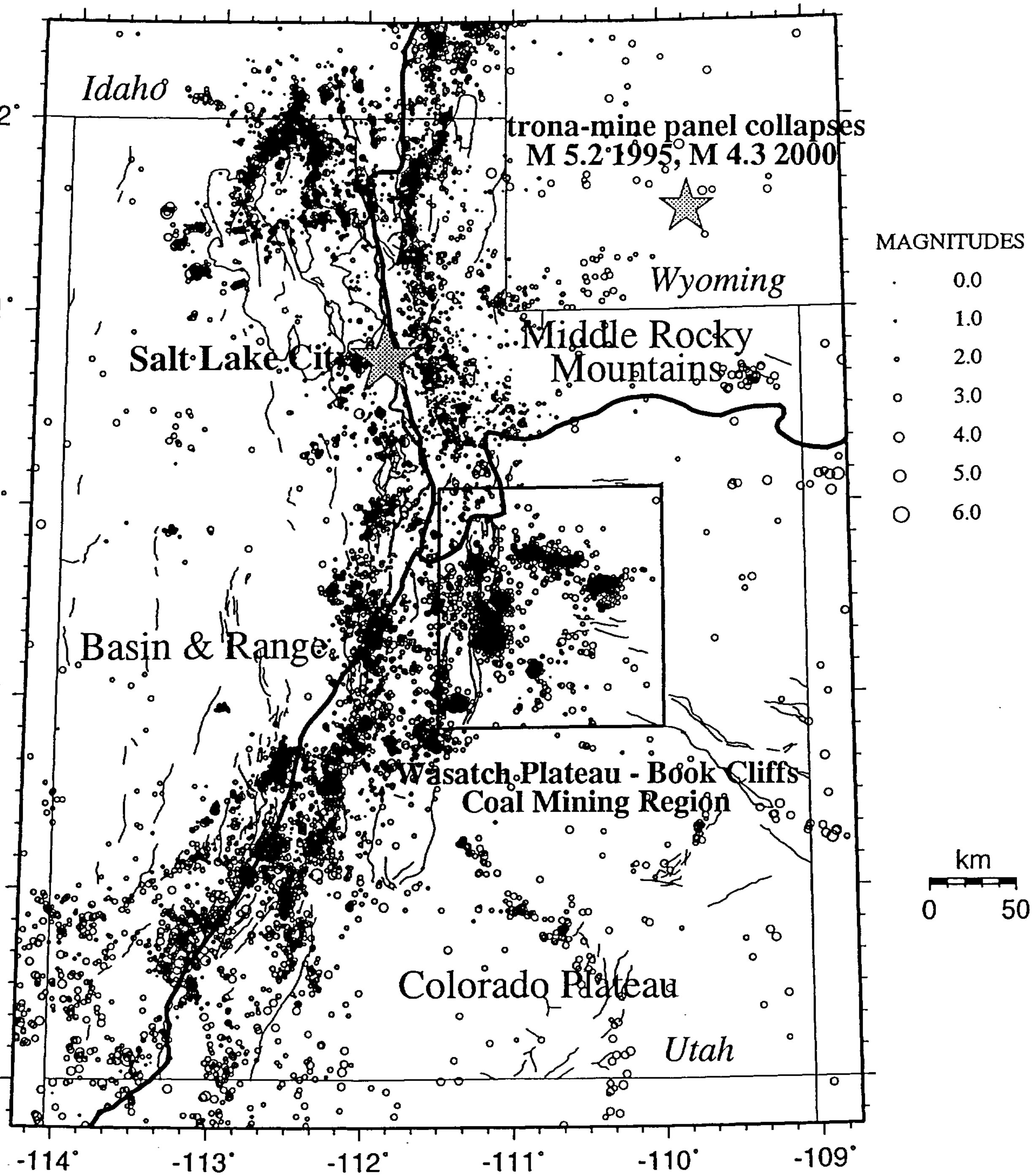

Figure 1-1. Seismicity map of the Utah region, 1978-2000, showing the location and setting of the Wasatch Plateau-Book Cliffs coal mining region (Figure 1-2). Heavy lines indicate boundaries of major physiographic provinces; light lines, geologically young faults. Star in SW Wyoming marks the location of significant seismic events related to trona mining. Earthquake data from the University of Utah Seismograph Stations.

Wasatch Plateau - Book Cliffs Coal Mining Region

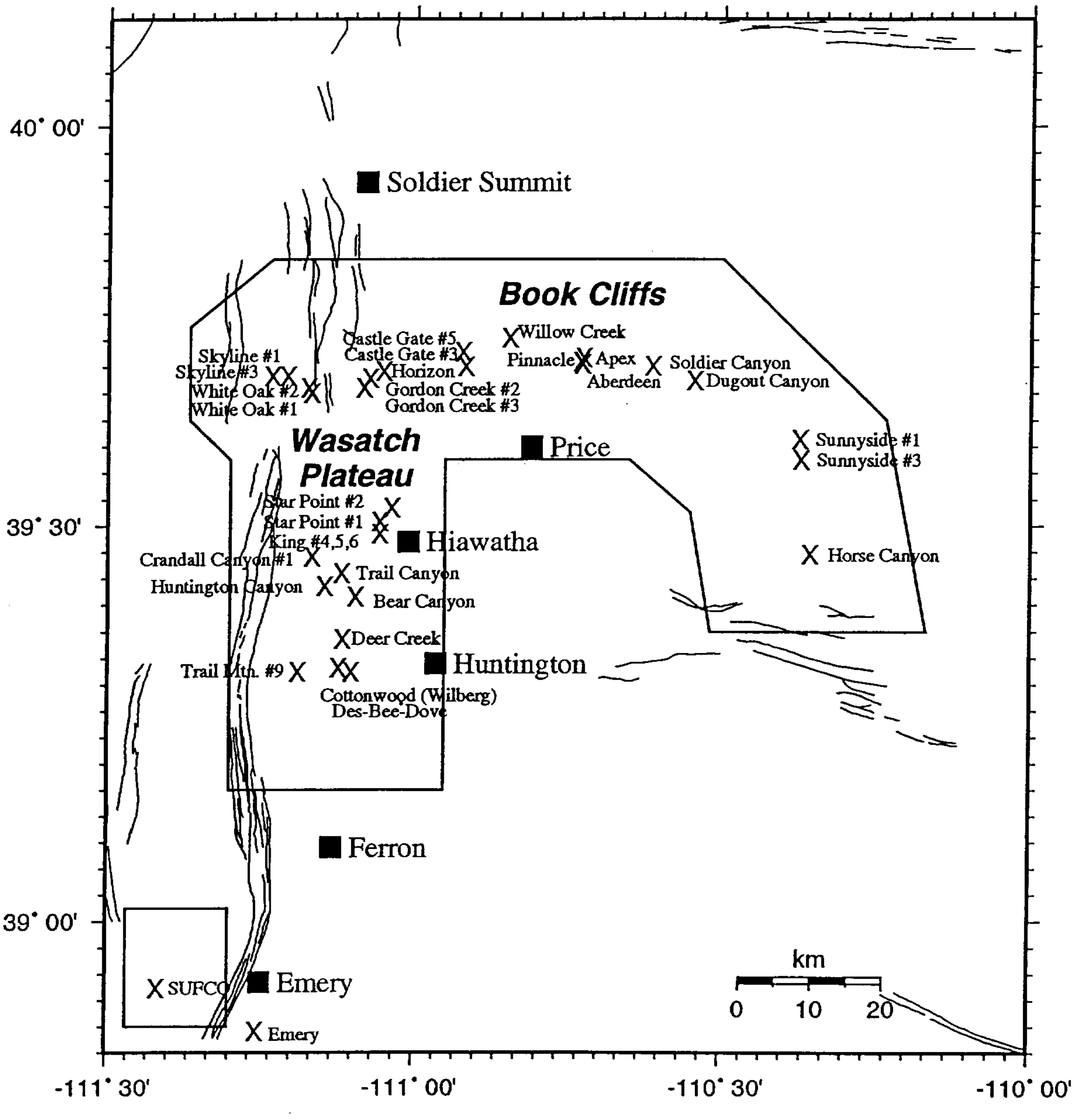

Figure 1-2. Location map of coal mines (X's) in the northerly-trending Wasatch Plateau (WP) and easterly-trending Book Cliffs (BC) coal fields (all mines east of and including the Castle Gate mines lie within the BC field; the remainder, within the WP field). Polygons (after Arabasz et al. 1997) bound areas within which nearly all seismicity is inferred to be mining-related. Geologically young faults are shown by light lines.

2.0 BROADBAND DIGITAL SEISMIC STATION (SRU)

As proposed, we installed a broadband, 3-component digital telemetry station in the WP-BC region of Utah at the site of a preexisting station of the University of Utah regional seismic network, SRU (San Rafael Swell, Utah; see Figures 3-1 to 3-3). Prior to the completion of this installation on September 9, 1998, SRU was a short-period, vertical-component, analog telemetry station. We selected the SRU site because it (1) complements the azimuthal coverage of the WP-BC region provided by other broadband stations, (2) has a low seismic noise level, and (3) is at a roughly uniform distance of 70 ± 20 km from the coal mines in the area. At this distance range, SRU obtains good recordings of the $M_L \geq 3.0$ seismic events which are of primary interest with minimal interference from the frequent smaller-magnitude events (hundreds per day) which occur in the coal fields.

2.1 INSTALLATION

The sensor at the upgraded SRU station, selected in consultation with William Walter, is a Guralp CMG-3T 3-component broadband seismometer with a flat velocity response from .01 to 50 Hz. When we started recording data from this seismometer on September 9, 1998, we discovered that there was a high level of long-period (50-100 sec) instrumental noise on the east-west component. Consequently, the CMG-3T was removed on September 26, 1998, and sent back to Guralp Systems Limited in England for repair. In order to keep SRU operating, the CMG-3T was replaced with a Guralp CMG-40T 3-component broadband seismometer having a flat velocity response from .05 to 50 Hz. The CMG-3T was reinstalled on April 15, 1999, shortly after it was received back from Guralp.

Figure 2-1 illustrates the seismometer installation at the site. The seismometer is on a concrete pad on Jurassic Navajo Sandstone bedrock inside a cylindrical steel barrel 24" high and 30" in diameter. Thermal insulation is provided by a concrete and foam insulation enclosure inside the barrel, mixed fill surrounding the barrel, and sand on top of the barrel. The installation design was modified by Erwin McPherson from the U.C. Berkeley design described by Uhrhammer et al. (1998).

The signal from the seismometer is digitized at 100 samples/sec by a 24-bit REF TEK 72A-07 data logger and transmitted via FM radio to a State of Utah microwave communications facility located 10.6 km to the northwest on Cedar Mountain. From there, the data are sent via the State microwave system to a REF TEK 112-00 Modem-Decoder Assembly at the UUSS central recording laboratory in Salt Lake City. The REF TEK digital telemetry system provides full two-way error correction. Time stamping is done by the 72A-07 data logger using a clock synchronized via radio to a REF TEK 111A-02 GPS Receiver/Clock at the central recording laboratory. From the REF TEK 112-00, the data are currently sent through a serial SDLC line, a router, and a local area network to our USGS-supplied Earthworm data acquisition system.

2.2 CALIBRATION

We analyzed the observed and predicted outputs from remotely-generated step function calibration inputs to check and revise the manufacturer-supplied instrument response parameters. This simple calibration method, illustrated in Figure 2-2 (from Pechmann et al., 1999), appears to work well at periods longer than about one-twentieth of the seismometer free period. However, its absolute accuracy depends on the accuracy of the manufacturer-supplied feedback coil constants, which relate calibration input to acceleration. The software we used for our step function calibrations (a Seismic Analysis Code macro) is available via anonymous FTP to <ftp.seis.utah.edu> in the file <pub/misc/calcheck.m>.

Table 2-1 lists the calibrated displacement responses at SRU for three different time periods: September 9, 1998, to September 26, 1998, 21:00 UTC, the time period immediately following the first installation of the Guralp CMG-3T; September 26, 1998, 21:00 UTC to April 15, 1999, 15:00 UTC, the time period during which the CMG-3T was out for repair and a Guralp CMG-40T was operating in its place; and April 15, 1999, 15:00 UTC to the present, the time period after the CMG-3T was reinstalled. The responses are specified as poles and zeros of a ratio of polynomials in the Laplace transform variable "s", plus a gain constant. Also listed in Table 2-1 are the calibration resistances and feedback coil constants supplied by Guralp Systems Limited, and the free periods and damping factors of the various seismometer components determined by our calibrations.

Both before and after the repair work, the Guralp-supplied values for the CMG-3T gain, free period, and damping were within 2% of the values we obtained with our calibration. For the CMG-40T, the differences between the Guralp-supplied values for these parameters and our calibrated values were a bit larger—up to 4%. We have found that gains, free periods, and damping factors of CMG-40T seismometers can differ by up to 15%, 9%, and 7%, respectively, from the nominal values (Pechmann et al., 1999).

2.3 RECORDING, PROCESSING, AND ARCHIVING OF DATA

The data from station SRU, and the other five REF TEK broadband digital telemetry stations in the UUSS network, are recorded by the UUSS Earthworm data acquisition system (see the web documentation at <www.cnss.org/EWAB>) using software written at REF TEK, the University of Nevada at Reno, the University of Utah, and the U.S. Geological Survey. The Earthworm system writes the REF TEK waveform data to continuous binary disk files in Seismic Analysis Code (SAC) format. It writes the non-waveform data packets, which contain station/channel and state-of-health information, to binary disk files in REF TEK format. UUSS technicians regularly look at the state-of-health data to detect and diagnose problems with the REF TEK stations.

The Earthworm system uses the waveform data from most stations in the network, including SRU, to automatically identify local seismic events and compute preliminary locations and magnitudes for them. The Earthworm system also exports triggered 40 sample/sec waveform data from selected stations, including all of the REF TEK stations, via an Internet link to the

U.S. National Seismograph Network (USNSN) data center in Golden, Colorado. These exported data are publicly available from the data center via the USNSN AutoDRM system. Finally, the Earthworm system creates digital "Webcorder" (simulated drum recorder) displays of the data from SRU and other selected stations in the UUSS network which may be accessed by anyone through the UUSS web site <www.quake.utah.edu>.

Waveform data from selected time windows are extracted from the continuous SAC-format data files and stored in both SAC and UW-1 format. The selected time windows are those identified by the UUSS analog telemetry data acquisition system, a Masscomp 7200 computer running University of Washington HAWK software, as possibly containing seismic events. Each of these "triggers" is reviewed by a seismic analyst and classified as a local earthquake, blast, distant seismic event, or noise. The analyst attempts to determine locations and magnitudes for all local earthquakes recorded. All REF TEK data from seismic event triggers, and usable data from other stations, are archived onto optical disks and 8-mm tapes. In addition, these triggered data are periodically archived in SEED format at the IRIS Data Management Center in Seattle, Washington.

The continuous SAC-format 100 sample/sec data files from the REF TEK stations are kept on-line at UUSS for five days. Since June 19, 2000, the continuous data files have been converted to SEED format and sent via FTP to the IRIS data center by an automatic background process which runs once per day. At the IRIS data center, these data are permanently archived and made available to all interested users.

2.4 SIGNIFICANCE OF DATA FOR CTBT MONITORING

External users of our network waveform data have commented on the excellent quality of the data from station SRU. The seismic analyst who is primarily responsible for routine UUSS data processing, Jeff Fotheringham, judges that SRU is now the best seismic station in Utah. During its first two years of operation, SRU has recorded high-quality data from hundreds of seismic events including local earthquakes, blasts, and mining-related events in the Wasatch Plateau-Book Cliffs coal-mining region. These data, along with data from other broadband digital telemetry stations in Utah, will be extremely valuable for future research on seismic discriminants which can be used to distinguish earthquakes, mine collapses, and explosions. To date, we have used the SRU data primarily for computing Richter local magnitudes for local earthquakes and mining-related seismic events. Woods et al. (1993) have proposed using the ratio of local magnitude to seismic moment as a means for discriminating explosions from earthquakes.

Table 2-1

Hardware and Calibration Information for Station SRU*

	Component	Sept. 9, 1998 to Sept. 26, 1998, 21:00 UTC	Sept. 26, 1998, 21:00 UTC to April 15, 1999, 15:00 UTC	April 15, 1999, 15:00 UTC to present
		Refraction Technology (REF TEK) Digitizer		
Model and Serial No.	All	72A-07 7789	72A-07 7789	72A-07 7789
Digitizing Constant, volts/count	All	1.9073×10^{-6}	1.9073×10^{-6}	1.9073×10^{-6}
		Guralp Systems Seismometer		
Model and Serial No.	All	CMG-3T T3650	CMG-40T T4182	CMG-3T T3650
Calibration Resistance, Ohms	All	51000	10000	51000
Feedback Coil Constant, amp/(m/sec^2)	Vertical	.03207	.004448	.03207
	East	.03383	.003862	.03383
	North	.03144	.004001	.03144
Free Period, sec	*Vertical*	*99.96*	*20.75*	*99.81*
	East	*101.44*	*20.13*	*100.91*
	North	*100.41*	*20.21*	*100.28*
Damping Factor	*Vertical*	*.7026*	*.6812*	*.7004*
	East	*.7077*	*.7002*	*.7094*
	North	*.7113*	*.7062*	*.7053*
		Total System Pole-Zero Response		
Zeros, rad/sec	All	0.0 + 0.0i	0.0 + 0.0i	0.0 + 0.0i
	All	0.0 + 0.0i	0.0 + 0.0i	0.0 + 0.0i
	All	0.0 + 0.0i	0.0 + 0.0i	0.0 + 0.0i
	All	945.6 + 0.0i	923.6 + 0.0i	945.6 + 0.0i
Seismometer Poles, rad/sec	*Vertical*	*-.04417 ± .04473i*	*-.2063 ± .2217i*	*-.04409 ± .04493i*
	East	*-.04384 ± .04376i*	*-.2185 ± .2228i*	*-.04417 ± .04388i*
	North	*-.04451 ± .04398i*	*-.2196 ± .2202i*	*-.04420 ± .04442i*
Other Poles, rad/sec	All	-505.8 ± 193.5i	-305.4 + 0.0i	-505.8 ± 193.5i
Gain Constant, counts/micron	*Vertical*	*-250347*	*-143.2*	*-249304*
	East	*-249126*	*-142.3*	*-250340*
	North	*-249705*	*-143.3*	*-248435*

* Values in italics are from UUSS calibrations. All others are from the equipment manufacturers.
The station coordinates are 39° 6.65′ N, 110° 31.43′ W, 1804 m elevation.

SRU Broadband Seismometer Installation

August 31, 2000

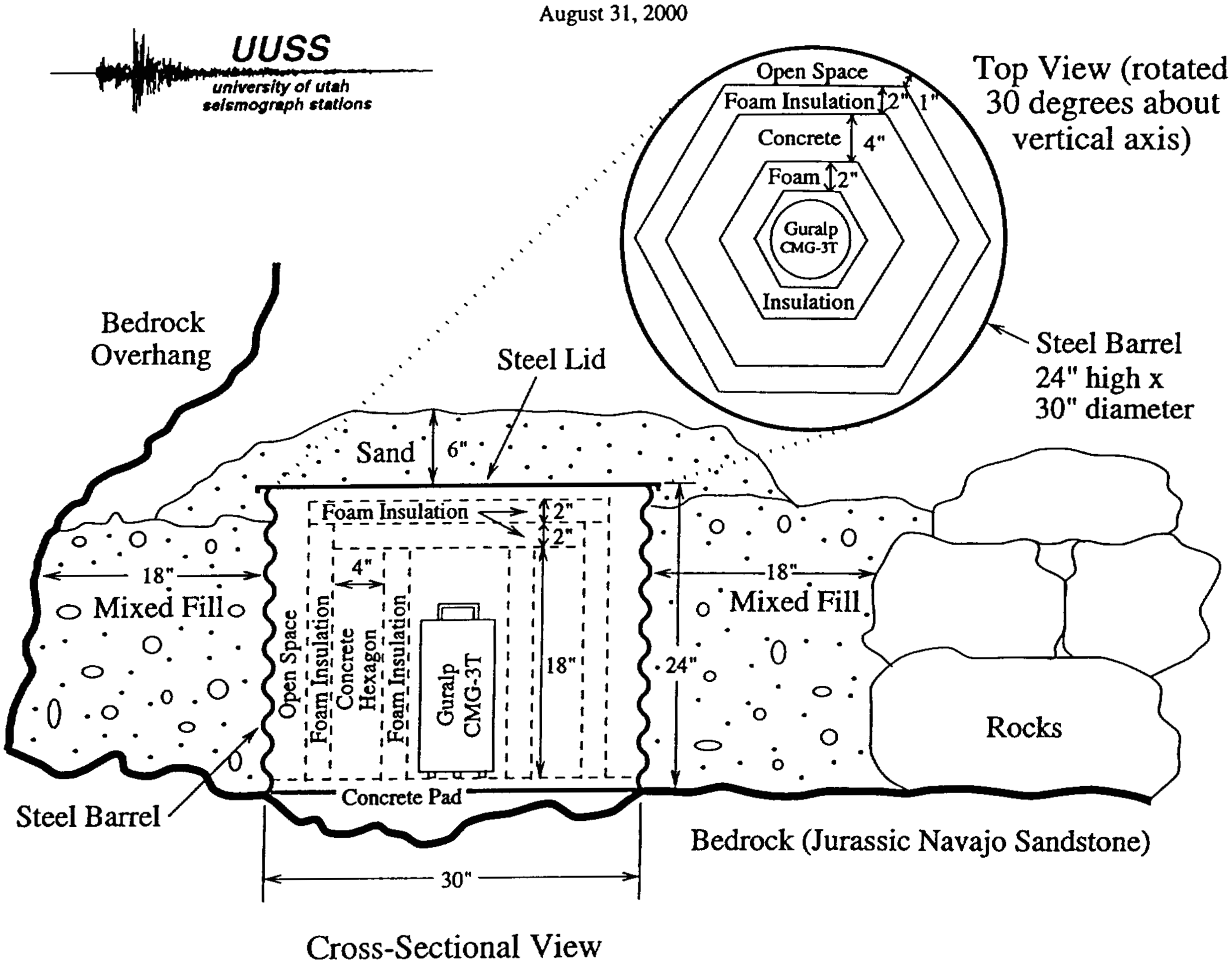

Figure 2-1. Installation diagram for the broadband, 3-component, Guralp CMG-3T seismometer at the digital telemetry station SRU.

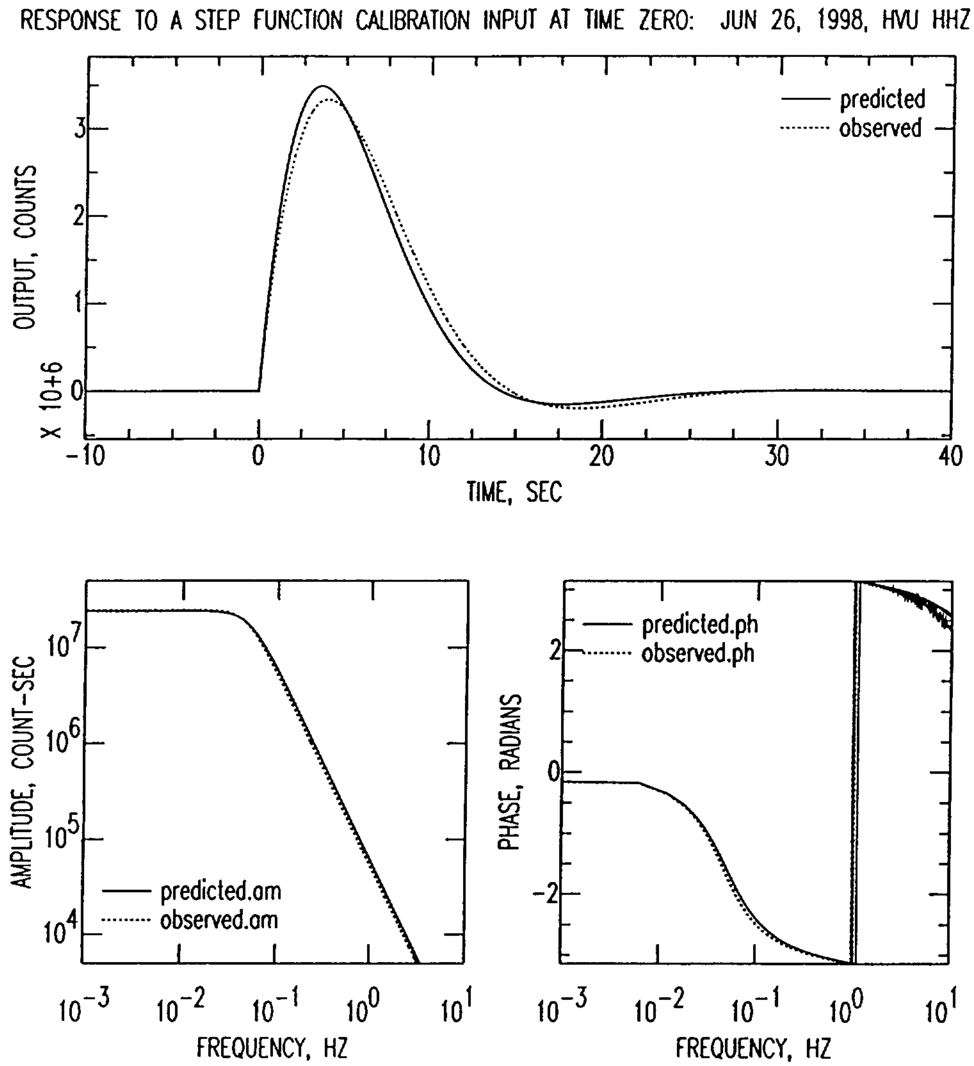

Calibration Step 1: Compare observed and predicted step function responses in the time domain (top) and frequency domain (bottom). Note that the time domain signal is primarily controlled by the seismometer response at periods longer than its free period (20 sec in this case). Therefore, time domain comparison of raw step function responses is not a good indicator of instrument response accuracy at periods shorter than the free period, i.e., within the passband of the seismometer.

Figure 2-2. The four steps in the calibration procedure we used to check and revise the manufacturer-supplied instrument response parameters for station SRU (from Pechmann et al., 1999).

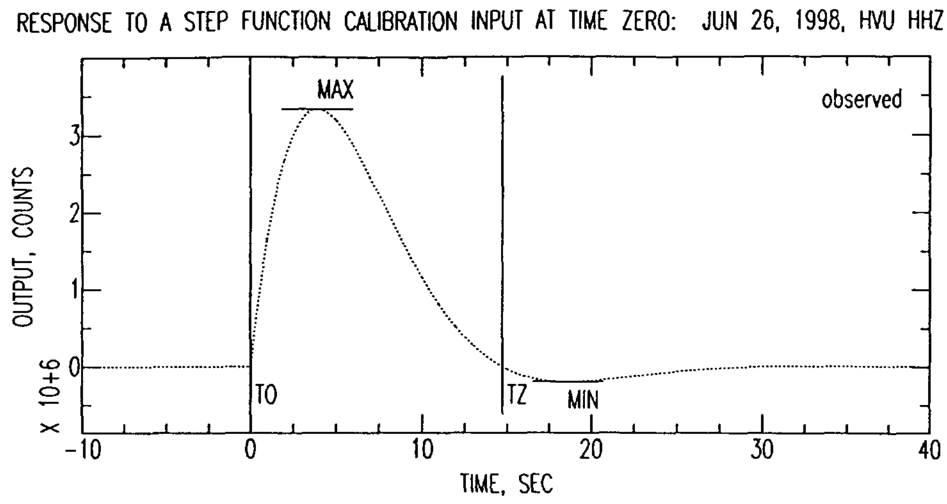

Calibration Step 2: Measure the damping ratio, |MAX/MIN|, and the initial pulse width (TZ - TO) for the observed step function response. Then use these measurements, together with relations derived from the standard seismometer equation, to calculate the seismometer damping factor and free period. This calculation assumes that the seismometer equation is applicable—as is the case for our Guralp CMG-40T and CMG-3T seismometers.

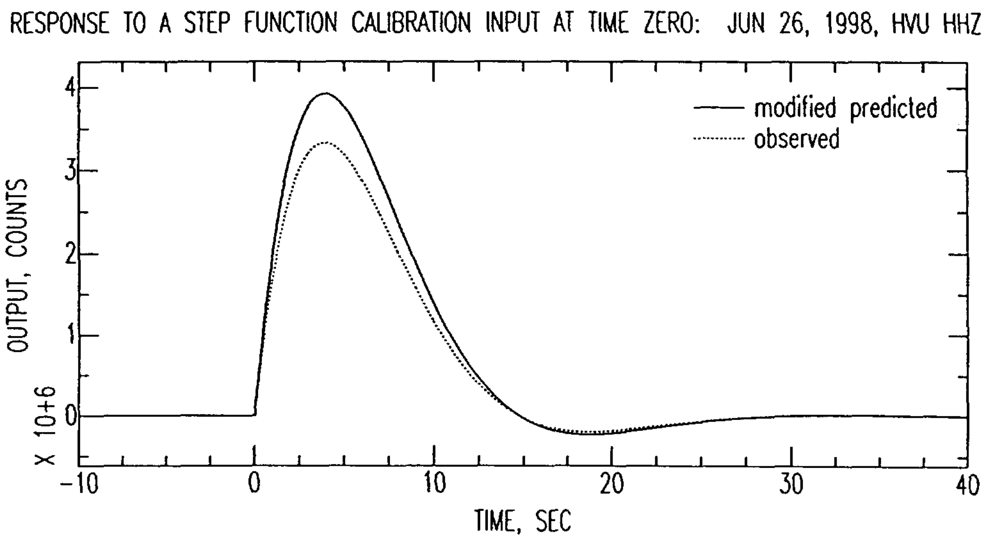

Calibration Step 3: In the frequency domain, correct the predicted step function response for the differences between the predicted and observed free period and damping. Then, use the ratio between the peak-to-peak amplitudes of the observed and modified predicted responses to compute the observed gain constant from the predicted one.

Figure 2-2 (continued).

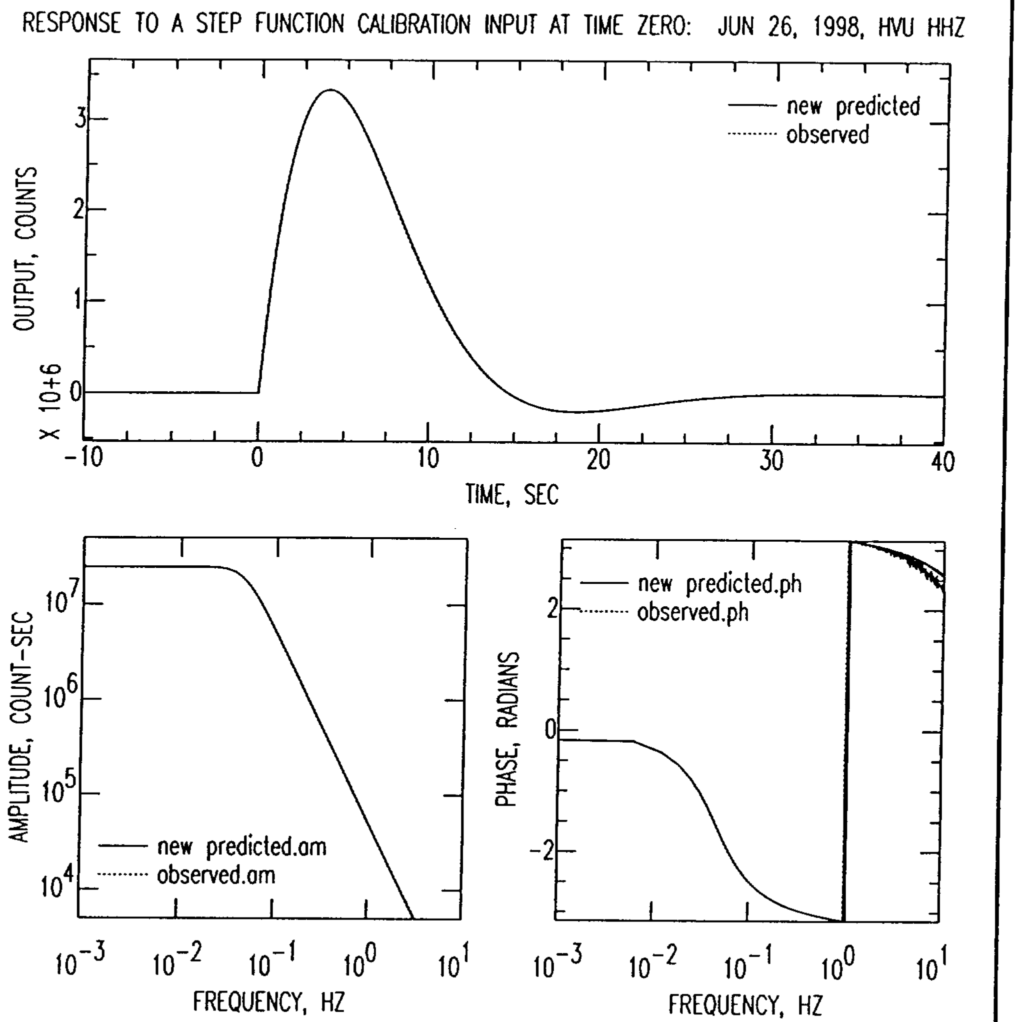

Calibration Step 4: Finally, revise the response file using the information obtained in Steps 1-3. Test the new response file by recomputing the predicted step function response and comparing it to the observed one. In the case shown here, the observed response has a good signal-to-noise ratio up to at least 1 Hz.

Figure 2-2 (continued).

3.0 MINING SEISMICITY AND "GROUND TRUTH"—AN UPDATE

Mining seismicity generally includes both seismic events induced by underground mining and mine blasts at surface mines. Our attention here is restricted to the former and primarily focuses on the Wasatch Plateau (WP)-Book Cliffs (BC) coal-mining districts of east-central Utah—with secondary attention to the trona-mining district of southwestern Wyoming (see upper right-hand corner of Figure 1-1). "Ground truth" in the context of mining seismicity simply means information on what actually happened in or near a mine at the time of some discrete event that produced observable seismic signals.

We use the term mine tremor as synonymous with a seismic event induced by mining, and we restrict the term rockburst or "coal bump" to those seismic events associated with damage in accessible areas of a mine due to violent failure of rock (see Arabasz et al., 1997). One of the major challenges in studying mining seismicity in the WP-BC area is the ability to determine unambiguously the primary source of seismic energy release when material suddenly fails at a mining opening. The failure can be caused either by local static stresses in the direct vicinity of mining openings or by dynamic effects from seismic slip on a fault hundreds to thousands of meters away (e.g., Gibowicz, 1990; Knoll and Kuhnt, 1990).

An overview of mining seismicity in the WP-BC area was given by Arabasz et al. (1997), including a description of available seismological data, the correlation of seismicity and mining, and outstanding issues and seismological challenges. Arabasz and Wyss (1999) reported a follow-up study on spatial variations in b-value (the slope of the frequency-magnitude distribution) in the WP-BC area. General issues posed by mine seismicity for mining engineers and seismologists, chiefly based on examples in the Utah region, were recently summarized by Arabasz and McCarter (2000).

Our chief purpose in the remainder of this section is to extend and update the information summarized by Arabasz et al. (1997) for mining seismicity in the WP-BC area in order to provide a useful reference for LLNL researchers. First, we describe the University of Utah's current monitoring capabilities, and we summarize incident reports communicated to LLNL during the course of this project (section 3.1). Second, we provide background information necessary to understand our approach to developing a homogeneous catalog of mining seismicity for the period January 1, 1978-June 30, 2000 (section 3.2). Third, we update information on coal production in the WP-BC area and compare the data to observed seismicity (section 3.3). Fourth, we describe "ground truth" information to which we were able to gain access for significant mine tremors (section 3.4)—referring the reader to Appendix C for documentation.

3.1 CONTINUOUS MONITORING AND INCIDENT REPORTS TO LLNL

The University of Utah Seismograph Stations (UUSS) operates a regional seismic network, with 105 stations in July 2000 (Figure 3-1), that has continuously monitored the Utah region, with progressively evolving instrumentation, since 1962. Telemetered data from the network have been centrally recorded on the University of Utah campus in Salt Lake City since 1974. Digital triggered recording of the UUSS network dates from 1981.

As evident in Figure 3-1, short-period, analog-telemetry stations predominate in the UUSS regional seismic network. Broadband stations in Utah include five UUSS stations installed and calibrated during 1997 and 1998 (Pechmann et al., 1999) that strategically complement six broadband stations of the U.S. National Seismograph Network (USNSN) in and near Utah, currently resulting in a broadband station spacing of 100 to 200 km or better.

UUSS network operations are cooperatively funded by the U.S. Geological Survey, the state of Utah, the U.S. Bureau of Reclamation, and (for the Yellowstone National Park area) the U.S. National Park Service. For additional details regarding the regional seismic network, see <www.quake.utah.edu>.

Figure 3-2 (from Arabasz et al., 1997) shows the WP-BC study area in relation to the regional seismic network. The post-1978 distribution of stations allows fair to good map locations of seismic events in the vicinity of mines within the study area, but focal-depth control for shallow events is poor. Epicentral precision (95% bounds), on average, is about ±3 km for the post-1978 data. This does not apply, however, to the eastern Book Cliffs area where poor azimuthal station control results in greater epicentral errors. Analysis of the UUSS catalog indicates that seismic monitoring of the mining areas shown in Figure 3-2 has been complete above about magnitude 1.8 since 1978 (Arabasz et al., 1997).

Figure 3-3 gives a current and future view of the location of seismographic stations in the WP-BC area, updating beyond 1994 the depiction shown in Figure 3-2. Comparing with Figure 3-2, Figure 3-3 indicates: (1) the continued operation of stations EMU, which dates from October 1986, and SRU, dating from November 1990; (2) the operation of station SRU as a broadband, digitally-telemetered station (see section 2.0) beginning in September 1998; (3) the recent addition of station DBD, which earlier operated on a temporary basis in 1995 for a four-month period; (4) the location of four planned short-period vertical-component stations (open triangles); and (5) the location of a temporary special-study array of accelerographs and short-period stations (installed in late 2000) for ground-motion studies of mining-induced seismic events in the Trail Mountain area. Station SKYM (not shown on Fig. 3-3), operated at 39°41.63'N, 111°12.27'W, from June 29, 1995, until June 22, 1999.

Based on continuous monitoring with the UUSS regional seismic network, the following incident reports were made by e-mail and/or telephone to William Walter of LLNL during the project period:

1. February 5, 1998 — Report of an M_L 3.7 (later revised to M_L 3.8) seismic event that occurred the previous night in the vicinity of the Willow Creek Mine in the WP-BC area. (On July 14, 1998, a detailed follow-up report was made summarizing available information on ground truth for the February 5 seismic event.)

2. April 13, 1999 — Confirmation that an M_L 4.5 seismic event in south-central Wyoming on April 6, 1999 (UTC date) was a tectonic earthquake and not a mining-related event.

3. December 22, 1999 — Report of an M_L 3.9 seismic event in central Utah earlier in the day and confirmation that the event was a tectonic earthquake and not a mining-related event.

4. January 30, 2000 — Report of an M_L 4.4 (later revised to M_L 4.3) seismic event earlier that morning near the Solvay Trona Mine in southwestern Wyoming—and confirmation that this was a mining-related event.

5. March 6, 2000 — Report of an M_L 4.1 (later revised to M_L 4.2) seismic event that occurred less than two hours earlier that evening close to the Willow Creek Mine in the WP-BC area. (Subsequent communications reported on available ground-truth information, the precise hypocentral location, a velocity model for the source, and a focal mechanism for the source.)

6. July 19, 2000 — Report of an M_L 3.2 (later revised to M_L 3.0) seismic event three days earlier on July 16 in the trona mining district of southwestern Wyoming, west of Green River, Wyoming. Report included a refined epicentral location placing the event in the vicinity of the TG Soda Ash and FMC mines, but local observations gave no indication of a simple association with either mine. P-wave first-motion information was also reported indicating the event did not appear to be of a collapse type.

7. August 22, 2000 — Report of an M_L 3.3 (later revised to M_L 3.1) seismic event that occurred five days earlier on August 17 in the trona mining district of southwestern Wyoming. Report included a refined epicentral location and a brief summary of waveform and first-motion information suggestive of a collapse-type mechanism. However, no information was available to confirm that the event was associated with a specific mine.

3.2 DEVELOPING A HOMOGENEOUS CATALOG

Most earthquake catalogs are heterogeneous in time, particularly in terms of non-uniform estimates of event size (e.g., Habermann, 1995; Zuniga and Wyss, 1995). Arabasz et al. (1997) made a major effort to address this issue in the case of the University of Utah's earthquake catalog, and they determined homogeneous magnitudes for mining-related seismic events in the WP-BC area for the period July 1962 through March 1996. Here we extend their revised catalog through June 2000.

For review, magnitude is reported in the University of Utah's earthquake catalog as either local Richter magnitude, M_L, based on amplitude measurements of standard Wood-Anderson (W-A) seismograms, or coda-duration magnitude, M_C, an empirical estimate of M_L typically made for events smaller than about magnitude 3. Inadvertent temporal changes in the M_C scale can arise variously from factors such as changes in network configuration, the type of instrumentation and its ground-motion magnification, or analysis software and procedures (Pechmann et al., 2000; Wiemer and Wyss, 1994, and references therein).

3.21 Methodology

Arabasz et al. (1997) did two basic things to achieve a catalog of homogeneous magnitudes for the WP-BC area. First, they used quantitative tools available in the interactive software package ZMAP (Wiemer et al., 1995) to derive time-varying correction terms for values of M_C in the catalog between January 1, 1978, and March 31, 1996, designating the corrected values as M_C'. Their correction terms are given in Table 3-1 here. Second, in order to develop robust estimates of size anchored to the University of Utah's Wood-Anderson-based M_L for the larger events in the catalog since 1962, they used empirical relations to convert all available magnitudes to an M_L equivalent and then calculated a weighted average, designated M_L'. The practical reason for doing this was that prior to 1994, only a few W-A seismographs were in operation in the Utah region.

Since early 1994, UUSS has routinely determined values of M_L using synthetic W-A seismograms from several USNSN stations in the region and from five UUSS broadband digital telemetry stations in Utah installed during 1997 and 1998 (see section 3.1 and Figure 3-1). This has greatly increased the fraction of earthquakes for which M_L can be robustly determined using recordings from multiple stations. With these new data in hand, a major project is under way at UUSS to review and revise, as appropriate, all magnitude estimates in the UUSS catalog since January 1981 when digital triggered recording of our network began. Here we continue the approach taken by Arabasz et al. (1997), and demonstrate its validity, but we caution that future revisions of the UUSS catalog may result in minor differences with the corrected magnitudes presented here.

The revised catalog of Arabasz et al. (1997) for mining seismicity in the WP-BC area was extended from March 31, 1996, to October 31, 1999, by Arabasz and Wyss (1999) as part of a special topical study. Their correction terms, given in Table 3-2, reflect the following: First, they justified the extension of equation (4) in Table 3-1 beyond March 1996, and we have lengthened the extension from October 1999 to June 2000. Second, when they analyzed the whole revised catalog from 1978 through October 1999 using ZMAP, they discovered a small bias of 0.1 unit for values of M_C prior to 1995, and they subtracted 0.1 to correct for this. (Note: Recognizing that M_C also factored into some of the weighted-average estimates of M_L' made by Arabasz et al. [1997], those values of M_L' were recalculated to be consistent with the adjustment of 0.1 in Mc for events before 1995. Consequently, some of the values of M_L' reported herein may differ from those of Arabasz et al. [1997] by 0.1 unit or less.)

To test the validity of their corrected values of M_C' as reliable estimators of M_L, Arabasz and Wyss (1999) compared M_C' with M_L for 85 events in the WP-BC area for which an estimate of M_L was available. With one exception, all estimates of M_L prior to 1994 were based on one station; those for 1994 and later, on two or more stations. The results of the comparison are shown in Figure 3-4. (Note: The sample includes eight tectonic earthquakes with M_L values in the range 2.5 to 4.4.) The lower panel of Figure 3-4 shows a plot of M_C' versus M_L and the line for perfect agreement. The mean residual for the 85 data points is -0.002 ± 0.273 (one standard deviation), indicating very good correlation. The upper panel is a plot of differences between M_C' and M_L as a function of time. The running average indicates random rather than systematic differences with time about the mean of -0.002. Thus, we believe that the revised coda magnitudes, M_C', together with available values of M_L, provide reliable, homogeneous estimates of size for mining seismicity in the WP-BC area.

3.22 Revised Catalog

Figure 3-5 shows an epicenter map of 6,851 seismic events in our revised catalog for the WP-BC area for the period January 1978 through June 2000. The events are restricted to two polygons, following Arabasz et al. (1997), which bound what is judged to be almost entirely mining-related seismicity located within (1) an arcuate crescent encompassing the Wasatch Plateau and Book Cliffs coal fields and (2) an isolated area of mining in the southern Wasatch Plateau. In Figure 3-5, the locations of the three largest seismic events are indicated by large stars. These include a shock of M_L 4.2 on March 7, 2000, one of M_L 3.8 on February 5, 1998, and another of M_L' 3.8 on May 14, 1981. Coincidentally, these three shocks are the largest not only since 1978 but also since systematic instrumental monitoring in this region began in July 1962.

A listing of all events of magnitude 2.5 and greater (N=148) in the revised catalog for 1978-2000 is presented in Appendix A. For special reference, a listing of all events in the revised catalog of magnitude 3.0 or greater, ordered by decreasing size, is presented in Table 3-3. We refer the reader to Table 1 of Arabasz et al. (1997) for the identification of larger mining-related seismic events in the WP-BC area that occurred after July 1962 but before January 1978, when the revised catalog here begins. The largest event in the 1962-1977 period was one of magnitude (M_L') 3.7 that occurred in April 1966.

3.23 Focal Depths

We emphasized earlier that focal-depth control in the WP-BC area based on the UUSS regional seismic network is generally poor because of the large station spacing, and computed focal depths such as included in Appendix A are not reliable. As part of the study reported by Arabasz and Wyss (1999), Arabasz investigated focal-depth control for events in the polygonal areas of Figure 3-5 to determine whether there might be a mixed sample of mining seismicity and deeper tectonic seismicity.

Of 5,063 events between January 1978 and October 1999, Arabasz was able to find only 15 for which the data arguably supported a focal depth greater than 6 km. None of these events was larger than magnitude 2.1. The results, combined with those of local studies (Williams and Arabasz, 1989; Wong et al., 1989) allow and suggest that virtually all the events clustering in the vicinity of the active coal mines in the WP-BC area are relatively shallow events occurring less than 6 km in depth. Because of the close spatial and temporal association of the seismicity with active mining (elaborated in section 3.3), we believe that nearly all this seismicity probably occurs at or within hundreds of meters above or below mine level and is mining-related.

3.3 ASSOCIATION OF SEISMICITY WITH MINING

In this section, we present and briefly discuss data and information relevant to the spatial and temporal association of seismicity with underground coal mining in the WP-BC area. In order to provide a useful "bridge" between results reported by Arabasz et al. (1997) for 1978-1994 and this report, data are presented here for an 8.5-year period beginning in January 1992 and ending in June 2000. While detailed analyses are beyond the scope of this project, the data summaries alone provide abundant information that (1) gives a useful overview and (2) can guide future studies relating to the correlation of mining activity and associated seismicity on a mine-by-mine basis.

Because the seismicity data inherently lack fine spatial resolution, we purposely make only general observations. Causal relationships between mining operations and seismic energy release are highly complex, and more detailed data are needed to confidently attribute specific seismic events to a particular mining operation.

3.31 Spatial Association

Figures 3-6 through 3-14 show the epicentral distribution, on an annual basis, for seismicity located within the WP-BC coal mining region using the University of Utah's regional seismic network. Also shown are the portal locations of all mines active in this region since 1978. Thus, each figure includes not only active mines but inactive ones as well, which in some cases may be associated with seismic failures.

Because distal parts of an active mine may commonly be 5 km or more from the portal, epicentral clustering may not coincide with the plotted location of an associated mine. Another consideration in comparing observed seismicity with locations of mining, separate from epicentral precision (i.e., the relative location of one event compared to another), is the possibility of systematic bias due to network configuration and non-uniform seismic velocities. Our experience suggests, for example, that computed epicenters in the Wasatch Plateau coal field tend to lie a few kilometers westward of their true locations.

A first-order feature of the annual epicenter maps, at their plotted regional scale, is the spatial clustering of seismicity in known areas of active mining. In general, one observes tighter clustering in the Wasatch Plateau coal field than in the Book Cliffs field, due in part to better epicentral control. In the Sunnyside area of the eastern Book Cliffs, an area marginal to the seismic network, there is an apparent scattering of epicenters in an ENE-WSW direction (see Figures 3-6 and 3-7) due to inadequate azimuthal station control. Higher rates of seismic activity in the Wasatch Plateau coal field during the sample period generally reflect higher extraction rates compared to the Book Cliffs coal field (see, for example, Appendix B).

Inspecting the series of annual epicenter maps from 1992 to 2000 (Figures 3-6 through 3-16), one can observe distinct clusters of seismic events in the vicinity of mines known to be active at the time. Temporal variations in the observed seismic clustering correlate in some cases with the start or completion of mining; in other cases, where extraction was relatively continuous over several years, seismic clustering has occurred in distinct episodes. We proceed to examine such changes with time.

3.32 Temporal Association

Arabasz et al. (1997) cross-correlated time series of observed seismicity with tons of extracted coal, on a quarterly basis from 1978 through 1994, for nine local areas in the WP-BC region. Seismicity was measured both in terms of counts of seismic events above a threshold magnitude and seismic energy release. In order to gain an updated view, we did the following.

First, we extended our database for quarterly coal mine production in the WP-BC region with tabulations for 1995 through 1998, the last year for which data were available. These data, which give a representative view of contemporary mining activity in the study area, were compiled by J. D. McKenzie and are presented in Appendix B.

Second, we plotted all seismic events in our revised catalog above magnitude 1.8 for the period January 1992-June 2000. The resulting map, shown in Figure 3-15 allowed twelve areas of clustered seismicity to be isolated for special analysis, following the approach of Arabasz et al. (1997). Index data for these twelve sample areas are summarized in Table 3-4.

Third, for each sample area and for the period January 1992-June 2000, we constructed composite time-series plots that show: (a) reported quarterly coal production within the sample area, (b) quarterly counts of seismic events above a magnitude threshold of uniform detection, and (c) magnitude versus time of occurrence. For (b) and (c), a magnitude threshold of 1.75 was generally adopted, except for areas 1, 8, 11, and 12 where a threshold of 1.85 was used.

The resulting composite plots for the twelve sample areas are shown in Figures 3-16 through 3-21 (note changes in the vertical scales from plot to plot). Referring to the plots sequentially, we make these observations:

- S. Wasatch Plateau area (Figure 3-16): Production throughout the sample period was from longwall mining. Annual tonnage progressively increased with time, but seismicity was variable with some notably quiet periods—longer than a few weeks duration typical of a longwall move—that are not due to gaps in seismic recording.

- S. Joes Valley area (Figure 3-16): Tonnage and seismicity both increased after late 1995 with the beginning of a longwall operation, and the seismicity rate later increased significantly in late 1998. Prior to 1995, minor production was from room-and-pillar mining.

- East Mountain and Rilda Canyon areas (Figure 3-17): These two plots are complicated by the fact that extraction attributed to one particular mine occurred in both areas, and the partition of tonnage to each area is unclear. Thus, while we can spatially distinguish two separate clusters of seismicity in map view (Figure 3-15), we have incomplete information for reliably characterizing the time series for quarterly tonnage in each area. One of two longwalls operating in the East Mountain area ended production in late 1995, which corresponds to the timing of a marked decrease in seismicity in that area. In the plot for the Rilda Canyon area, observed seismicity increases significantly in early 1995 but does not persist continuously thereafter.

- Lower Huntington Canyon area (Figure 3-18): Relatively low production in this area came from room-and-pillar mining. Most of the observed seismicity notably occurred in two episodes, one during 1995 and the other during 1999-2000.

- Upper Huntington Canyon area (Figure 3-18): Coal production progressively increased in this area. There was a change from room-and-pillar to longwall mining about 1996, but there is no evident contrast in the observed seismicity before and after this date.

- Gentry Mountain area (Figure 3-19): The cessation of a longwall operation in 1997 was accompanied by a marked decrease in seismicity, providing a good correlation between extraction and seismicity in this area.

- Pleasant Valley area (Figure 3-19): Seismicity in this area is predominantly related to longwall mining that occurred throughout the entire sample period at relatively high levels of production. The marked decrease in observed seismicity after mid-1996, despite continued coal production, emphasizes that seismic energy release depends not only on rate of extraction but also on other mine-specific variables, including local geology and depth of cover.

- Castle Gate area (Figure 3-20): Sparse but relatively continuous seismicity occurred in this area between 1992 and 1997 while mines in this area were inactive. The start of coal production in 1996 relates to development work in a new mine in which a longwall began operating in mid-1998, but discontinuously thereafter. The two prominent seismic events of magnitude 3.8 in 1998 and 4.2 in 2000 are discussed in sections 4.22 and 4.21, respectively.

- W. Book Cliffs area (Figure 3-20): Both coal production and seismicity in this area—as generally true for mining areas in the Book Cliffs—are lower than for counterpart mining areas in the Wasatch Plateau. A change from room-and-pillar mining to longwall mining in mid-1994 is reflected by a step increase in the tonnage plot. The seismicity plots show at least one episode of increased seismicity in 1998-1999.

- Central Book Cliffs area (Figure (3-21): Relatively low levels of coal production in this area were from room-and-pillar mining. Production ceased after 1998. Perhaps the most notable aspect of the observed seismicity was the occurrence of two distinct episodes of seismic energy release, one in 1992-1993 and another in 1996-1997, each including a seismic event in the magnitude 3 range.

- E. Book Cliffs area (Figure 3-21): Longwall mining in this area ceased in early 1994, as reflected in the tonnage graph. In 1995-1996, a distinct episode of seismic events occurred after the mine had closed.

3.4 GROUND TRUTH FOR SIGNIFICANT EVENTS

Part of Objective 3 for this study was to gather and report available information on "ground truth"—what actually happened in or near a mine at the time of a discrete event that produced observable seismic signals—for significant mining-related seismic events. In section 1.1 we described guidance from LLNL's Technical Representative for this contract, William Walter, which indicated special interest in three particular mining-related events—two in the WP-BC coal-mining region in February 1998 and March 2000, respectively, and one in the trona-mining region of southwestern Wyoming in January 2000.

To help acquire and organize the ground-truth information in a systematic way, we engaged the assistance of Dr. Michael K. McCarter, chair of the University of Utah's Department of Mining Engineering. Information was successfully gathered for the three events of special interest as well as for five other events. The total of eight events includes seven events ($3.1 \leq M_L \leq 4.2$) related to underground coal mining in the WP-BC area between 1981 and 2000 and the January 2000 trona-mining-related event ($M_L = 4.3$) in southwestern Wyoming. The WP-BC data include information for the four largest seismic events listed in Table 3-3 plus three other events for which information was recoverable.

We refer the reader to Appendix C for a listing (Table C-1) of the seismic events for which ground-truth information was compiled and for data sheets that document the observations.

Table 3-1

Correction Terms Used by Arabasz et al. (1997) for Revised Coda Magnitudes, M_C', in the Wasatch Plateau-Book Cliffs Area

Time Period	Equation	
1978 01/01 – 1978 07/31	$M_C' = M_C + 0.25$	(1)
1978 08/01 – 1987 10/31	$M_C' = M_C$	(2)
1987 11/01 – 1992 06/14	$M_C' = 0.90\ M_C - 0.09$	(3)
1992 06/15 – 1996 03/31	$M_C' = 0.747\ M_C + 0.207$	(4)

Table 3-2

Correction Terms Used in This Report, Following Arabasz and Wyss (1999), for Revised Coda Magnitudes, M_C', in the Wasatch Plateau-Book Cliffs Area

Time Period	Equation	
1978 01/01 – 1978 07/31	$M_C' = (M_C + 0.25) - 0.10$	(5)
1978 08/01 – 1987 10/31	$M_C' = M_C - 0.10$	(6)
1987 11/01 – 1992 06/14	$M_C' = (0.90\ M_C - 0.09) - 0.10$	(7)
1992 06/15 – 1994 12/31	$M_C' = (0.747\ M_C + 0.207) - 0.10$	(8)
1995 01/01 – 2000 06/30	$M_C' = 0.747\ M_C + 0.207$	(9)

Table 3-3

Seismic Events of Magnitude 3.0 or Greater in the WP-BC Coal-Mining Area, January 1978-June 2000, Ranked by Size

ID	Yr	Mo/Da (UTC)	Hr:Min (UTC)	Lat N	Long W	Depth* (km)	Mag.**	Closest Active Mine
1	2000	03/07	02:16	39-44.95	110-50.19	1.8	ML 4.2	Willow Creek
2	1981	05/14	05:11	39-28.86	111-04.72	0.7	ML' 3.8	King #4
3	1998	02/05	05:19	39-45.05	110-50.73	1.3	ML 3.8	Willow Creek
4	1992	07/05	12:22	39-18.81	111-09.60	5.6	ML' 3.5	Cottonwood
5	1981	09/21	08:01	39-35.48	110-25.47	1.6	ML' 3.4	Sunnyside #3
6	1981	09/22	05:03	39-35.35	110.23.61	7.5	ML' 3.3	Sunnyside #3
7	1987	12/16	17:43	39-18.70	111-12.92	0.5	ML' 3.3	Trail Mountain
8	1992	06/03	05:08	39-19.04	111-09.80	0.7	ML' 3.2	Cottonwood
9	1991	02/06	13:46	39-29.99	111-04.61	4.3	ML' 3.1	Star Point #2
10	1996	10/25	18:32	39-42.12	110.39.24	3.3	ML 3.1	Soldier Canyon
11	1986	02/14	00:56	39-41.18	110.31.50	0.2	ML' 3.1	Soldier Canyon
12	1991	05/23	07:38	39-17.89	111-08.92	12.4	ML' 3.1	Cottonwood
13	1992	07/11	13:23	39-18.52	111-08.94	3.0	ML' 3.1	Cottonwood
14	1993	01/21	09:01	39-42.73	110-37.26	1.3	ML' 3.1	Soldier Canyon
15	1983	03/22	11:12	39-32.78	110-25.32	1.7	ML' 3.0	Sunnyside #3
16	1984	03/21	11:19	39-20.64	111-06.53	0.1	ML' 3.0	Deer Creek
17	1996	06/02	08:09	39-37.55	111-14.45	5.5	ML 3.0	(Skyline #3)***
18	1986	10/30	00:05	39-44.11	110-57.93	5.6	ML' 3.0	Castle Gate #3

* Unreliable
** ML' is a weighted-average estimate of local magnitude, ML (see Arabasz et al., 1997, and section 3.21 here)
*** Tectonic earthquake located 7 km south of Skyline Mine (see section 4.23)

Table 3-4

Information for Sample Areas in Figure 3-15 Used to Investigate the Association of Seismicity with Mining in the WP-BC Area During the Period 1992-2000

Area	Coordinates of Center (degrees–minutes)		Radius (km)	Mines Reporting Coal Production During Sample Period
1. S. Wasatch Plateau	38–58.0	111–22.0	6.0	Sufco
2. S. Joes Valley	39–17.5	111–13.5	4.0	Trail Mountain
3. East Mountain	39–19.0	111–08.5	4.0	Deer Creek; Cottonwood
4. Rilda Canyon	39–23.0	111–10.0	3.5	Deer Creek
5. Lower Huntington Canyon	39–24.5	111–06.0	3.5	Bear Canyon #1, #2
6. Upper Huntington Canyon	39–28.0	111–13.0	4.0	Crandall Canyon
7. Gentry Mountain	39–30.0	111–07.0	5.0	Starpoint #2; King #4, #6
8. Pleasant Valley	39–41.5	111–14.5	6.0	Skyline #1, #3; White Oak #1, #2 (formerly Belina #1, #2)
9. Castle Gate	39–45.0	110–50.5	5.0	Willow Creek
10. W. Book Cliffs	39–42.5	110–44.0	4.0	Aberdeen; Apex; Pinnacle
11. Central Book Cliffs	39–42.0	110–38.0	4.0	Soldier Canyon
12. E. Book Cliffs	39–34.5	110–24.0	9.0	Sunnyside #1

University of Utah Regional Seismic Network

July 2000

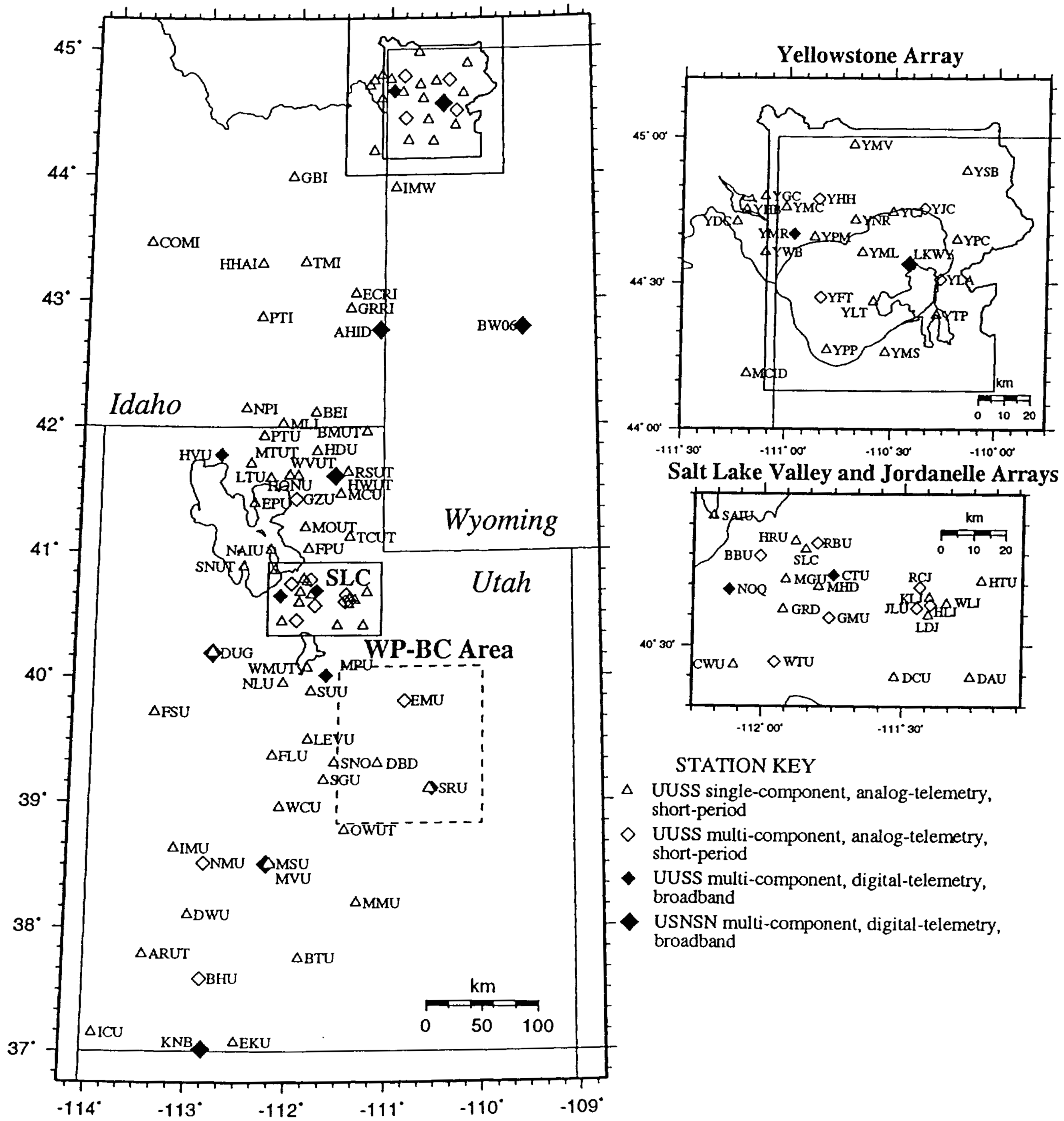

Figure 3-1. Location map of seismograph stations (symbols with letter codes) making up the University of Utah regional seismic network, July 2000. The network extends from Yellowstone National Park to southern Utah. Seismic data from each station are transmitted continuously by radio, telephone, and/or microwave to Salt Lake City (SLC) for central recording on the University of Utah campus. WP-BC study area outlined by dashed rectangle.

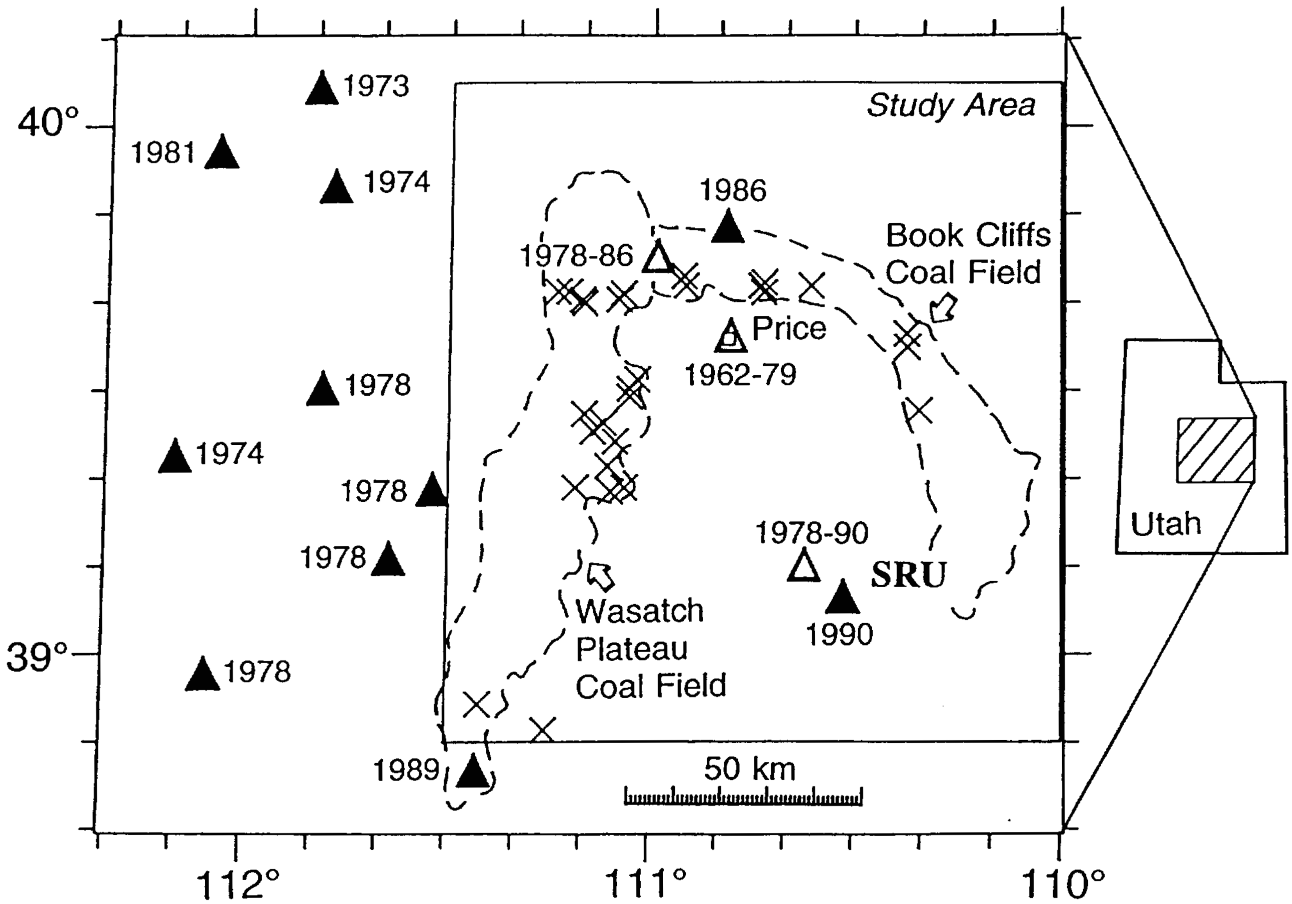

Figure 3-2. Map showing the location of the Wasatch Plateau-Book Cliffs study area (inset rectangle) with respect to the distribution of stations in the University of Utah regional seismic network in 1994 (from Arabasz et al., 1997). X's = sites of 32 underground coal mines active during the 1978-1994 period. Triangles = sites of seismographs (filled triangles = stations operating in 1994, with start date indicated; open triangles, inactive stations,with start and end dates shown). The filled triangle labeled SRU is the site of the new broadband digital telemetry station cooperatively funded and installed as part of this project.

Existing and Planned Seismograph Stations in the WP-BC Area, July 2000

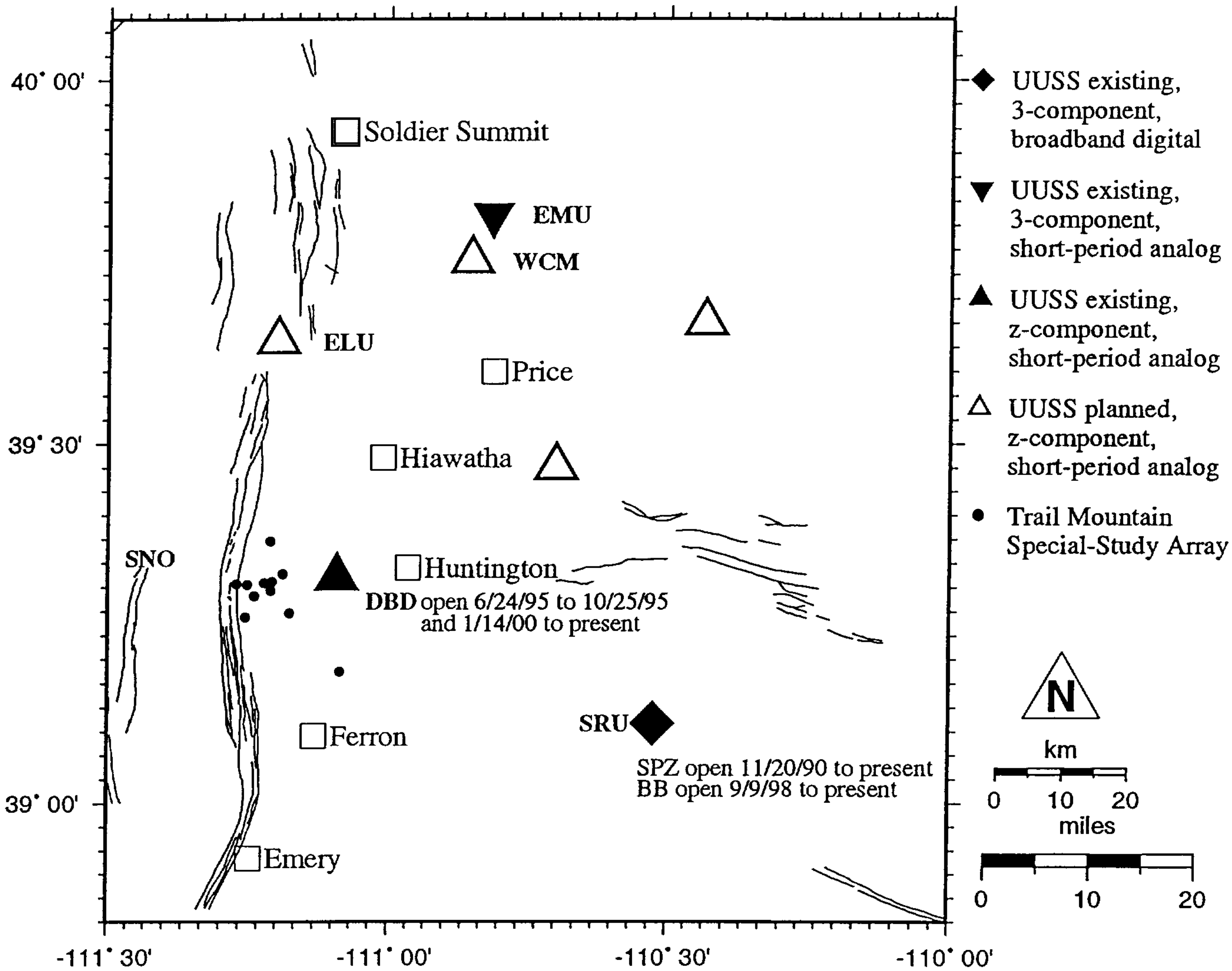

Figure 3-3. Map of Wasatch Plateau-Book Cliffs study area showing existing and planned seismograph stations, July 2000, for comparison with earlier instrumental coverage shown in Figure 3-2.

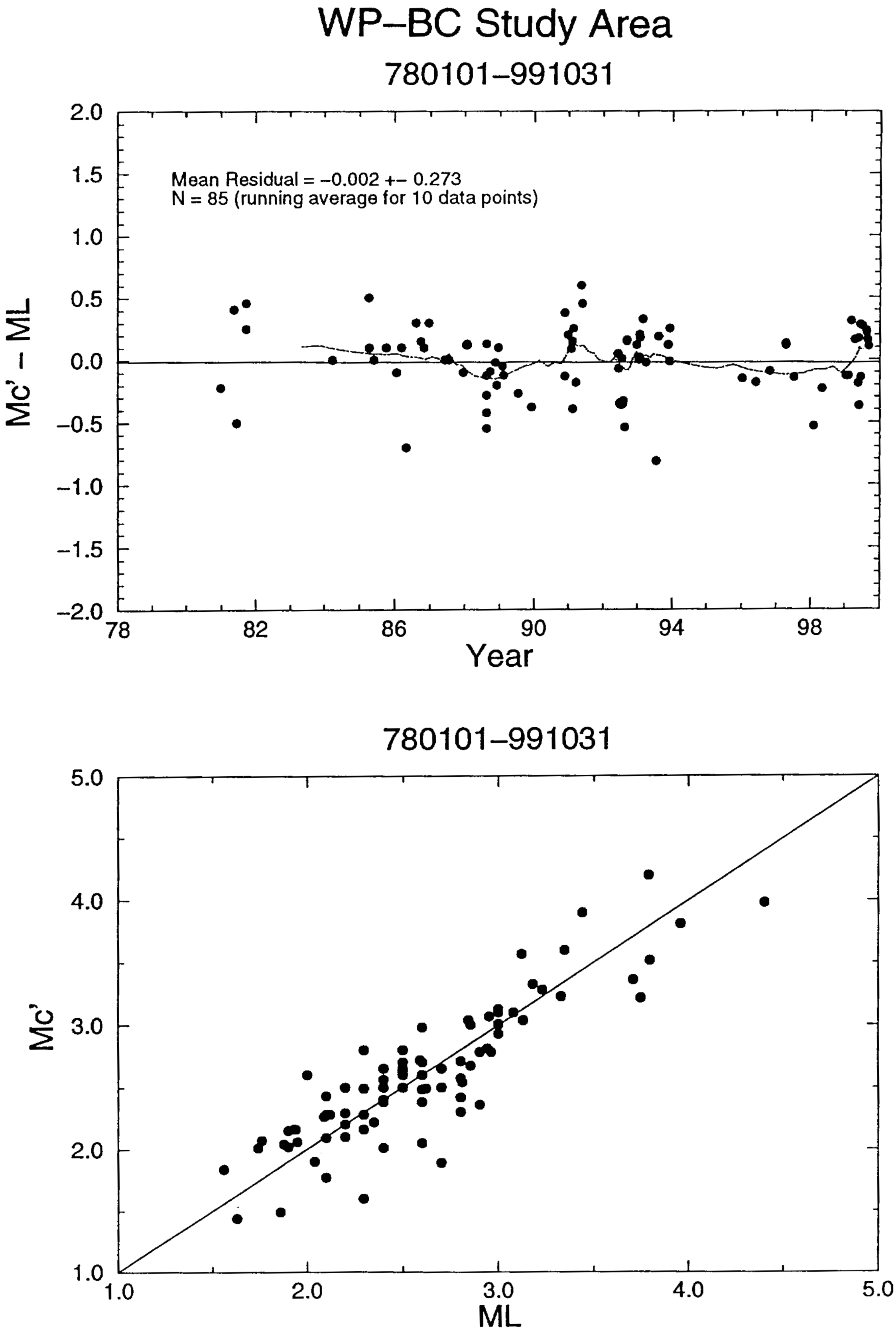

Figure 3-4. Plots comparing values of corrected coda-duration magnitude (M_C') to measured values of local Richter magnitude, M_L. (Above) Difference between M_C' and M_L as a function of time for 85 seismic events in the WP-BC study area. (Below) M_C' versus M_L for the same data. Sloping line indicates locus of perfect agreement.

Mining-Related Seismicity in the WP-BC Coal Mining Region Jan 1978 - Jun 2000

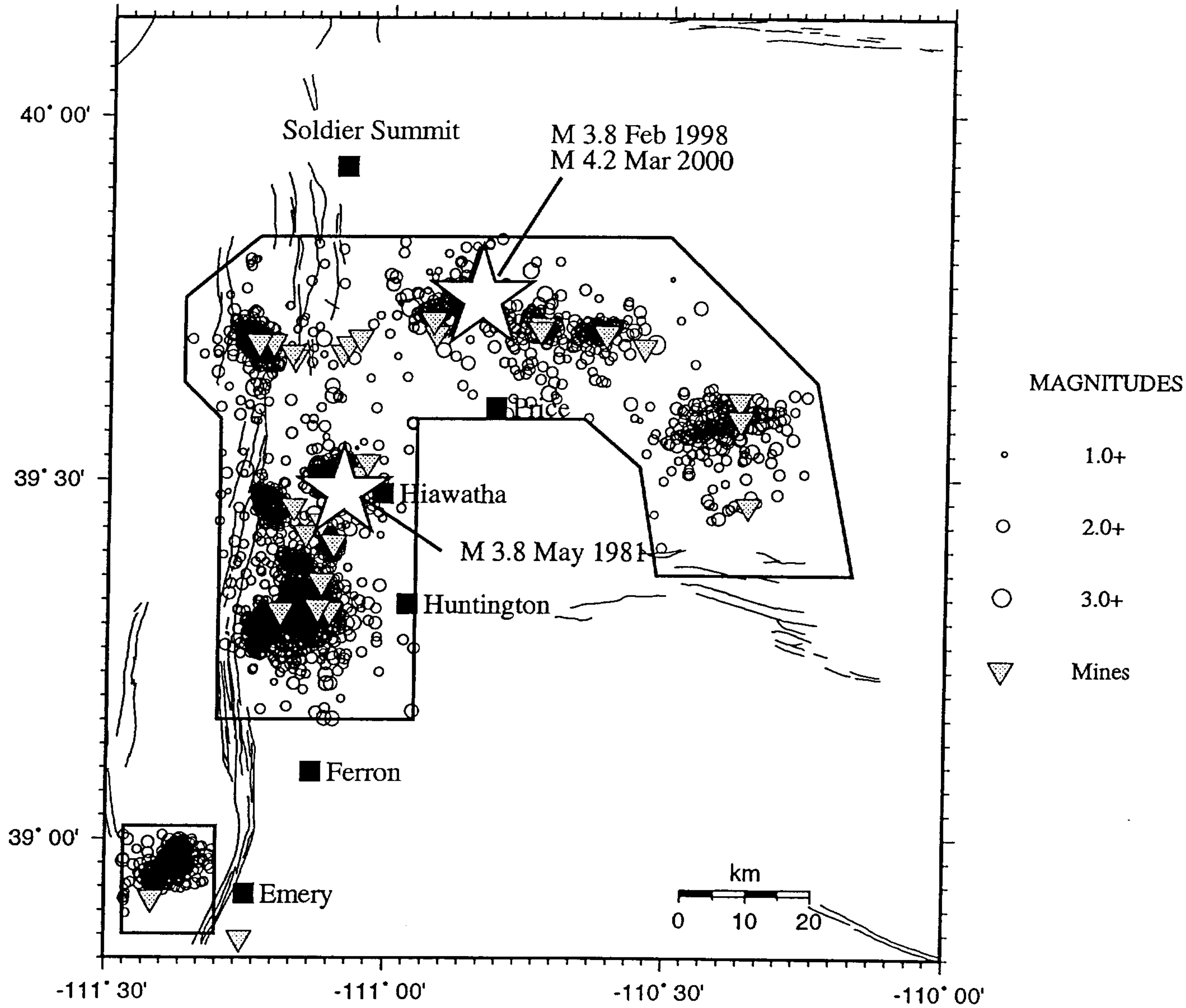

Figure 3-5. Epicenter map of all seismic events located by the University of Utah regional seismic network in the WP-BC coal mining region from January 1, 1978, through June 30, 2000. Polygons (after Arabasz et al., 1997) circumscribe areas within which nearly all seismicity is inferred to be mining-related. Stars (labeled) indicate the three largest mining-related seismic events in this area instrumentally recorded since 1962. Geologically young faults are shown by light lines.

WP-BC Coal Mining Region
Jan 1 - Dec 31, 1992

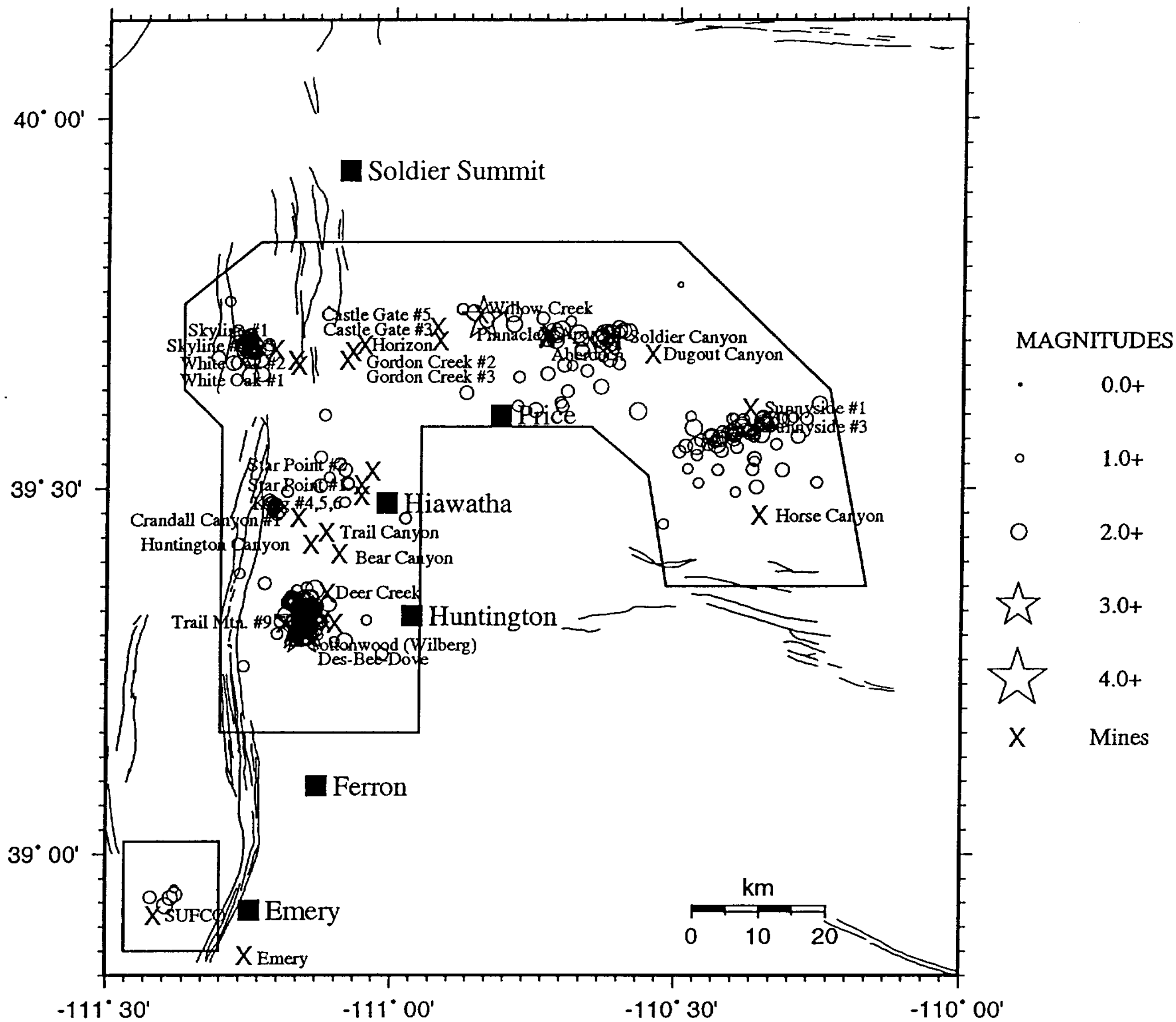

Figure 3-6. Epicenter map of mining-related seismicity in the WP-BC coal mining region for the year 1992. Base map as in Figure 3-5, except that mines are shown by X's and are labeled.

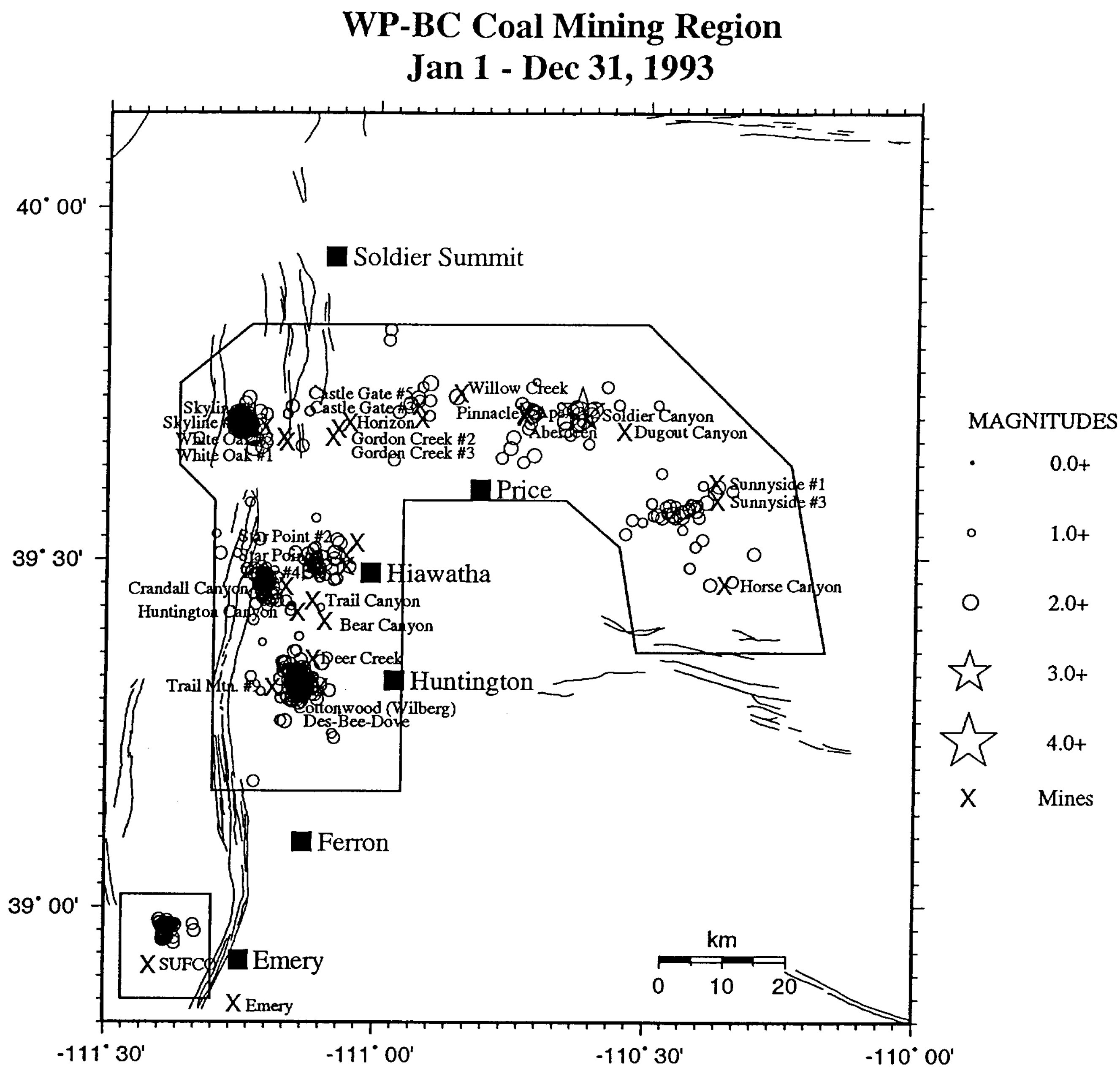

Figure 3-7. Epicenter map of mining-related seismicity in the WP-BC coal mining region for the year 1993. Base map as in Figure 3-5, except that mines are shown by X's and are labeled.

WP-BC Coal Mining Region
Jan 1 - Dec 31, 1994

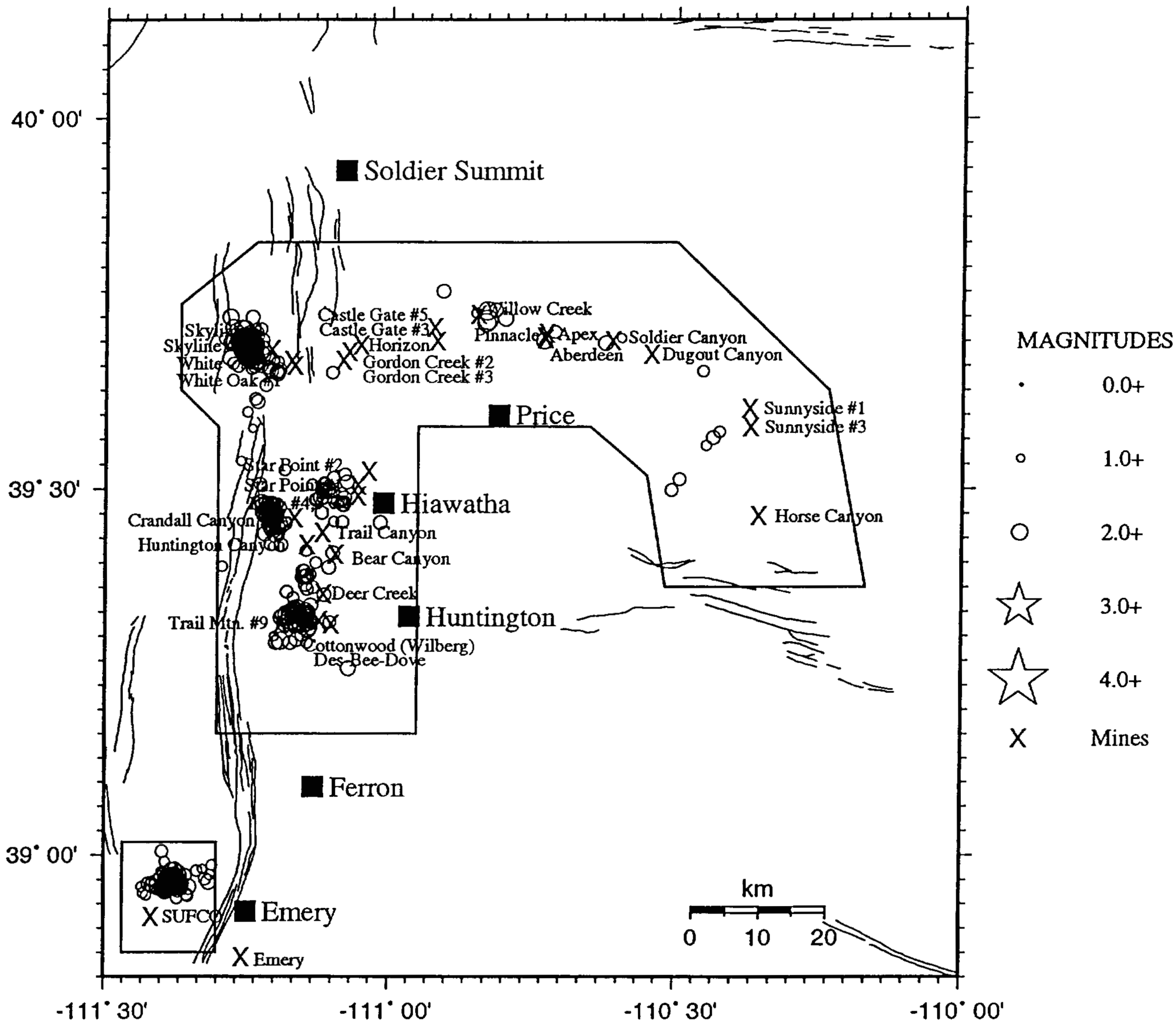

Figure 3-8. Epicenter map of mining-related seismicity in the WP-BC coal mining region for the year 1994. Base map as in Figure 3-5, except that mines are shown by X's and are labeled.

WP-BC Coal Mining Region
Jan 1 - Dec 31, 1995

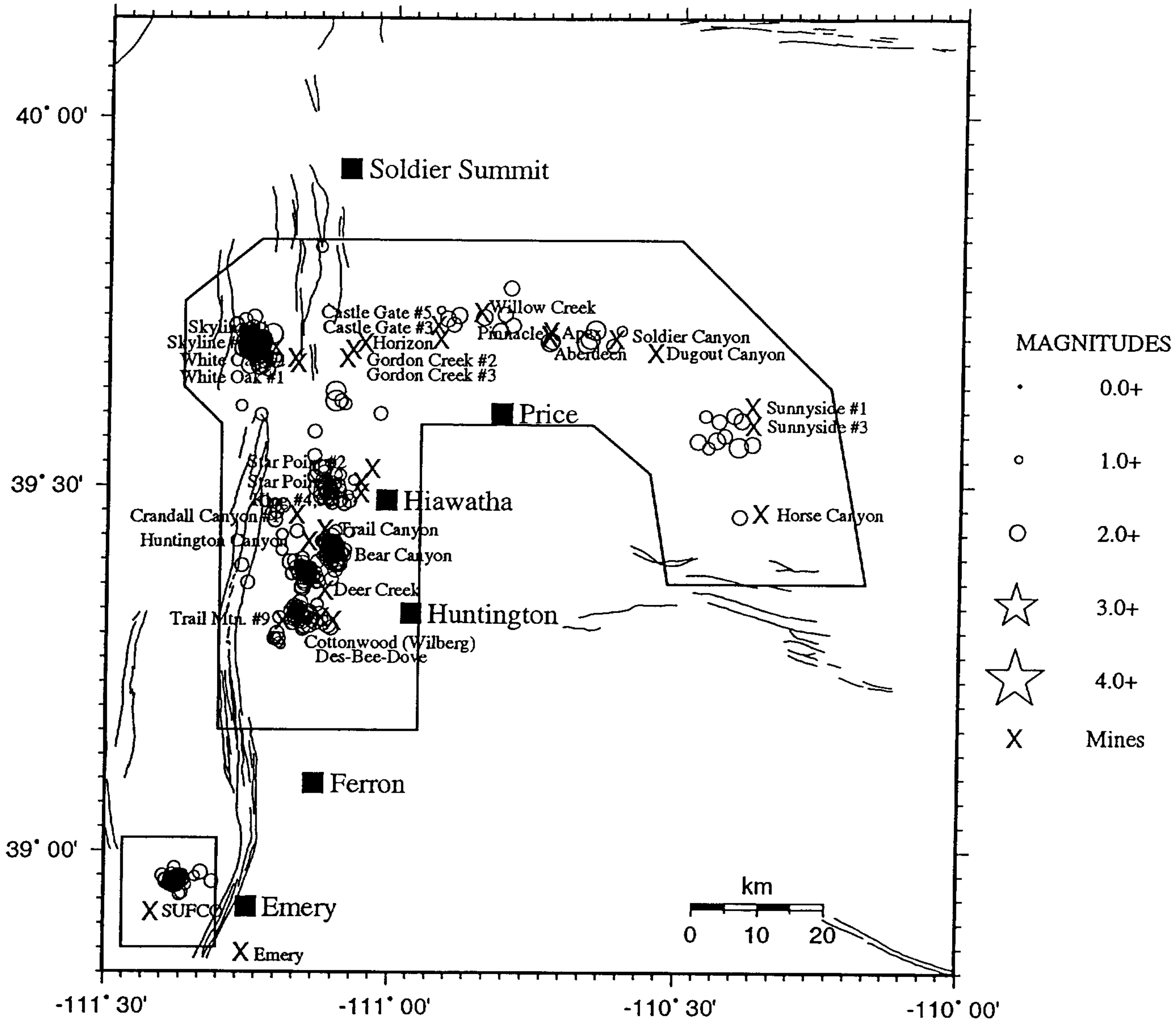

Figure 3-9. Epicenter map of mining-related seismicity in the WP-BC coal mining region for the year 1995. Base map as in Figure 3-5, except that mines are shown by X's and are labeled.

WP-BC Coal Mining Region
Jan 1 - Dec 31, 1996

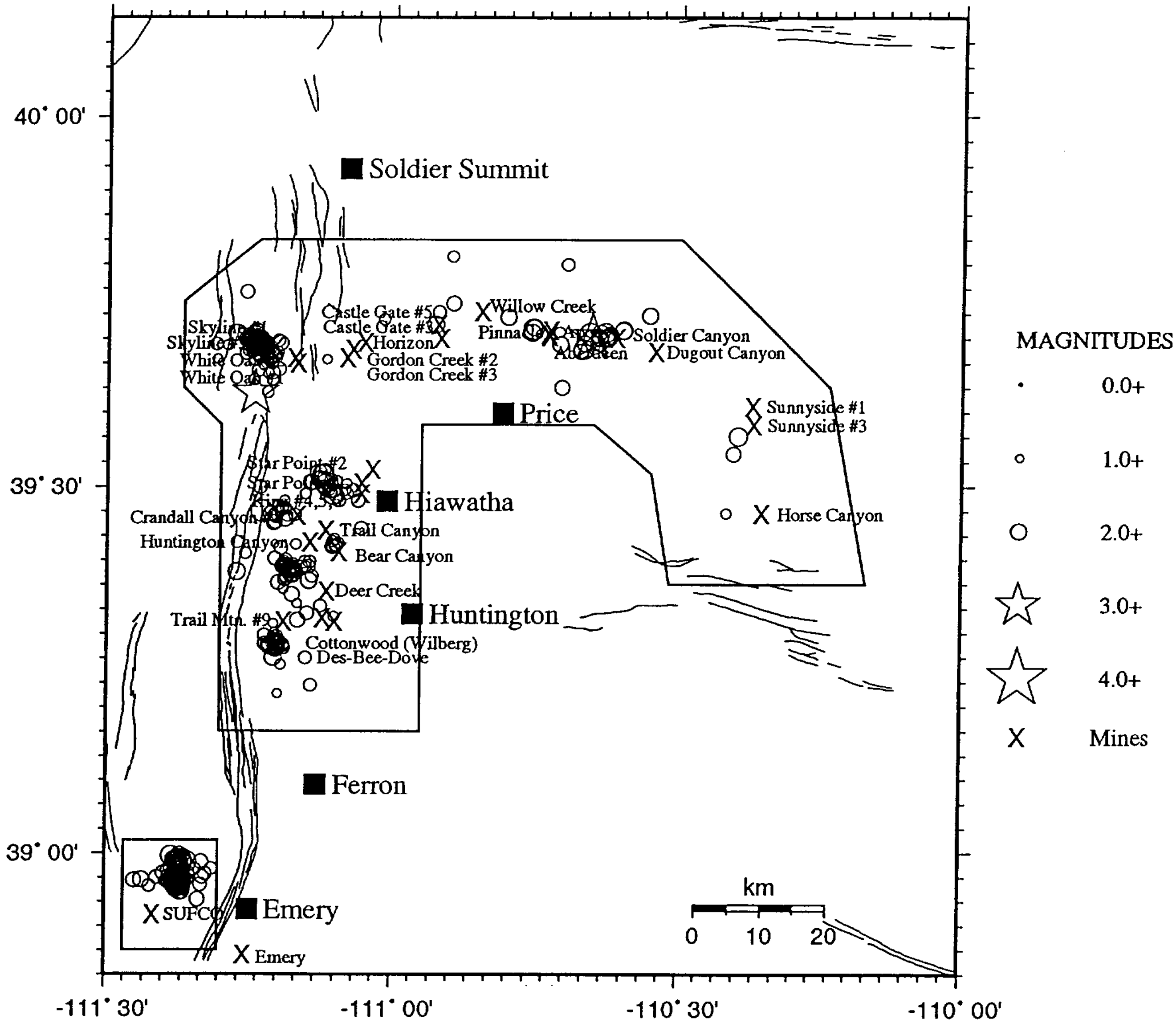

Figure 3-10. Epicenter map of mining-related seismicity in the WP-BC coal mining region for the year 1996. Base map as in Figure 3-5, except that mines are shown by X's and are labeled.

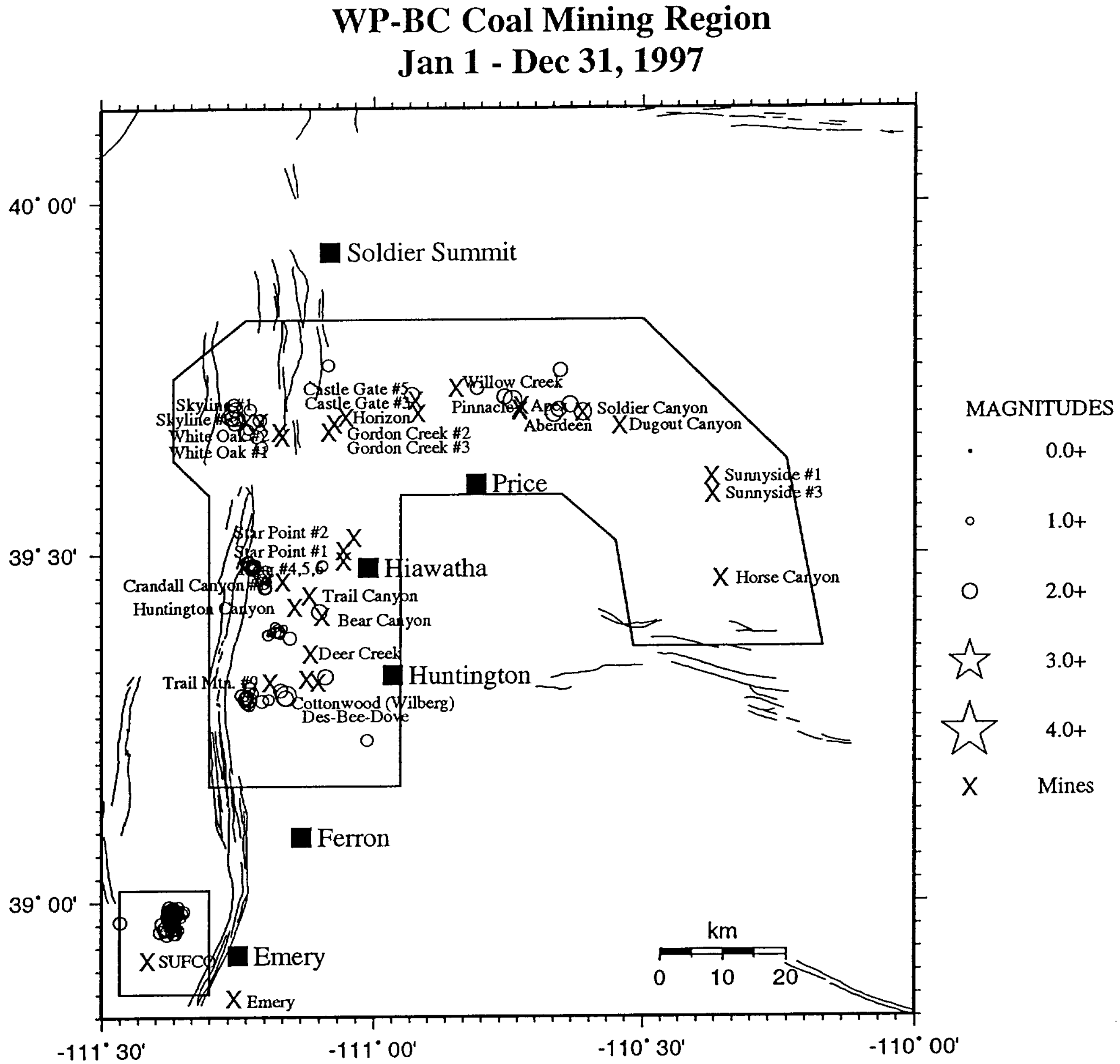

Figure 3-11. Epicenter map of mining-related seismicity in the WP-BC coal mining region for the year 1997. Base map as in Figure 3-5, except that mines are shown by X's and are labeled.

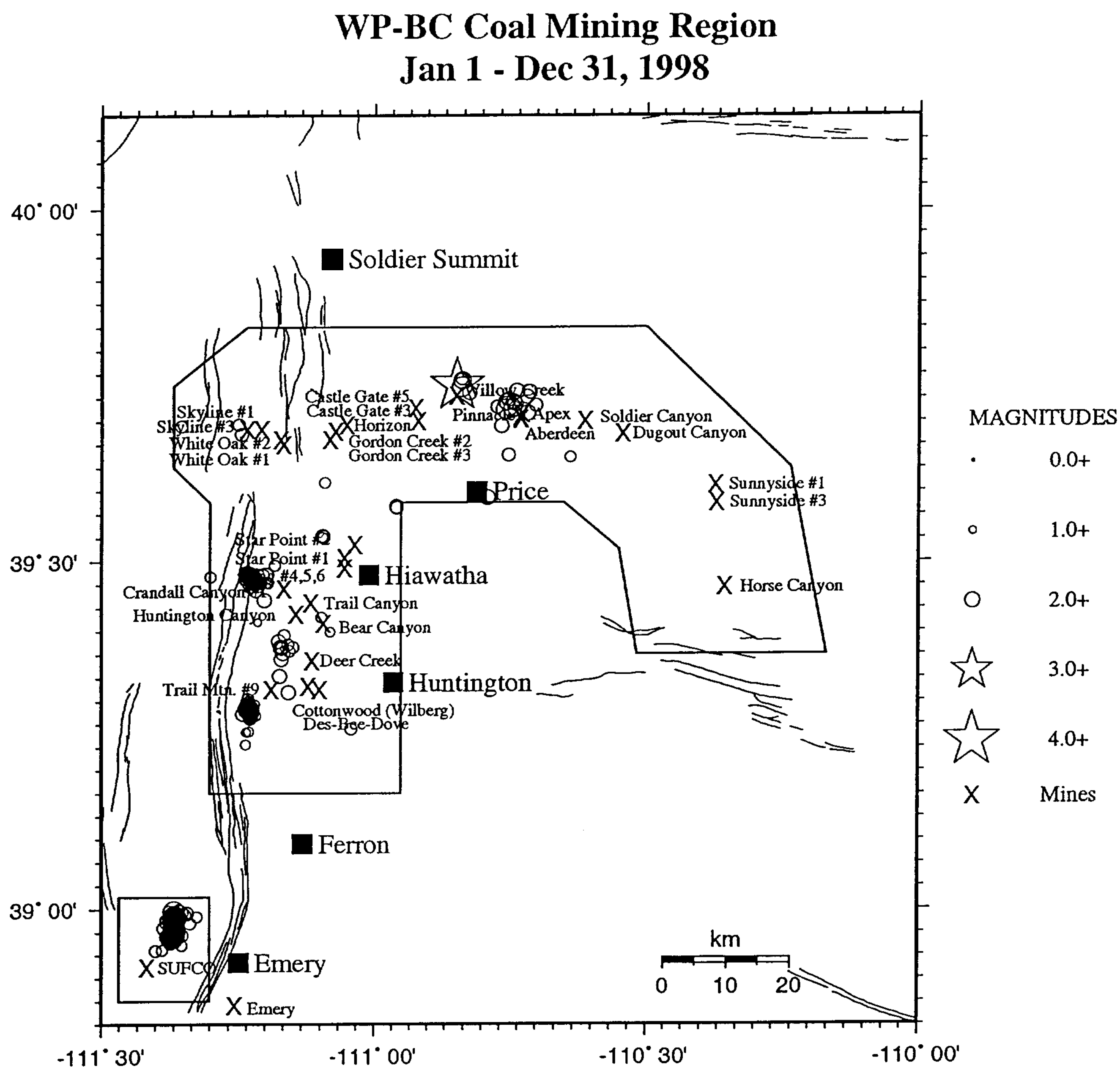

Figure 3-12. Epicenter map of mining-related seismicity in the WP-BC coal mining region for the year 1998. Base map as in Figure 3-5, except that mines are shown by X's and are labeled.

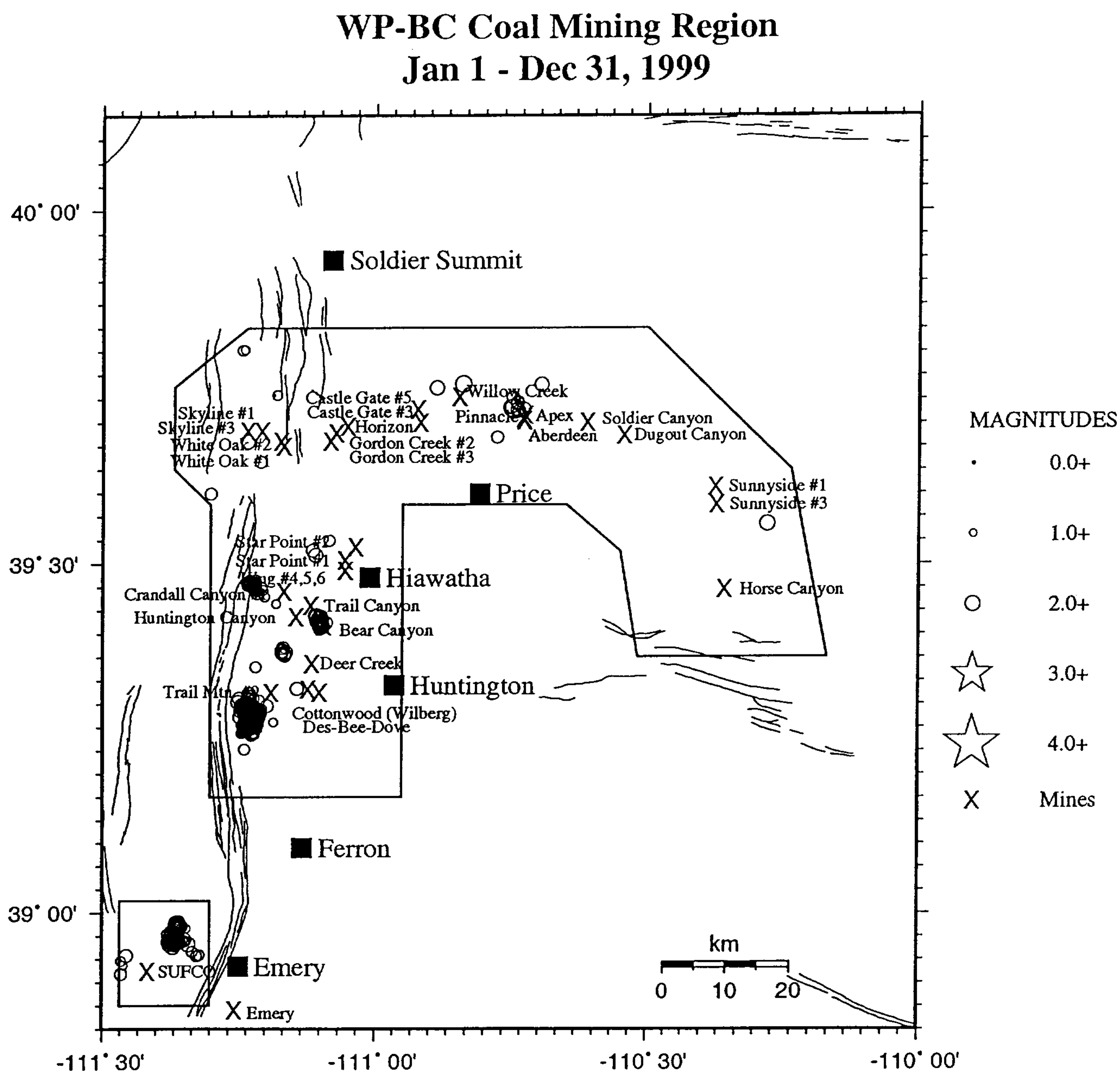

Figure 3-13. Epicenter map of mining-related seismicity in the WP-BC coal mining region for the year 1999. Base map as in Figure 3-5, except that mines are shown by X's and are labeled.

WP-BC Coal Mining Region
Jan 1 - Jun 30, 2000

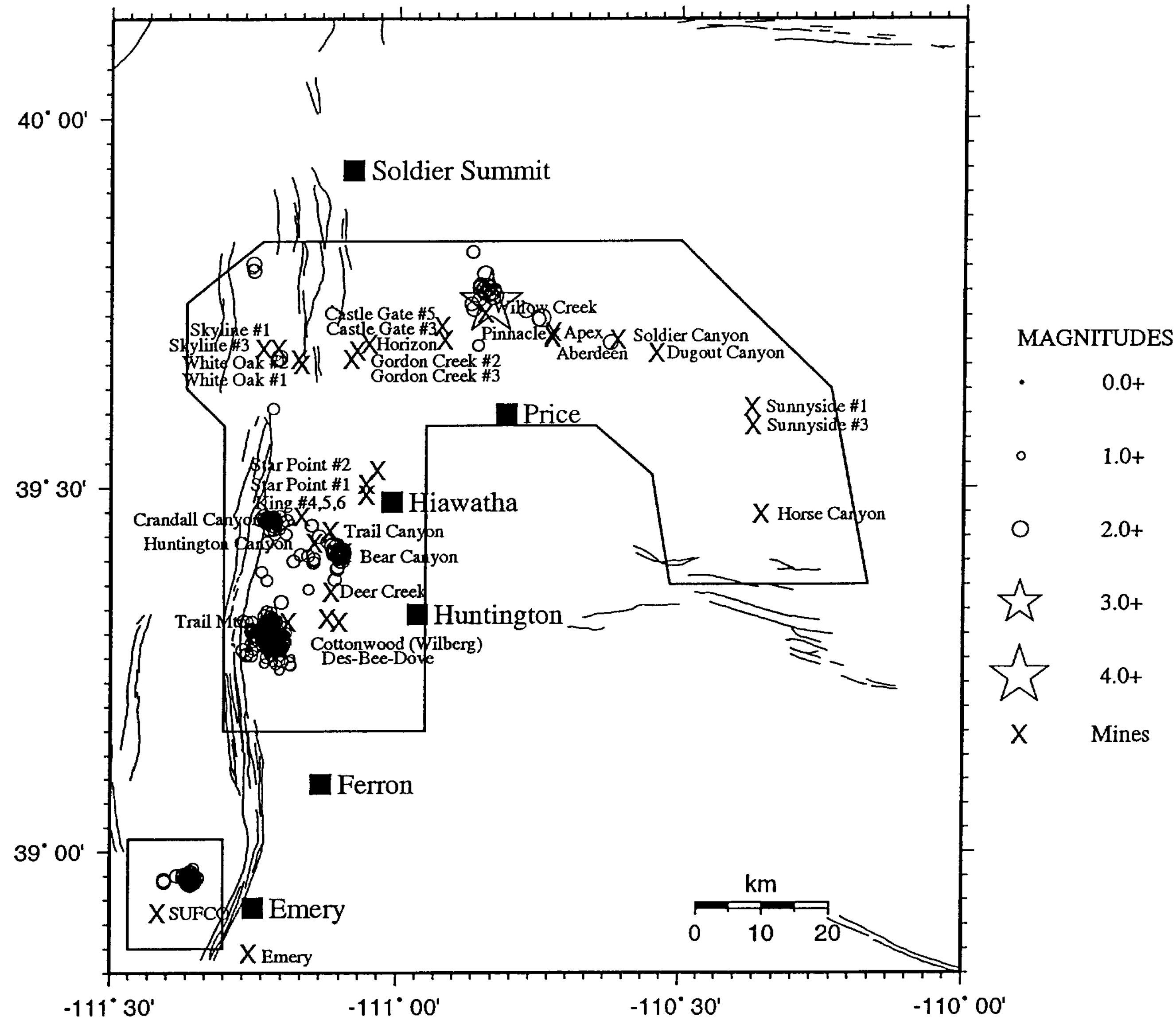

Figure 3-14. Epicenter map of mining-related seismicity in the WP-BC coal mining region for January through June 2000. Base map as in Figure 3-5, except that mines are shown by X's and are labeled.

WP-BC Coal Mining Region
Jan 1, 1992 - Jun 30, 2000

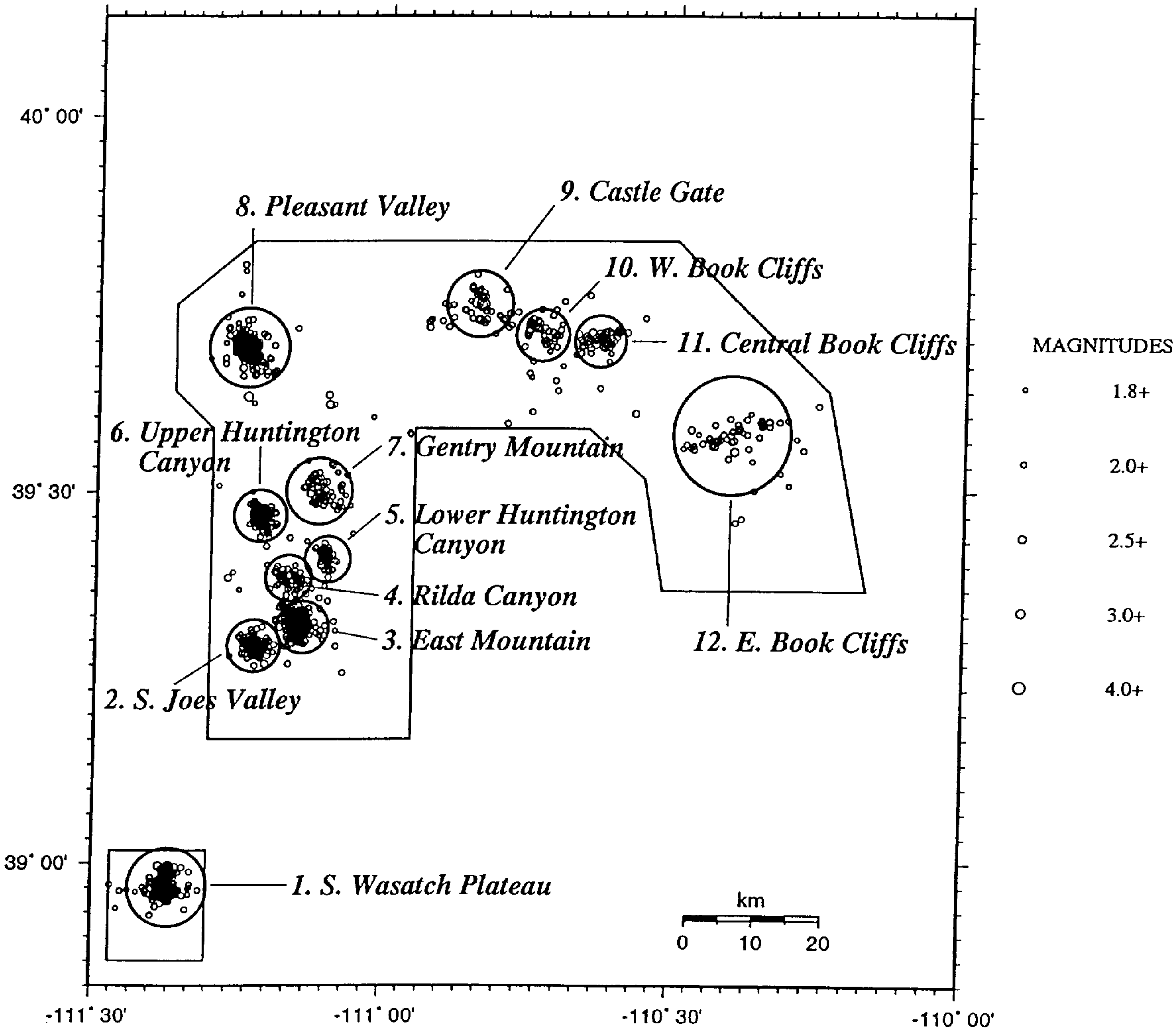

Figure 3-15. Index map, keyed to Table 3-4, outlining areas of concentrated mining-related seismicity (circumscribed by large circles) for which detailed characterizations are shown in Figures 3-16 through 3-21. Plotted seismicity includes events from January 1992 through June 2000 of magnitude 1.8 and greater.

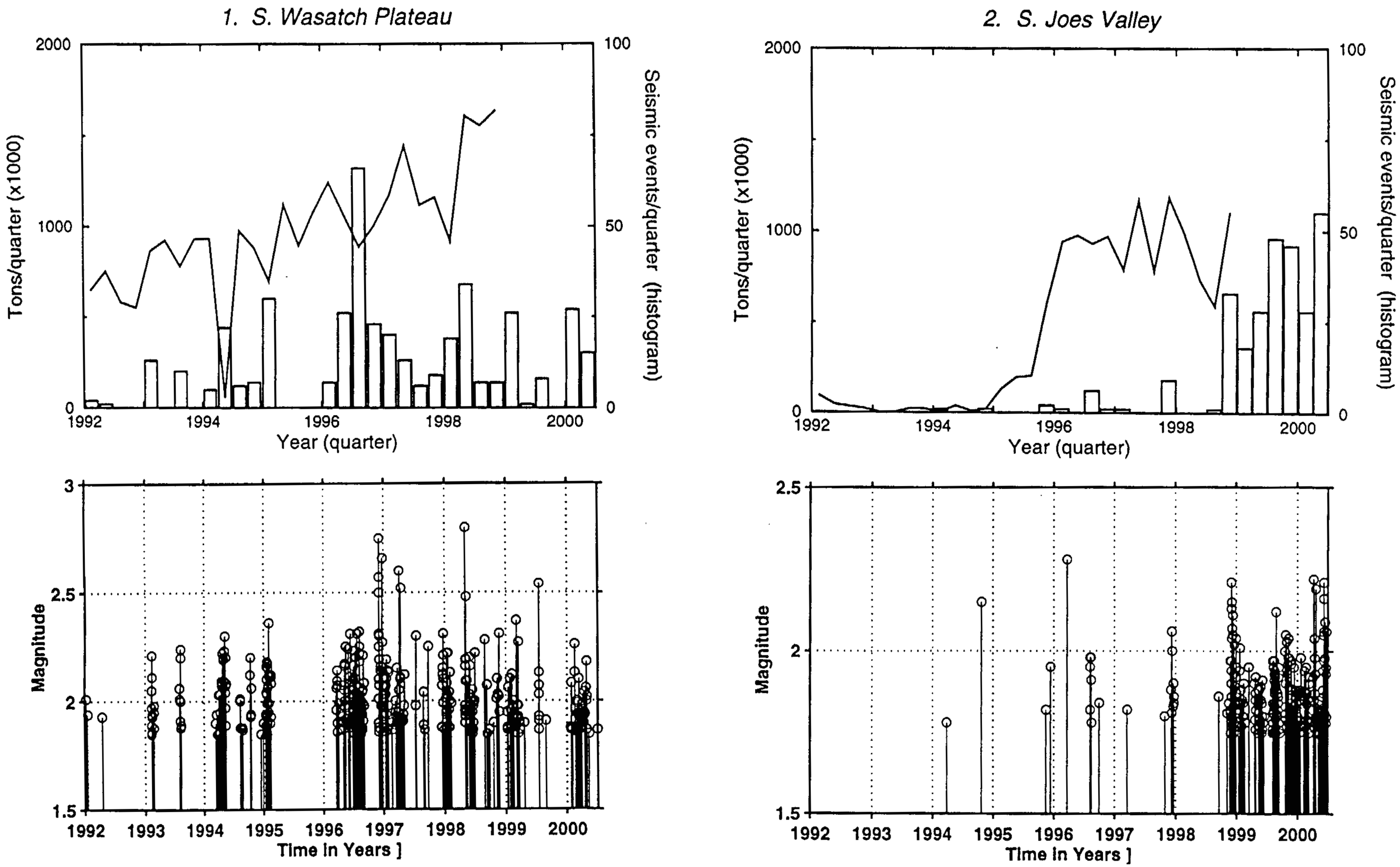

Figure 3-16. Temporal characterization of seismicity and coal production for sample areas identified in Figure 3-15. For each sample area, a composite plot is shown. The upper panel shows a time series of quarterly coal production, in tons, together with a histogram of the number of seismic events per quarter above a threshold magnitude (see text). The lower panel shows a corresponding plot of magnitude versus time. (Coal production data were available through 1998 only.)

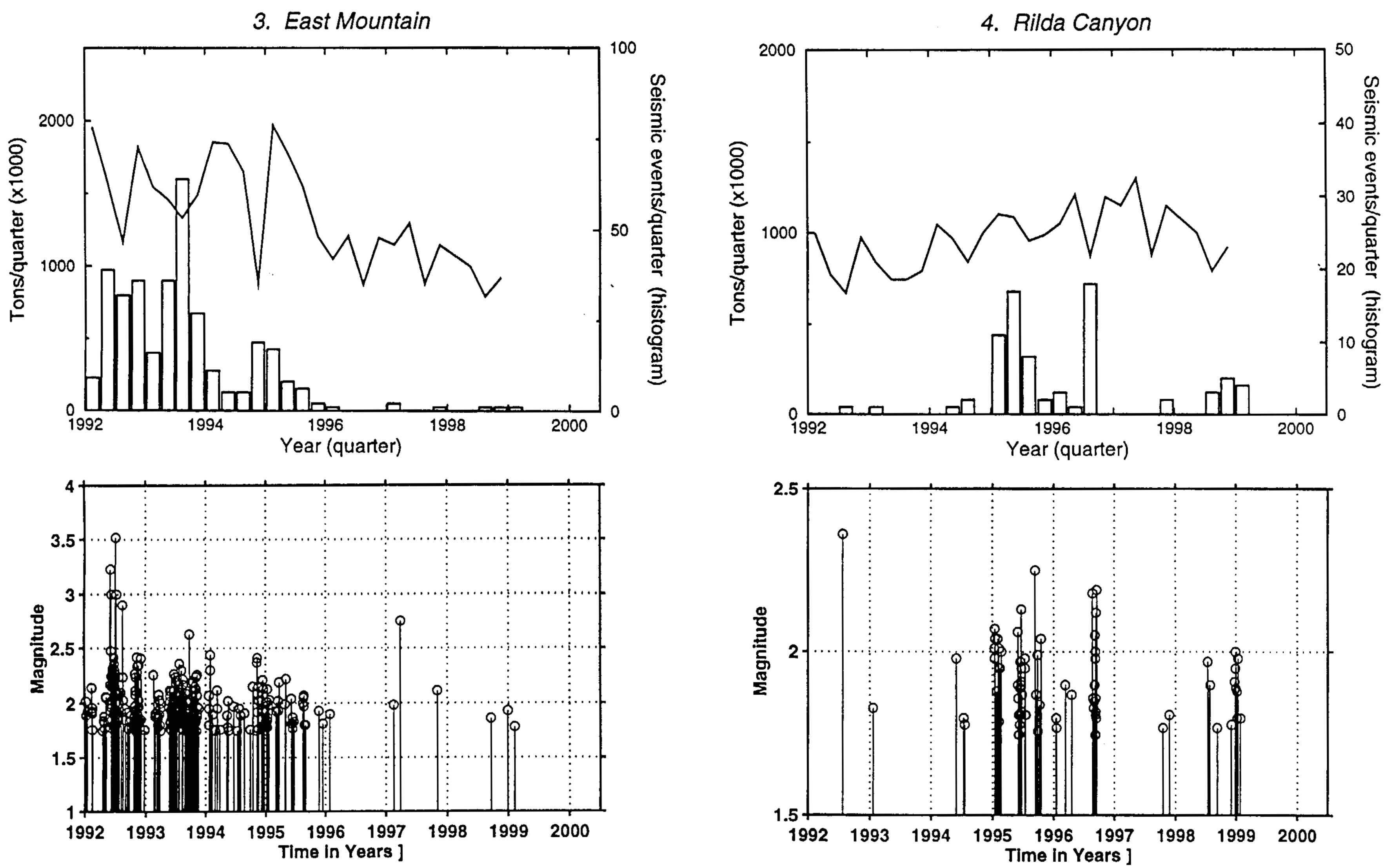

Figure 3-17. Temporal characterization of seismicity and coal production for sample areas identified in Figure 3-15. For each sample area, a composite plot is shown. The upper panel shows a time series of quarterly coal production, in tons, together with a histogram of the number of seismic events per quarter above a threshold magnitude (see text). The lower panel shows a corresponding plot of magnitude versus time. (Coal production data were available through 1998 only.)

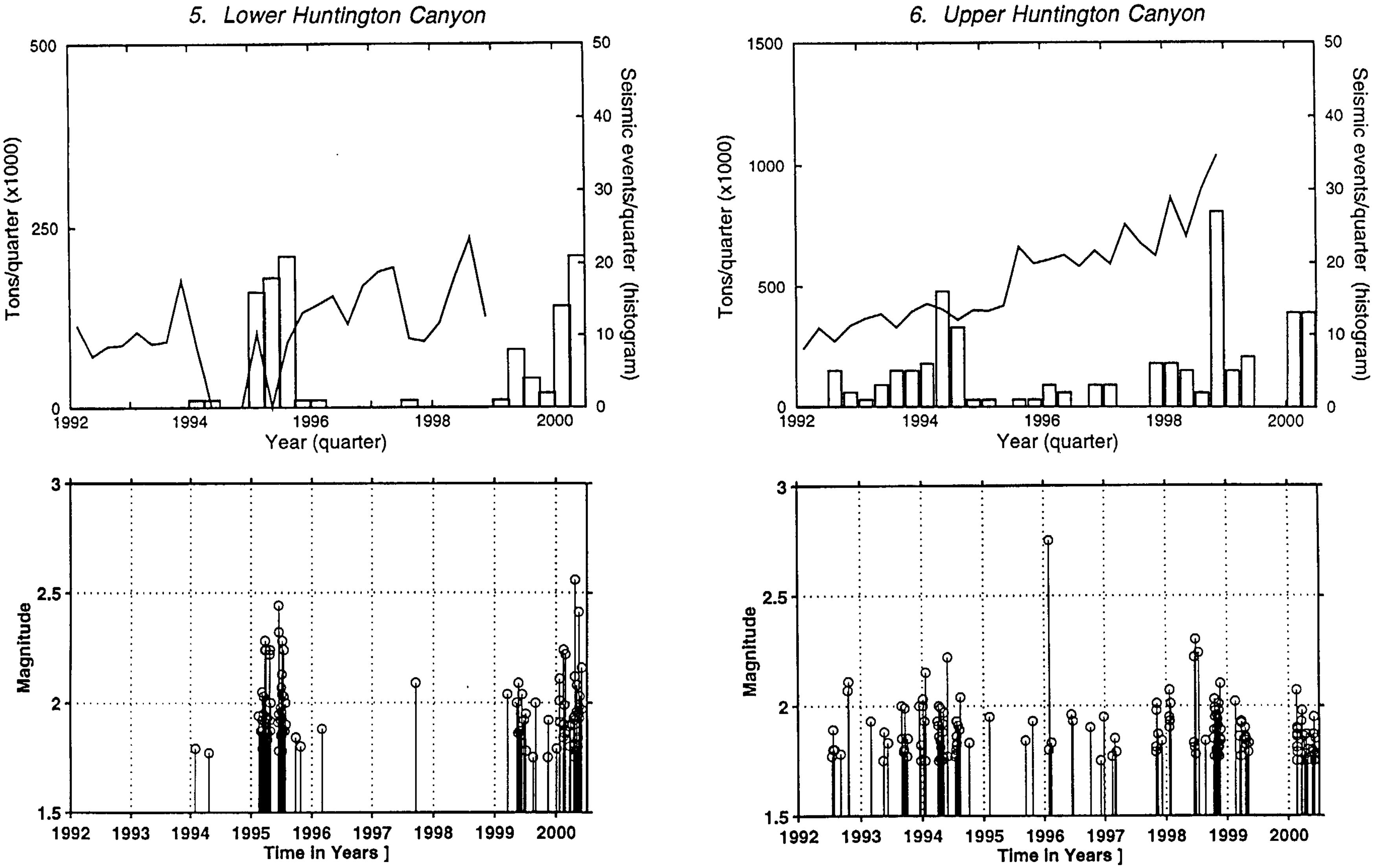

Figure 3-18. Temporal characterization of seismicity and coal production for sample areas identified in Figure 3-15. For each sample area, a composite plot is shown. The upper panel shows a time series of quarterly coal production, in tons, together with a histogram of the number of seismic events per quarter above a threshold magnitude (see text). The lower panel shows a corresponding plot of magnitude versus time. (Coal production data were available through 1998 only.)

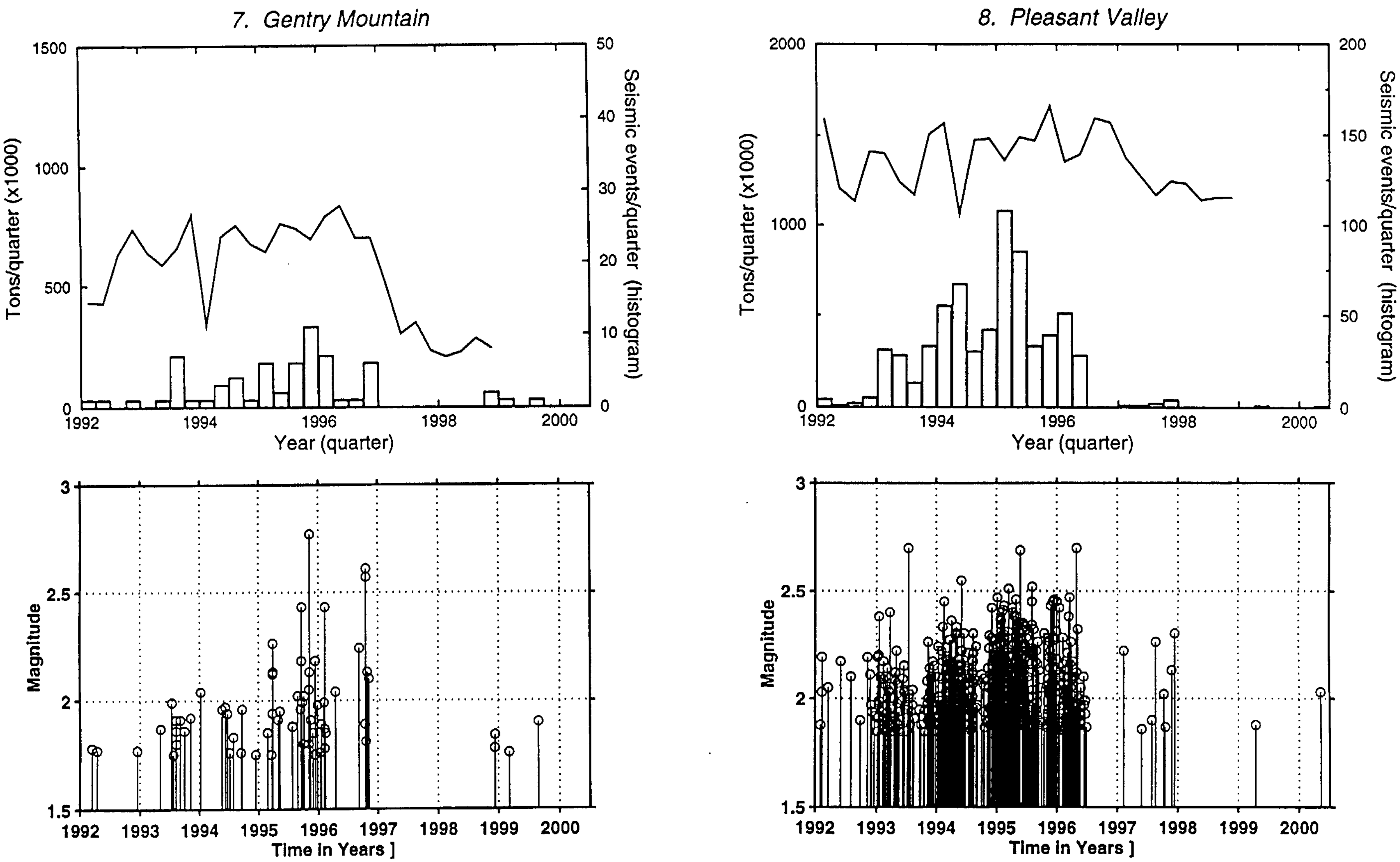

Figure 3-19. Temporal characterization of seismicity and coal production for sample areas identified in Figure 3-15. For each sample area, a composite plot is shown. The upper panel shows a time series of quarterly coal production, in tons, together with a histogram of the number of seismic events per quarter above a threshold magnitude (see text). The lower panel shows a corresponding plot of magnitude versus time. (Coal production data were available through 1998 only.)

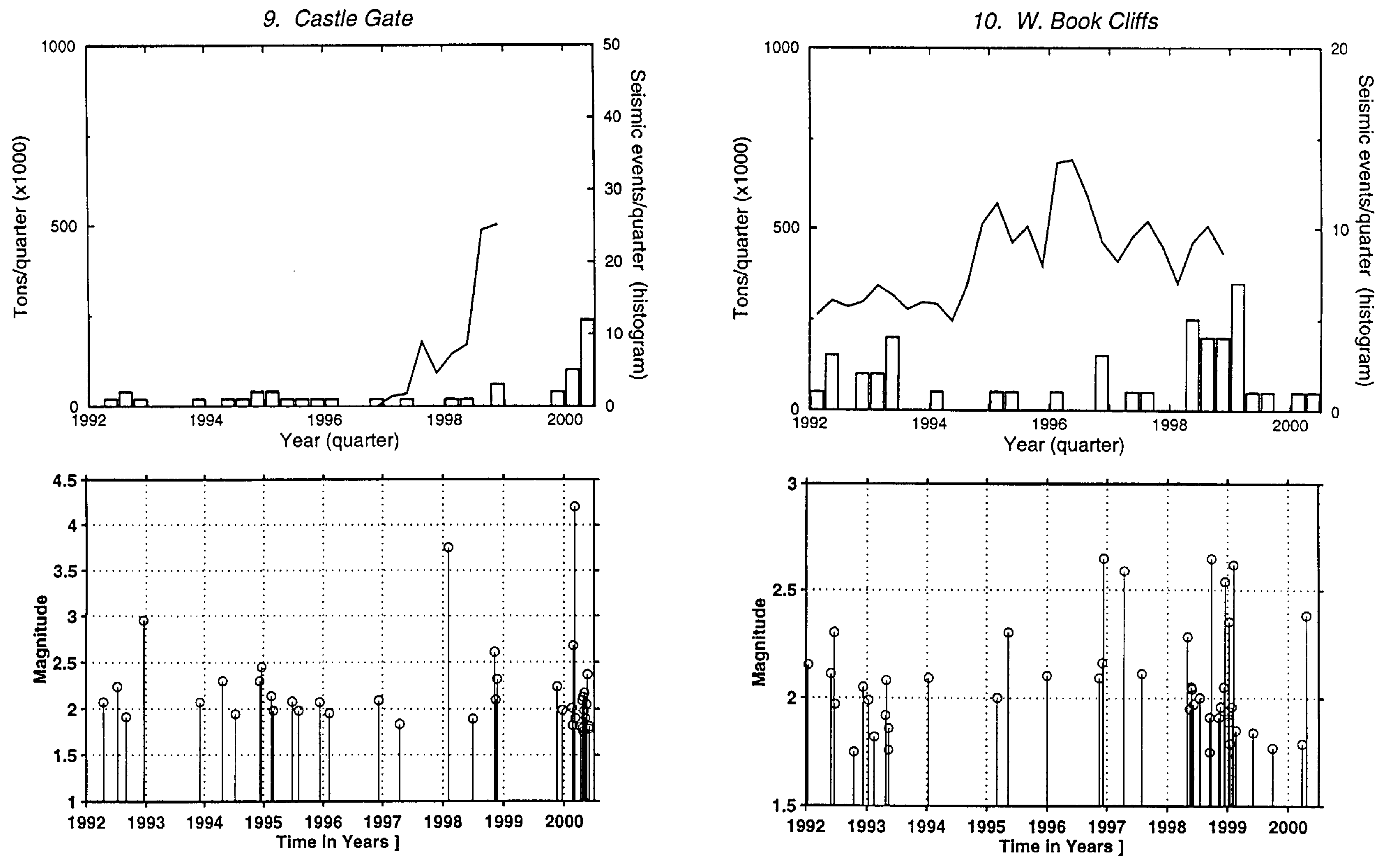

Figure 3-20. Temporal characterization of seismicity and coal production for sample areas identified in Figure 3-15. For each sample area, a composite plot is shown. The upper panel shows a time series of quarterly coal production, in tons, together with a histogram of the number of seismic events per quarter above a threshold magnitude (see text). The lower panel shows a corresponding plot of magnitude versus time. (Coal production data were available through 1998 only.)

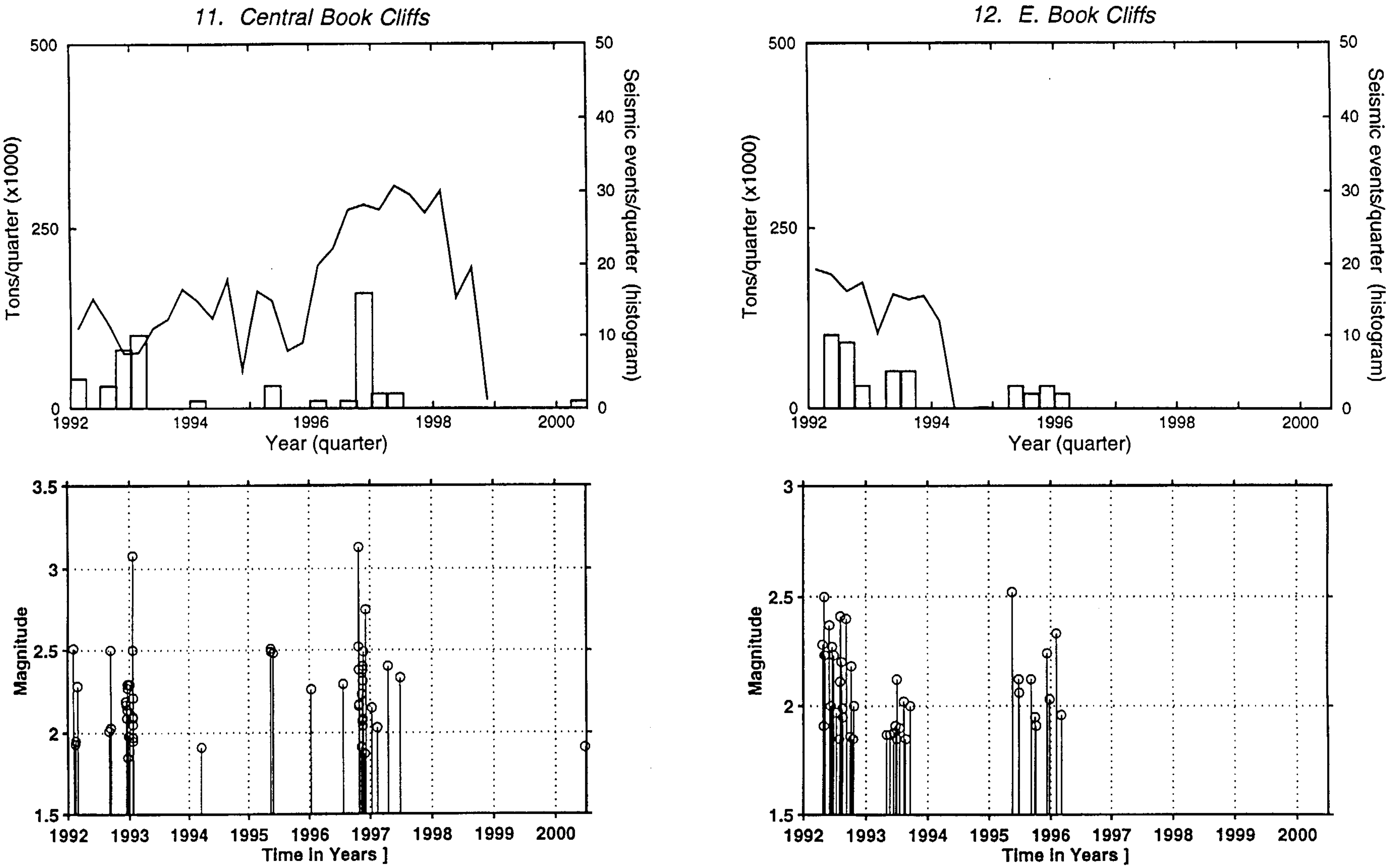

Figure 3-21. Temporal characterization of seismicity and coal production for sample areas identified in Figure 3-15. For each sample area, a composite plot is shown. The upper panel shows a time series of quarterly coal production, in tons, together with a histogram of the number of seismic events per quarter above a threshold magnitude (see text). The lower panel shows a corresponding plot of magnitude versus time. (Coal production data were available through 1998 only.)

4.0 MECHANISMS OF SIGNIFICANT SEISMIC EVENTS

In this section we report results for Objective 2 relating to investigations of source mechanisms of mine seismicity—primarily in the Wasatch Plateau-Book Cliffs region but also including some seismic events in the trona mining region of southwest Wyoming (see section 1.1 regarding guidance from LLNL for emphasizing some specific seismic events). Figure 4-1 gives a simplified overview of four types of source mechanisms known to be associated with mine seismicity. Given our focus on underground mining, explosional source mechanisms will not be considered. Use of explosives in underground coal and trona mines is not a routine practice, and when explosives *are* used in such settings the "permissible" amount is small and generally far below the detection threshold of regional seismic monitoring. For example, the use of explosives in the Wyoming trona mines is reportedly rare and involves only a few pounds, and rules for underground coal mines limits the "permissible" amount to 60 pounds unless special permission is obtained from the Mine Safety and Health Administration (M. K. McCarter, personal communication, October 2000).

Of the other mechanisms depicted in Figure 4-1, our discussion will relate chiefly to shear-slip mechanisms and implosional or collapse-type mechanisms, which involve sudden roof-floor closure. Such closure can result from either tabular collapse or loss of pillar support that causes only partial roof-floor closure. The mechanism of a tensile fracture or opening crack (Figure 4-1) represents a variation of a collapse-type mechanism reported for an explosively induced mine collapse at a room-and-pillar copper mine in Michigan (Yang et al., 1998; Phillips et al., 1999).

Because of constraints of available data and resources, we investigated source mechanisms by using the conventional approach of analyzing P-wave first motions. The framework we have established lays the groundwork for complementary moment-tensor analyses—feasible now for only a few of the largest, relatively recent events in our data set, but increasingly feasible for future events in our study region, thanks to new broadband seismographs such as station SRU.

4.01 Overview—Events Analyzed and Presentation of Results

Table 4-1 (based on Table 3-3) lists all events of magnitude 3.0 or larger in the WP-BC area from January 1978 through June 2000; Figure 4-2 shows their map distribution. For each event, Table 4-1 also indicates the closest active mine, the inferred focal-mechanism type, and whether ground-truth information is available (Appendix C). We used this list of events as a starting point for our analysis and systematically examined P-wave first-motion data for all events in this set. We were able to distinguish two groups of events. The first group consists of shear-slip events having a clear mixture of compressional and dilatational first motions. The second consists of events for which only dilatational first motions were observed, making them possible candidates for collapse-type events. In addition to this sample of larger seismic events in the WP-BC area, we also investigated P-wave first motions and selected waveforms for three seismic events (M_L 3.0-4.3) in the trona mining district of southwestern Wyoming that occurred between January and August 2000 (see section 3.1) in order to assess their likely mechanisms.

We have organized the remainder of section 4.0 as follows. We begin, in section 4.1, by describing velocity modeling that was a prerequisite for constructing focal mechanisms in the WP-BC area. Next, in section 4.2, we describe and discuss three events in the WP-BC sample of larger events (Table 4-1) that have unambiguous shear-slip mechanisms. In section 4.3 we then describe and discuss 13 events in the WP-BC sample that were possible collapse-type events. Table 4-1 includes a total of 18 events, but as the table indicates the P-wave first motions for two events were obscured by small preceding events, so their mechanisms could not be evaluated from a first-motion analysis. Finally, in section 4.4, we address the three seismic events in the trona-mining district of southwestern Wyoming.

4.1 VELOCITY MODELS FOR FOCAL MECHANISMS

We constructed two different sets of velocity models for our focal mechanism investigations in the WP-BC area: the Willow Creek Composite (WCC) model for the Willow Creek Mine area and the Trail Mountain Composite (TMC) model for the Trail Mountain Mine area (Tables 4-2 and 4-3; Figure 4-2). We refer to these models as composite models because each one consists of two or more one-dimensional velocity models designed for use with recording stations in different regions. We used the WCC and TMC models for seismic events north and south of 39° 32′ N, respectively, as this latitude is halfway between the Willow Creek and Trail Mountain mines.

4.11 The Willow Creek Composite Velocity Model

We began by examining reduced travel-time plots from the March 7, 2000, Willow Creek earthquake to evaluate the accuracy of existing velocity models. The Willow Creek earthquake was especially suitable for this purpose because its hypocenter had been accurately and independently determined using travel-time data from a dense seismic network in and above the Willow Creek Mine, as discussed in section 4.21. The travel-time plots for this event showed that no single, one-dimensional velocity model could provide an adequate fit to all of the data. The East Mountain velocity model of Williams and Arabasz (1989) predicts travel times that fit reasonably well the observed travel times from the earthquake at Colorado Plateau stations out to 200 km distance (20° to 210° azimuth). However, at stations in the Basin and Range Province (azimuth 210° to 355°, the observed apparent velocity at distances of 50 to 150 km is significantly slower than that predicted by the model. The ideal solution to this problem would be to use a three-dimensional velocity model. However, there are no such models available which include the WP-BC region.

To approximate the laterally-varying velocity structure in the region from which our first motion data for the Willow Creek earthquake came, we developed a set of three one-dimensional models to use with three groups of stations: (1) surface stations located along the eastern edge of the Basin and Range province in Utah (210° to 355° azimuth from the Willow Creek event), (2) surface stations located in the Colorado Plateau Province of eastern Utah (20° to 210° azimuth), and (3) stations located underground in the Willow Creek Mine in the Colorado Plateau. The second model was also used for a few distant stations in easternmost Idaho and western Wyoming (355° to 20° azimuth). We will refer to this set of models as the Willow Creek Composite (WCC) velocity model (Table 4-2).

The datum for the first two WCC models is 2400 m above sea level—the mean elevation of the 7 surface stations located within 1 km of the Willow Creek epicenter. The datum for the third model, the Willow Creek Mine model, is 1900 m: 21 m above the elevation of the highest underground station and 25 m above the minimum source depth. The Willow Creek Mine model is the same as the WCC Colorado Plateau model except that the top 0.5 km of the latter has been removed. The use of two datums is necessary because the location program we used, Hypoinverse (Klein, 1978), assumes that all stations are at the elevation of the datum for the purpose of the takeoff angle calculations. For the 2000 Willow Creek earthquake, the takeoff angles for the closest stations are sensitive to the choice of the datum because the focal depth of the source is so shallow.

We computed elevation corrections for the travel times using a P-wave velocity of 4.0 km/sec. This velocity was chosen because it is the velocity of the top layer in the Willow Creek Mine model and the velocity of the layer immediately beneath the 0.1-km-thick low-velocity near-surface layer in the other two models. The assumption underlying this choice is that a similar low-velocity layer is present near the surface everywhere, regardless of elevation, but is above the level of the mine stations.

The uppermost 4.4 km of all three WCC velocity models is the same, except for the 0.5 km removed from the top of the Willow Creek Mine model. The top 0.9 km of the models was generalized with the assistance of Julie Bernier using sonic logs from two boreholes located near the epicenter of the M_L 4.2 earthquake: 96-25-3 (0.8 km west-northwest, surface elevation of 2056.1 m) and 96-30-3 (1.4 km east-northeast, surface elevation of 2092.6 m). Because the datum for two of the velocity models is higher than the surface elevations of these sonic logs, it was necessary to extrapolate the sonic log velocities beyond the elevation range of the data. This was done by extending the second, 4.0 km/sec layer in these models upward, for consistency with the elevation correction calculations.

The model between 0.9 km and 4.4 km below the 2400 m datum was modified from the East Mountain model of Williams and Arabasz (1989). East Mountain is located 55 km SSW of Willow Creek in an area of similar geology. Williams and Arabasz derived the relevant part of their model from sonic logs of an oil well located roughly 10 km south of East Mountain. We based the modifications to their model on a comparison between the stratigraphic column in Figure 3 of their paper and a generalized stratigraphic column for the Helper-Price-Wellington area (chart 65, p. 170 in Hintze, 1988) using the 1821 m elevation for the base of the Castlegate sandstone near the epicenter as a reference elevation (see section 4.21).

The lower part of the WCC Basin and Range model is modified from model B of Keller et al. (1975). This model is from an unreversed seismic refraction profile beginning at an open-pit mine near Salt Lake City and extending 245 km southward along the Basin and Range/Colorado Plateau transition zone. The lower part of the WCC Colorado Plateau model is modified from the model determined by Roller (1965) for the northern end of a 300-km-long reversed refraction line across the Colorado Plateau in southeastern Utah and northwestern Arizona. The modifications to both models are based on analyses of travel-time data from local and near-regional earthquakes and blasts recorded on the University of Utah seismic network (Loeb, 1986; Loeb and Pechmann, 1986). Figure 4-3 shows that these models provide reasonably good fits to the travel-time data for their respective regions.

4.12 The Trail Mountain Composite Velocity Model

The Trail Mountain Composite (TMC) model (Table 4-3) consists of two different one-dimensional models for use with two different groups of stations: (1) surface stations located along the eastern edge of the Basin and Range province in Utah (approximately 210 to 360 degrees azimuth from Trail Mountain), and (2) surface stations located in the Colorado Plateau region of eastern Utah (approximately 0 to 210 degrees from Trail Mountain). The second model is also used for stations in eastern Idaho and Western Wyoming north of 42° 30′. As discussed in section 4.11, the two separate models are needed because of the significant differences in crustal structure between the eastern Basin and Range Province and the Colorado Plateau interior. For this study, we did not need a version of the Trail Mountain model for underground stations.

The datum for both of the TMC models is 2600 m above sea level—the approximate elevation above the active part of the Trail Mountain Mine in 2000. As with the WCC model, we computed elevation corrections for the travel times using the P-wave velocity of the second layer in the models, which is 4.0 km/sec.

The uppermost 4.14 km of both TMC velocity models is the same. The top 0.8 km is based on a stratigraphic column for the Trail Mountain area which we constructed from a geologic map (Larsen, 1997), and some average formation velocities computed from the two sonic logs obtained near the Willow Creek Mine. We used the sonic logs from the Willow Creek region because the available sonic logs from the Trail Mountain region do not sample the uppermost 0.8 km of the stratigraphic section. Williams and Arabasz (1989) used mean vertical-interval velocities from high-resolution seismic reflection profiles on East Mountain, centered ~6 km ENE of the Trail Mountain Mine, to construct the uppermost kilometer of their velocity model for the East Mountain area. However, this part of their model consists of a strong velocity gradient with a P-wave velocity increase from 2.4 to 4.04 km/sec. Sonic log data from this depth range elsewhere in the region indicate a much thinner near-surface velocity gradient. Based on these sonic logs, including those from the Willow Creek area, we decided to replace the Williams and Arabasz (1989) near-surface gradient by a 0.1-km-thick top layer with a P-wave velocity of 3.5 km/sec.

The TMC model between 0.8 and 2.4 km below the 2600 m datum was generalized from sonic logs from two boreholes in the Trail Mountain Mine area (analyzed by Matthew Jensen): Indian Green 02-176-1, located 8 km north of the mine, and Federal 41-33, located

12 km southeast of the mine. The formation boundaries in both wells are estimated to be at comparable elevations, but ~0.4 km higher than their elevations in the Trail Mountain area. Consequently, we adjusted the depths of the velocities from these logs for this ~0.4 km difference in stratigraphic level. The Federal 41-33 log provides velocity information to greater depths. Williams and Arabasz used this log in constructing their East Mountain model, which is a reasonable fit to the data. Therefore, to obtain the TMC model from 2.4 to 4.14 km below the datum, we modified their East Mountain model by decreasing the layer boundary elevations by 0.4 km. The TMC models below 4.14 km depth are identical to the corresponding parts of the WCC models. Figure 4-4 shows that the TMC models provide acceptable fits to the travel-time data from one of the larger seismic events to occur in the Trail Mountain vicinity—the 1992 M_L 3.5 seismic event in the East Mountain area.

4.2 SHEAR-SLIP EVENTS IN THE WP-BC AREA

4.21 The M_L 4.2 Seismic Event Near the Willow Creek Mine on March 7, 2000

The March 7, 2000, UTC (March 6, 2000, MST) M_L 4.2 Willow Creek earthquake is the largest mining-related seismic event to occur in the WP-BC region of Utah since the University of Utah seismic network began operating in 1962 (Table 4-3; Arabasz et al., 1997). This event triggered several small rock falls, one of which briefly blocked U.S. Highway 6 and the Denver and Rio Grande railroad tracks adjacent to the highway (Miller, 2000; Francis X. Ashland, written communication, 2000). This event was also accompanied by seven roof falls at various locations in the nearby Willow Creek Mine (Appendix C).

We report here on our determination of a focal mechanism for this event using P-wave first-motion data from three sources: (1) a dense, 23-station temporary seismic network which Dr. Peter L. Swanson of the National Institute for Occupational Safety and Health (NIOSH) was operating in and above the Willow Creek Mine, (2) one accelerograph and two portable digital seismographs which we had temporarily deployed near this mine, and (3) the University of Utah regional seismic network. The hypocentral location which we use for this focal mechanism determination was computed by Dr. Swanson using arrival-time data from his network and a simple, preliminary velocity model based on apparent seismic velocities across this network. Dr. Swanson provided us first-motion readings from his stations, but did not provide the corresponding arrival time data because of some timing problems which he was trying to resolve. Consequently, we have not been able to recompute the hypocenter with the same velocity model which we employed for the focal mechanism determination.

In the following sections, we first discuss the hypocentral location for the 2000 Willow Creek earthquake and then our focal mechanism determination. Our preferred focal mechanism indicates that the Willow Creek earthquake was caused by oblique reverse faulting on a plane dipping steeply to the south or shallowly to the north-northwest. Thus, it appears that the roof falls which occurred in the Willow Creek Mine at the time of the earthquake were a result of the earthquake and not the cause.

Hypocentral Location. Dr. P. L. Swanson provided the following information on the hypocentral location for the March 7, 2000, Willow Creek earthquake: (1) "The initiation point was centered right above the face (the location of active mining) at a distance we estimate at 400 to 700 feet (122 to 213 m) above the seam", (2) the seam elevation is 5450 feet (1661 m), and (3) "The location coincides with the base of the Castlegate sandstone where it is most massive." The epicentral location corresponding to this description is 39° 45.10′ N, 110° 51.08′ W, and the elevation above sea level is 1829 ± 46 m (6000 ± 150 ft). The source elevation is in good agreement with the elevation of the base of the Castlegate sandstone in the two nearby boreholes from which the sonic logs used in the velocity modeling were obtained: 1821 m in the closest borehole and 1859 m in the other (John Mercier, personal communication, 2000).

The focal depth depends on the datum chosen. The elevation varies by hundreds of meters in the mine area, but is approximately 2475 m (8120 ft) at the epicenter and averages 2400 m at the seven surface stations within 1 km of this point. Selecting 2400 m as the datum, as noted above, the focal depth is 0.57 ± .05 km.

The range of possible focal depths spans a discontinuity in the velocity model. At this discontinuity, which is at a depth of 0.6 km below the 2400 m datum, the P-wave velocity increases downward from 4.0 to 4.3 km/sec. The sonic logs from which this part of the velocity model was derived show good evidence for a sharp increase in average velocity of at least this magnitude near source depth. Thus, despite the excellent focal depth control for this event, it was necessary to investigate the sensitivity of the focal mechanism to the focal depth.

Focal mechanism. We determined the focal mechanism for three fixed focal depths spanning the range of the focal-depth uncertainty: 0.52 km, 0.57 km, and 0.62 km. For each of these focal depths, we used the location program Hypoinverse to compute the best-fitting origin times, the station azimuths, and the takeoff angles for the surface stations and some of the stations located underground in the mine.

Determination of the takeoff angles for the underground stations required special care. The elevation range of these stations is 1561 m to 1879 m, which encompasses both the source elevation of 1829 ± 46 m and the 1800 m elevation of a discontinuity in the velocity model. The takeoff angles for the underground stations between 1800 m and 1900 m elevation were calculated by Hypoinverse assuming station elevations equal to a datum elevation of 1900 m. For source locations above the 1800 m discontinuity, the first arrivals at these stations are all modeled as refractions off the 1800 m discontinuity. The corresponding takeoff angles are therefore independent of the exact station elevation. For source locations below the 1800 m discontinuity, the first arrivals at these stations are modeled as direct waves. The corresponding takeoff angles are near horizontal, and are also insensitive to the exact station elevation.

The takeoff angles for the underground stations below the 1800 m velocity discontinuity could not be calculated using Hypoinverse because the P-wave first arrivals at these stations are all downgoing direct rays. The takeoff angles for these arrivals were calculated by hand to an accuracy of ±3 degrees, which is adequate in light of the velocity model uncertainties.

Fortunately, the best-fit focal mechanism turns out not to be very sensitive to focal depth over the range of depth uncertainty (Figure 4-5). The best-fit focal mechanisms for all three depths show oblique reverse faulting on a plane dipping steeply to the south or shallowly to the northwest or north-northwest. Our preferred focal mechanism is the one for the 0.62 km depth, because this is the only one of the three for which the best-fit focal mechanism fits all of the first motion data. This choice does not necessarily mean that this depth is more accurate in an absolute sense. But it does suggest that this depth is more accurate relative to the depths of the velocity model discontinuities.

For our preferred focal mechanism, the strike, dip, and rake are, respectively, 88° ± 4°, 75° ± 4° and 99° ± 2° for one nodal plane and 238° ± 12°, 17° ± 4°, and 61° ± 9° for the other nodal plane. These error bars reflect only the uncertainties in fitting the nodal planes to the preferred first motion plot. They do not incorporate the uncertainties related to the focal depth or velocity model.

It is not possible to identify which of the two nodal planes is the fault plane based on the information presently available to us. The second nodal plane, which dips 13° to 21° towards N20°W to N44°W, can be interpreted as subparallel to the bedding, which dips 8.5° to the north (Richardson et al., 1996). It can also be interpreted as dipping in the opposite direction of the longwall advance at the time of the earthquake, which was toward the southeast (Appendix C). Finally, the strike of this shallowly-dipping nodal plane can be interpreted as subparallel to one of two major fracture trends in the Willow Creek Mine area mentioned in Richardson et al. 1996), N75°E. (The other trend is N60°W). Any one of these interpretations could be used to argue that the shallowly-dipping nodal plane is the fault plane. On the other hand, the slip direction on the steeply-dipping plane is more consistent with the maximum horizontal stress direction determined by overcoring, which is N30°W to N60°W (Richardson et al., 1996).

4.22 The M_L 3.8 Seismic Event Near Willow Creek Mine on February 5, 1998

The M_L 4.2 Willow Creek earthquake of March 2000 was preceded by an M_L 3.8 earthquake in nearly the same place on February 5, 1998, UTC (February 4, 2000, MST; Table 4-1). The 1998 earthquake occurred while gate-road development was underway in the nearby Willow Creek Mine in preparation for longwall mining which began in July 1998. The 1998 earthquake caused no significant damage to the mine, but triggered some rock falls in a nearby canyon (John Mercier, Willow Creek Mine geologist, personal communication, 2000). Some coal sluffed from a mine pillar during a second, smaller seismic event 48 minutes later (Appendix C).

We relocated the 1998 M_L 3.8 earthquake relative to the 2000 M_L 4.2 earthquake and attempted to determine a focal mechanism for it from P-wave first motions. The data we used were from the University of Utah regional seismic network, the closest station of which was

8 km from the 1998 event. The closer NIOSH and University of Utah temporary seismic stations which we used to analyze the 2000 event had not yet been installed when the 1998 event occurred. Although we were unable to constrain the focal mechanism of the 1998 event, the first motion data clearly indicate that this event, like the 2000 event, was caused by slip on a fault and not a mine collapse. Within the constraints of our data, the fault orientations and slip directions could have been the same in both earthquakes.

Hypocentral location. We located the 1998 earthquake relative to Dr. Swanson's hypocenter for the 2000 earthquake using the master event technique of Johnson and Hadley (1976) and the Willow Creek Composite velocity model discussed in Section 4.11. In our implementation of this technique, we attempted to correct the arrival times of the 1998 event for velocity model inaccuracies by subtracting the travel-time residuals for the 2000 event (observed arrival time minus calculated arrival time) before locating the 1998 event with Hypoinverse. In computing this location, we used only those stations for which we had determined a station delay, and we applied no distance weighting. The first trial hypocenter for the location was the preferred hypocenter of the 2000 event at 0.62 km depth.

If the focal depth is allowed to vary, then the 1998 event locates at a depth of 0.59 km. This depth falls within the depth range of 0.57 ± .05 km calculated by Dr. Swanson for the 2000 event. However, this depth is poorly constrained due to the lack of nearby stations. Locations computed with any fixed focal depth shallower than 2 km have root-mean-square travel-time residuals within 0.01 sec of the minimum value of 0.09 sec.

Fixing the focal depth of the 1998 event at the preferred focal depth for the 2000 event, 0.62 km, gives an epicenter of 39° 45.01′ N, 110° 51.94′ W. This epicenter is 1.2 km WSW of the 2000 epicenter. However, the difference between these two epicenters is not significant in light of the location uncertainties.

Focal mechanism. The first motion data for the 1998 event are inadequate to constrain its focal mechanism regardless of the focal depth. If the focal depth is fixed at 0.62 km, then the first motion data can be fit by the preferred nodal planes for the 2000 event (Figure 4-6). Thus, it is possible that both the 1998 and 2000 earthquakes had the same oblique-reverse faulting focal mechanism.

Jochen Braunmiller obtained a "not well constrained" moment tensor solution for the 1998 earthquake by modeling regionally recorded broadband seismograms (see the Oregon State University web page <quakes.oce.orst.edu/moment-tensor>). His best-fitting double-couple solution, which is for a source depth of 4 km, shows oblique-reverse faulting on a plane dipping 31° south or 63° north-northeast. This focal mechanism does not fit our first-motion data distribution for a focal depth of 4 km or any other reasonable focal depth.

4.23 The M_L 3.0 Seismic Event in the Northern Wasatch Plateau on June 2, 1996

We relocated the June 2, 1996, earthquake in the northern Wasatch Plateau and determined its' focal mechanism using the Willow Creek Composite velocity model and data from the

University of Utah regional seismic network, supplemented by data from an accelerograph which we were temporarily operating at a site 7 km from the epicenter (the closest station). In computing the location with Hypoinverse, we downweighted the arrival times from the more distant regional network stations using a cosine taper with a weight of one at a distance "dmin" of 100 km and a weight of zero at a distance "dmax" of 200 km (see Klein, 1978). Our revised hypocenter is at 39° 37.70′ N, 111° 14.53′ W, with a well-constrained focal depth of 11.0 ± 1.5 km (95% confidence limits). The relatively large focal depth indicates that this earthquake is not mining related.

Our focal mechanism for this event (Figure 4-7) shows normal faulting on a plane dipping moderately to the east (strike = 2° ± 4°, dip = 40° ± 2°, rake = −116° ± 1°) or west-northwest (strike = 214° ± 5°, dip = 55° ± 2°, rake = −70° ± 2°). The tension (T) axis of this focal mechanism is nearly horizontal and trends west-northwest, nearly parallel to the average T-axis direction found in studies of focal mechanisms in the Basin and Range – Colorado Plateau transition zone of southern Utah, where this earthquake is located (Arabasz and Julander, 1986; Bjarnason and Pechmann, 1989; Patton and Zandt, 1991). Based on the focal mechanism and the depth, we interpret the June 2, 1996, M_L 3.0 northern Wasatch Plateau earthquake to be a tectonic event caused by regional east-southeast/west-northwest extension in the WP-BC area.

4.3 POSSIBLE COLLAPSE-TYPE EVENTS IN THE WP-BC AREA

One of the notable results of our analysis of P-wave first motions for the larger seismic events in the WP-BC area listed in Table 4-1 is that only three events had an unambiguous shear-slip mechanism. The majority were possible collapse-type events—that is, only dilatational first-motions were observed. The latter observation alone is insufficient to conclude that the focal mechanism was implosional because one must have confidence that the focal sphere was adequately sampled to preclude a double-couple, shear-slip type of mechanism (e.g., Wong and McGarr, 1990). One must have additional confidence that ubiquitous dilatations on the focal sphere are at geometrically correct positions, i.e., that true take-off angles have been plotted using a reliable source focal depth and velocity model (e.g., Williams and Arabasz, 1989, Figure 12).

We discuss individually the two largest collapse-type events, for which various information—including ground truth—makes it highly probable that the source mechanisms were implosional. Separately, we systematically quantify available data for 11 other events in Table 4-1 having a possible collapse-type mechanism.

4.31 Event #2—M_L' 3.8, Gentry Mountain Area, May 14, 1981

The M_L' 3.8 seismic event on May 14, 1981 in the Gentry Mountain area was associated with a major collapse which occurred during pillar recovery operations at the U.S. Fuel Company King Mine. The collapse area may have been as large as 150 m by 150 m (Taylor, 1984; Appendix C).

Bjarnason (1987, Appendix B) presents an "unconstrained" normal-faulting focal mechanism for this event, based on his observations of 29 dilatational and no compressional P-wave first motions. In contrast, Wong and Humphrey (1989) report a reverse-faulting focal mechanism. Their first motion plot shows both compressions and dilatations, with some inconsistencies, but the dilatations are much more numerous. Finally, Taylor (1994) modeled a broadband recording of this event using a tabular collapse source mechanism. He cites the following observations as supporting evidence for this type of mechanism: the small size of the Love waves generated, the low Lg/Pg amplitude ratio, the relative lack of high frequency energy in the seismic waves, the large implosional component to Patton and Zandt's (1991) surface-wave moment-tensor solution, and the apparently contemporaneous mine collapse which he estimates is large enough to account for the size of the event.

The P-wave first-motion plots for the Gentry Mountain event in Figure 4-8 illustrate the typical difficulties with using regional network first-motion data to constrain the focal mechanisms of shallow mining-related events. The first-motion data shown are from Bjarnason (1987). They include readings from both the University of Utah regional network and a network in the Canyonlands district of southeastern Utah, which Woodward-Clyde Consultants operated from 1979 to 1987. We checked Bjarnason's first-motion and arrival-time picks from the University of Utah network, and concur that all of them are dilatational. We cannot easily check his picks from the Canyonlands network, because we do not have the waveform data he used. We note, however, that some of Wong and Humphrey's (1989) compressional first-motion picks appear to be from the University of Utah network.

The azimuths and takeoff angles for the first motions in Figure 4-8 are for locations which we computed using Bjarnason's arrival-time picks, the Trail Mountain Composite velocity model, distance weighing with a "dmin" of 150 km and a "dmax" of 200 km, and fixed focal depths of 0.06, 0.6, and 6.0 km. We evaluated the focal mechanism for this set of fixed focal depths because the actual focal depth is poorly constrained by the available data, none of which is from a station closer than 56 km. The root-mean-square travel-time residuals are the same for the locations at both .06 and 0.6 km depth, and 10% larger for the location at 6 km depth. Our preferred focal depth is 0.6 km, the approximate depth of the commercial coal seams in the Trail Mountain model. (The corresponding epicenter is 39° 28.74′ N, 111° 7.11′ W.) However, first-motion plots for any depth between 0.36 km and 2.48 km should be very similar, because this range of depths encompasses two layers in the Trail Mountain Composite velocity model with similar P-wave velocities of 4.3 and 4.4 km/sec (Table 4-3).

The P-wave first motion data from the May 14, 1981, M_L' 3.8 Gentry Mountain event are consistent with a wide variety of normal and oblique-normal faulting mechanisms if the focal depth is assumed to be 0.06 or 0.6 km (Figure 4-8), or probably any depth less than 2.48 km. Figure 4-8 illustrates only one of these possible focal mechanisms. For a focal depth of 6 km, the best double-couple fit to the data is a reverse-faulting mechanism similar to that published by Wong and Humphry (1989). Of course, the collapse mechanism proposed by Taylor (1994) satisfies the first-motion data in Figure 4-8 for any focal depth. In light of Taylor's work and the in-mine observations which he reports, we agree with his conclusion that this seismic event was most likely caused by a mine collapse.

4.32 Event #4—M_L' 3.5, East Mountain Area, July 5, 1992

The M_L' 3.5 seismic event in the East Mountain area on July 5, 1992, occurred at about the same time as some pillar damage adjacent to active longwall mining in the nearby Cottonwood Mine. The damage consisted primarily of ~0.3 m of height reduction in nine pillars over an area of about 30 by 270 m (Appendix C).

We relocated the East Mountain event and attempted to determine its focal mechanism using the Trail Mountain Composite velocity model and data from the University of Utah regional seismic network. In locating this event with Hypoinverse, we used the same distance weighting and fixed focal depths as we did in locating the previously-discussed event. The focal depth is very poorly constrained due to the lack of recording stations closer than 32 km, as evidenced by the fact that the root-mean-square travel-time residuals are the same for all three focal depths. Our revised epicenter for the 0.6 km fixed focal depth is 39° 19.18′ N, 111° 9.70′ W.

If the July 5, 1992, M_L' 3.5 East Mountain event is assumed to have a focal depth of 0.06 or 0.6 km, then our P-wave first motion data can be fit with a wide range of normal and oblique-normal faulting mechanisms—one of which is illustrated in Figure 4-9. If the focal depth is assumed to be 6.0 km, then all but one of the first-motion observations can be fit by a reverse-faulting mechanism. Thus, the set of all dilatational first motions which we found for the East Mountain event can be explained not only by an implosional mechanism, but also by a variety of possible double-couple focal mechanisms. The available observations from the Cottonwood mine are more consistent with a collapse mechanism, but further work is needed to determine the correct focal mechanism for this event.

4.33 Eleven Other Seismic Events Having Only Dilatational P-wave First Motions

Thirteen events in Table 4-1 have an indicated "collapse-type?" mechanism. Focal-sphere plots for the two largest of these (#2 and #4) have just been discussed. For each of the other 11 events, the total number of available P-wave first-motion recordings was generally fewer, due to smaller size, less favorable station coverage, or both. Nevertheless, the absence of any compressional P-wave first motions for these events seems significant and warrants documentation, which we provide in Table 4-4.

Basis for Table 4-4. In scrutinizing available P-wave first-motion recordings for the 11 events, special care was taken to objectively assess the quality of the recordings. Care was also taken to accept only first motions whose arrival times were consistent with predicted first arrivals, especially beyond about 150 km where a weak P_n phase might be the true first arrival but mistakenly be missed (see travel-time curves in Figures 4-3 and 4-4).

Just as for the various focal-mechanism plots included in this report, we consistently used the signal-to-noise ratio (s/n) of the P-wave first motion to quantify its quality. Following Bjarnasson and Pechmann (1989), highest quality (labeled Q1 in Table 4-4) was assigned to readings for which s/n was 3 or greater, and a lesser quality (labeled Q2 in Table 4-4) to readings for which s/n was between 2 and 3. Readings for which s/n was less than 2, but which still appeared valid, were recorded in this exercise (labeled Q3 in Table 4-4), even though we routinely discarded such readings in constructing focal-mechanism plots. Despite the lower quality of these readings, they were significant in that none was compressional, thus decreasing the likelihood of a shear-slip, double-couple mechanism.

In lieu of a stereographic plot for each of the 11 events, the azimuthal range given in Table 4-4 conveys the relative coverage of the focal sphere by dilatational first motions. The larger the range, the less likely that a shear-slip mechanism could be accommodated. Ground-truth information is available for three of the 11 events, which we address individually.

Event #7—M_L 3.3, December 16, 1987. This seismic event occurred in the Wasatch Plateau coal field and was closely associated with room-and-pillar mining in the Trail Mountain Mine, prior to the beginning of longwall mining nearby in 1995. Ground-truth information that could be recovered for this event (Appendix C) is minimal, except to confirm the room-and-pillar setting and problematic mining conditions.

Event #8—M_L 3.2, June 3, 1992. This seismic event occurred in the Wasatch Plateau coal field and was closely associated with longwall mining in the Cottonwood Mine—the same source area as for event #4, the M_L 3.5 event that occurred one month later in July 1992 (discussed in section 4.32). As described in Appendix C, available ground-truth information for this event indicates that approximately five pillars immediately adjacent to the longwall face were reduced in height by ~0.3 m at the time of event #8. We consider this event to be a smaller counterpart of event #4 and judge that both seismic events were likely caused by sudden roof-floor closure due to loss of pillar support.

Event #14—M_L 3.1, January 21, 1993. This seismic event coincided with a catastrophic pillar failure in a room-and-pillar mine in the Book Cliffs coal field. Boler et al. (1997) published a detailed report of this incident (see also Appendix C here), describing that 24 pillars were crushed out over an area of nearly 15,000 m^2. Despite this pillar loss, they report that "the roof remained substantially intact and suspended above the crushed pillar array with . . . net roof-to-floor convergence of a few centimeters (estimated from photographs of support timbers that were broken in compression)."

Boler et al. include stereographic plots of first-motion distributions, assuming two different but shallow focal depths. In part because their interpreted data included three compressional first motions, Boler et al. (1997) concluded that a shear-slip focal mechanism (with normal-slip displacement) was involved and that the shear-slip event precipitated the pillar failure. In our reexamination of original data for this event from the University of Utah seismic network, including recordings whose azimuths and takeoff angles would closely coincide with the compressions plotted by Boler et al. (1997, Figure 8), we found no evidence of a reliable compressional first motion (Table 4-4). Figure 4-2 shows that event #14 lies 19 km to the east of event #1, the M_L 4.2 event near the Willow Creek Mine that had a reverse slip mechanism indicative of high horizontal compressive stress (see Figure 4-5). We consider the normal-slip mechanism interpreted by Boler et al. (1997) to be questionable and prefer the interpretation that the catastrophic pillar collapse described by Boler et al. (1997) was the seismic source of event #14.

Remainder of events. The remaining events in Table 4-4 identified as having a "collapse-type?" mechanism include the following: events #5, #6, and #15, all in the early 1980s, near the Sunnyside #3 Mine (longwall mining at the time); event #9 in 1991 near the Star Point #2 Mine (longwall mining); event #10 in 1996 near room-and-pillar mining in the same mine as event #14 discussed above and described by Boler et al. (1997); event #12 in 1991 near the Cottonwood Mine (longwall mining); event #16 in 1984 near the Deer Creek Mine (longwall mining); and event #18 in 1986 near the Castle Gate #3 Mine (longwall mining).

4.34 General Observations and Conclusions

The 13 events listed in Table 4-4 that have only dilatational first motions are distributed throughout both the WP and BC coal fields (Figure 4-2). Four can be associated with room-and-pillar mining and the other nine with longwall mining. Collapses or partial closures of mine openings are documented coincident with four of these events: #2, #4, #8, and #14 (see Appendix C and the descriptions above). For these four events, we have estimated the seismic moment and radiated seismic energy using empirical relations (developed for earthquakes) between these quantities and M_L. Based on these rough source parameter estimates, and calculations analogous to those in Pechmann et al. (1995) and Taylor (1994), it appears that the sizes of these four events can be accounted for by the accompanying implosions. However, we consider this conclusion to be preliminary in the absence of direct seismic moment and/or energy measurements.

In conclusion, based on ground-truth information and the data of Figure 4-8, Figure 4-9, and Table 4-4, we consider it highly likely that events #2, #4, #8, and #14 were collapse-type events with implosional focal mechanisms. We also consider it plausible that the other nine events had similar source mechanisms, with variable likelihood depending on available data.

4.4 THREE SEISMIC EVENTS (M_L 3.0-4.3) IN THE TRONA-MINING DISTRICT OF SOUTHWESTERN WYOMING, JANUARY-AUGUST 2000

On January 30, 2000, an M_L 4.3 seismic event accompanied by a major roof fall occurred at the Solvay Minerals trona mine in southwestern Wyoming (Appendix C; Gearino, 2000). This event appears to be a smaller-scale counterpart to an M_L 5.2 seismic event which occurred at the same mine on February 3, 1995. The M_L 5.2 event was generated by the collapse of a 1 by 2 km room and pillar section of the mine, as evidenced by long-period waveform modeling and surface subsidence of 0.6 to 0.9 m above the affected area, which is enough to account for the size of the seismic event (Pechmann et al., 1995). Similarly, at the time of the January 30, 2000, event, surface subsidence of up to 0.8 m occurred in an irregularly-shaped area of ~0.65 km^2 above three room and pillar sections of the mine rendered inaccessible by the accompanying roof falls. Pillar extractions had recently been completed within two of the three sections of the mine which apparently collapsed, and were underway in the third section when the collapse occurred (see Appendix C).

Walter et al. (2000, and written communication) has successfully modeled the long period waveforms from this event with the same collapsing crack model that Walter used to model the data from the 1995 event (see Pechmann et al., 1995). From this modeling, they obtained a preliminary collapse moment of 3×10^{22} dyne-cm—a factor of five smaller than the moment of 1.5×10^{23} dyne-cm obtained for the 1995 event. Considering that the maximum surface subsidence was similar for both the 1995 and 2000 events, but that the collapse area of the latter ($\leq$0.65 km) is a factor of three or more smaller, it appears that the 2000 collapse was large enough to account for the M_L 4.3 seismic event. A comparative analysis of subsidence maps from the two collapses would provide a more precise estimate of the expected collapse moment ratio.

Two other $M_L \geq 3$ events occurred during 2000 in the trona-mining region of southwestern Wyoming: an M_L 3.0 event on July 16 and an M_L 3.1 event on August 17 (Table 4-5). To date, we have not been able to find any ground truth information for either of these two events. We relocated these two events, plus the January 30 event, relative to the 1995 event to help determine if they might be associated with any active mines. We also compared P-wave first motions and regionally-recorded broadband waveforms from these two events to those of the January 30th event in order to evaluate their likely source mechanisms.

We relocated the three trona-mining district events using the master event technique discussed in Section 4.22. We began by fixing the location of the 1995 event in the center of the collapse area at a depth of 0.5 km—the approximate depth of the Solvay Mine. We calculated the best-fitting origin time for this hypocenter by using Hypoinverse, the southwestern Wyoming velocity model in Table 1 of Pechmann et al. (1995), and distance weighting with "dmin" equal to 200 km and "dmax" equal to 250 km. The travel-time residuals from this fixed location were then used as travel-time corrections for the relocations of the three events which occurred during 2000. In these relocations, we used only the stations for which we had determined a travel-time correction, no distance weighting, and the center of the 1995 collapse as the starting location. The distances to the nearest station used in the relocations ranged from 121 to 136 km, and the largest azimuthal gaps between stations ranged from 182 to 199 degrees. Because of the unfavorable station distribution, we found it helpful to stabilize the locations by fixing the focal depths to 0.5 km.

Our relocated epicenter for the January 30, 2000, event (Table 4-5) is near the southern end of the Solvay Mine, 1.1 km west-southwest of the center of the collapse area shown on the mine map in Appendix C (x = 228000, y = 302000; 41° 29.48′ N, 109° 44.57′ W) and 0.5 km from its closest edge. The agreement between our collapse location and the relocated epicenter is quite good, and well within the 95% confidence limit of 4.6 km (Table 4-5). Our relocated epicenters for the other two events both lie within mining lease areas mapped by Brown (1995), but we do know how close they are to any mine workings (Table 4-5).

All of the discernable first motions from the January 30 event are dilatational, as expected. There are a few clear P-wave first motions from the August 17 event and they are all dilatational as well. These first motions are consistent with either a collapse mechanism or with a normal faulting earthquake. In contrast, the July 16 event had a clear compressional P-wave first motion at the U.S. National Seismic Network station BW06 (Boulder, Wyoming), and a less certain compressional first motion at another station. Compressional first motions are inconsistent with a pure collapse mechanism.

We compared the waveforms from the three events recorded at three regional broadband digital telemetry stations, including SRU (Figure 4-10). The waveforms from the August 17 event are more similar to those from the January 30 Solvay mine collapse than those from the July 16 event. In particular, the waveforms from the July 16 event have more high-frequency energy, higher S/P amplitude ratios, and smaller surface waves compared to the other two events (Figure 4-10). Taylor (1994) recognized the same waveform differences between collapse-type and shear slip seismic events (see Section 4.31). Based on the waveform comparisons and the P-wave first motions, it appears that the August 17 event is probably another collapse but the July 16 event is not.

Table 4-1

Focal-Mechanism and Summary Information for Seismic Events of Magnitude 3.0 or Larger in the WP-BC Coal-Mining Area, January 1978-June 2000, Ranked by Size

ID	Yr	MoDa (UTC)	HrMin (UTC)	Lat N	Long W	Depth* (km)	Mag.**	Closest Active Mine	Focal Mechanism	Data Reference	Ground-Truth Info. Available?
1	2000	03/07	02:16	39-44.95	110-50.19	1.8	ML 4.2	Willow Creek	**Shear Slip**	Fig. 4-5	YES
2	1981	05/14	05:11	39-28.86	111-04.72	0.7	ML' 3.8	King #4	Collapse-type?	Fig. 4-8	YES
3	1998	02/05	05:19	39-45.05	110-50.73	1.3	ML 3.8	Willow Creek	**Shear Slip**	Fig. 4-6	YES
4	1992	07/05	12:22	39-18.81	111-09.60	5.6	ML' 3.5	Cottonwood	Collapse-type?	Fig. 4-9	YES
5	1981	09/21	08:01	39-35.48	110-25.47	1.6	ML' 3.4	Sunnyside #3	Collapse-type?	Table 4-3	
6	1981	09/22	05:03	39-35.35	110.23.61	7.5	ML' 3.3	Sunnyside #3	Collapse-type?	Table 4-3	
7	1987	12/16	17:43	39-18.70	111-12.92	0.5	ML' 3.3	Trail Mountain	Collapse-type?	Table 4-3	YES
8	1992	06/03	05:08	39-19.04	111-09.80	0.6	ML' 3.2	Cottonwood	Collapse-type?	Table 4-3	YES
9	1991	02/06	13:46	39-29.99	111-04.61	4.3	ML' 3.1	Star Point #2	Collapse-type?	Table 4-3	
10	1996	10/25	18:32	39-42.12	110.39.24	3.3	ML 3.1	Soldier Canyon	Collapse-type?	Table 4-3	
11	1986	02/14	00:56	39-41.18	110.31.50	0.2	ML' 3.1	Soldier Canyon	(data problem)***		
12	1991	05/23	07:38	39-17.89	111-08.92	12.4	ML' 3.1	Cottonwood	Collapse-type?	Table 4-3	
13	1992	07/11	13:23	39-18.52	111-08.94	9.3	ML' 3.1	Cottonwood	(data problem)***		
14	1993	01/21	09:01	39-42.73	110-37.26	1.3	ML' 3.1	Soldier Canyon	Collapse-type?	Table 4-3	YES
15	1983	03/22	11:12	39-32.78	110-25.32	1.6	ML' 3.0	Sunnyside #3	Collapse-type?	Table 4-3	
16	1984	03/21	11:19	39-20.64	111-06.53	0.1	ML' 3.0	Deer Creek	Collapse-type?	Table 4-3	
17	1996	06/02	08:09	39-37.55	111-14.45	5.5	ML 3.0	(Skyline #3)****	**Shear Slip**	Fig. 4-7	
18	1986	10/30	00:05	39-44.11	110-57.93	5.6	ML' 3.0	Castle Gate #3	Collapse-type?	Table 4-3	

* Unreliable
** ML' is a weighted-average estimate of local magnitude, ML (see Arabasz et al., 1997, and section 3.21 here)
*** P-wave first motions obscured by small preceding event
**** Tectonic earthquake located 7 km south of Skyline Mine

Table 4-2

The Willow Creek Composite Velocity Model

Eastern Basin and Range Province Stations (Datum =2400 m)		*Colorado Plateau Province Stations (Datum = 2400 m)*		*Willow Creek Mine Underground Stations (Datum = 1900 m)*	
P-Wave Velocity (km/sec)	**Depth to Top of Layer (km)**	**P-Wave Velocity (km/sec)**	**Depth to Top of Layer (km)**	**P-Wave Velocity (km/sec)**	**Depth to Top of Layer (km)**
3.40	0.0	3.40	0.0	4.00	0.0
4.00	0.1	4.00	0.1	4.30	0.1
4.30	0.6	4.30	0.6	4.40	2.0
4.40	2.5	4.40	2.5	4.84	2.4
4.84	2.9	4.84	2.9	5.81	3.5
5.81	4.0	5.81	4.0	6.20	3.9
5.90	4.4	6.20	4.4	6.80	30.2
6.40	19.9	6.80	30.7	7.90	44.5
7.50	32.0	7.90	45.0		
7.90	45.0				

Table 4-3

The Trail Mountain Composite Velocity Model

Eastern Basin and Range Province Stations (Datum =2600 m)		*Colorado Plateau Province Stations (Datum = 2600 m)*		*Stratigraphy (from this study and Williams and Arabasz, 1989)*	
P-Wave Velocity (km/sec)	**Depth to Top of Layer (km)**	**P-Wave Velocity (km/sec)**	**Depth to Top of Layer (km)**	**Formation at Bottom of Layer**	**Age of Bottom Formation**
3.50	0.00	3.50	0.00	North Horn	Tertiary
4.00	0.10	4.00	0.10	Castlegate Ss	Cretaceous
4.30	0.36	4.30	0.36	Mancos Sh	Cretaceous
4.40	2.04	4.40	2.04	Morrison	Jurassic
4.84	2.48	4.84	2.48	Moenkopi	Triassic
5.81	3.88	5.81	3.88	Kaibab Ls	Permian
5.90	4.14	6.20	4.14		
6.40	19.90	6.80	30.70		
7.50	32.00	7.90	45.00		
7.90	45.00				

Table 4-4

Data for Seismic Events in Table 4-1 Having Only
Dilatational P-wave First Motions

ID	Yr	Mo/Da (UT)	Hr:Min (UTC)	Observed First Motions* Q1	Q2	Q3	Azimuthal Range** (deg)
5	1981	09/21	08:01	3	4	3	138 (202 to 340)
6	1981	09/22	05:03	9	1	2	136 (203 to 339)
7	1987	12/16	17:43	9	2	3	285 (106 to 031)
8	1992	06/03	05:08	10	2	1	277 (111 to 028)
9	1991	02/06	13:46	11	2	5	270 (123 to 033)
10	1996	10/25	18:32	14	2	4	160 (170 to 330)
12	1991	05/23	07:38	6	2	2	277 (110 to 027)
14	1993	01/21	09:01	16	6	1	212 (136 to 348)
15	1983	03/22	11:12	8	1	1	121 (203 to 324)
16	1984	03/21	11:19	8	2	1	259 (114 to 013)
18	1986	10/30	00:05	3	2	2	153 (189 to 342)

* Quality (Q) based on signal-to-noise ratio (s/n) for first-motion reading: for Q1, s/n is 3 or greater; for Q2, between 2 and 3; for Q3, less than 2.

** Range of source-to-station azimuths, in degrees, within which first motions were observed (numbers in parentheses indicate azimuths at extremes of the range, beginning and ending in a clockwise direction).

Table 4-5

Location and Focal Mechanism Information for Seismic Events of Magnitude 3.0 or Larger in the Trona-Mining District of Southwestern Wyoming, January - August 2000

Yr	MoDa (UTC)	HrMin (UTC)	Lat N	Long W	Depth* (km)	Horizontal Error** (km)	Local Magnitude	Closest Active Mine	Focal Mechanism	Ground-Truth Info. Available?
2000	01/30	14:46	41-29.23	109-45.26	0.5	4.6	4.3	Solvay Minerals	Collapse-type	YES
2000	07/16	02:05	41-36.87	109-50.69	0.5	1.9	3.0	FMC Corporation	**Shear Slip**	
2000	08/17	23:02	41-32.42	109-41.47	0.5	1.4	3.1	General Chemical	Collapse-type?	

* Fixed

** 95% confidence limits

SOURCE MECHANISMS OF MINE SEISMICITY

TYPE		EXAMPLE
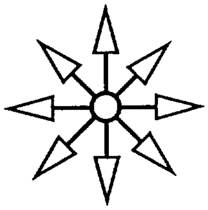	explosion	Surface mine blast
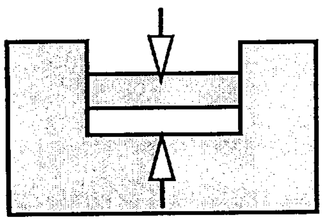	implosion	Sudden roof-floor closure due to tabular collapse (or partial closure due to loss of pillar support)
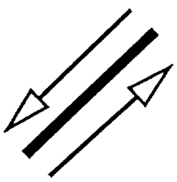	shear - slip	Shear fracture at mining opening or slip on nearby fault
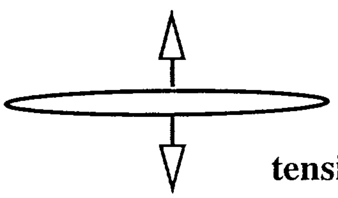	tensile fracture	Opening crack (e.g., due to parting of roof strata along horizontal interface)

Figure 4-1

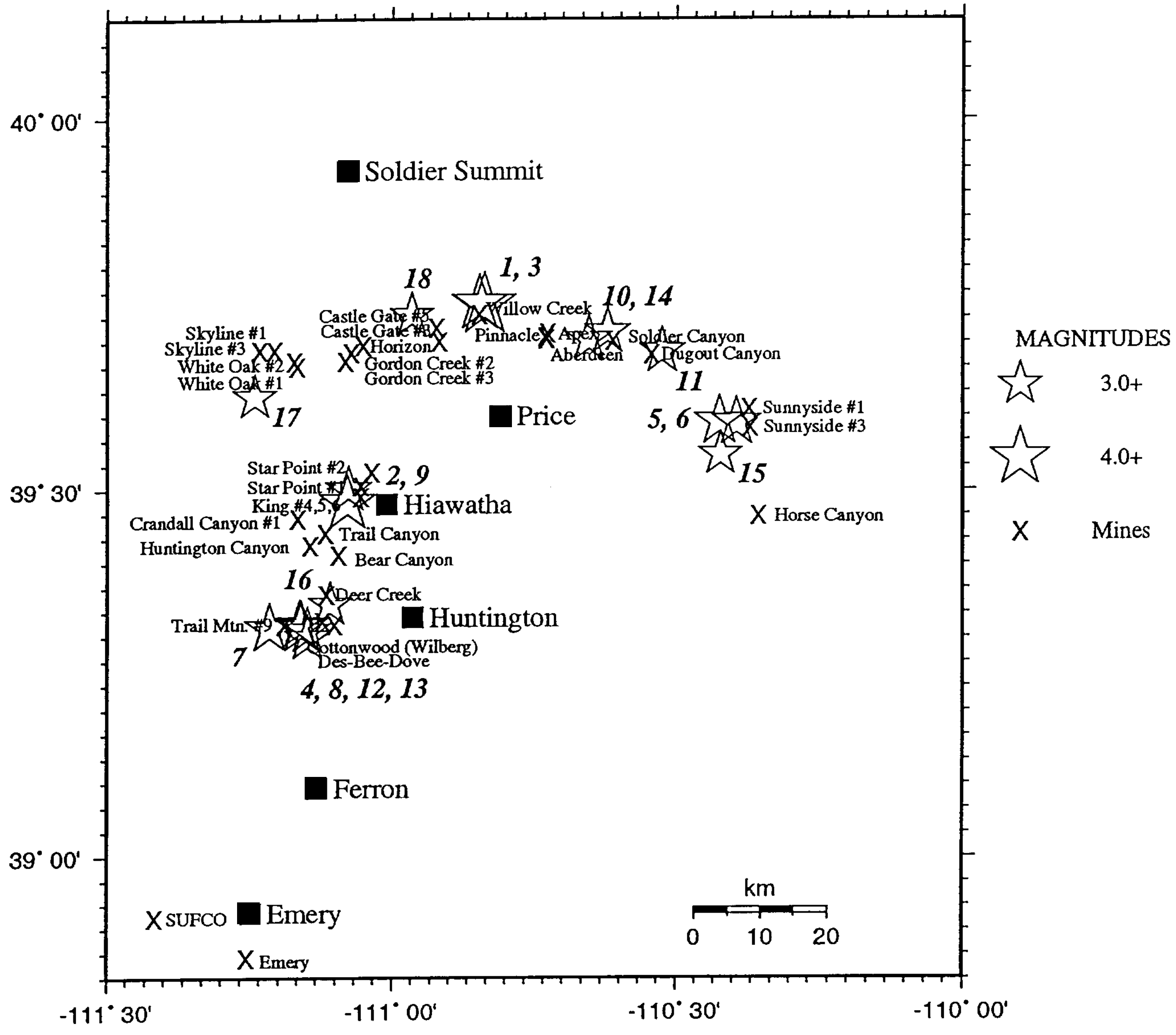

Figure 4-2. Epicenter map (keyed to Table 4-1) of seismic events of magnitude 3.0 or larger in the WP-BC coal-mining region, January 1978 through June 2000.

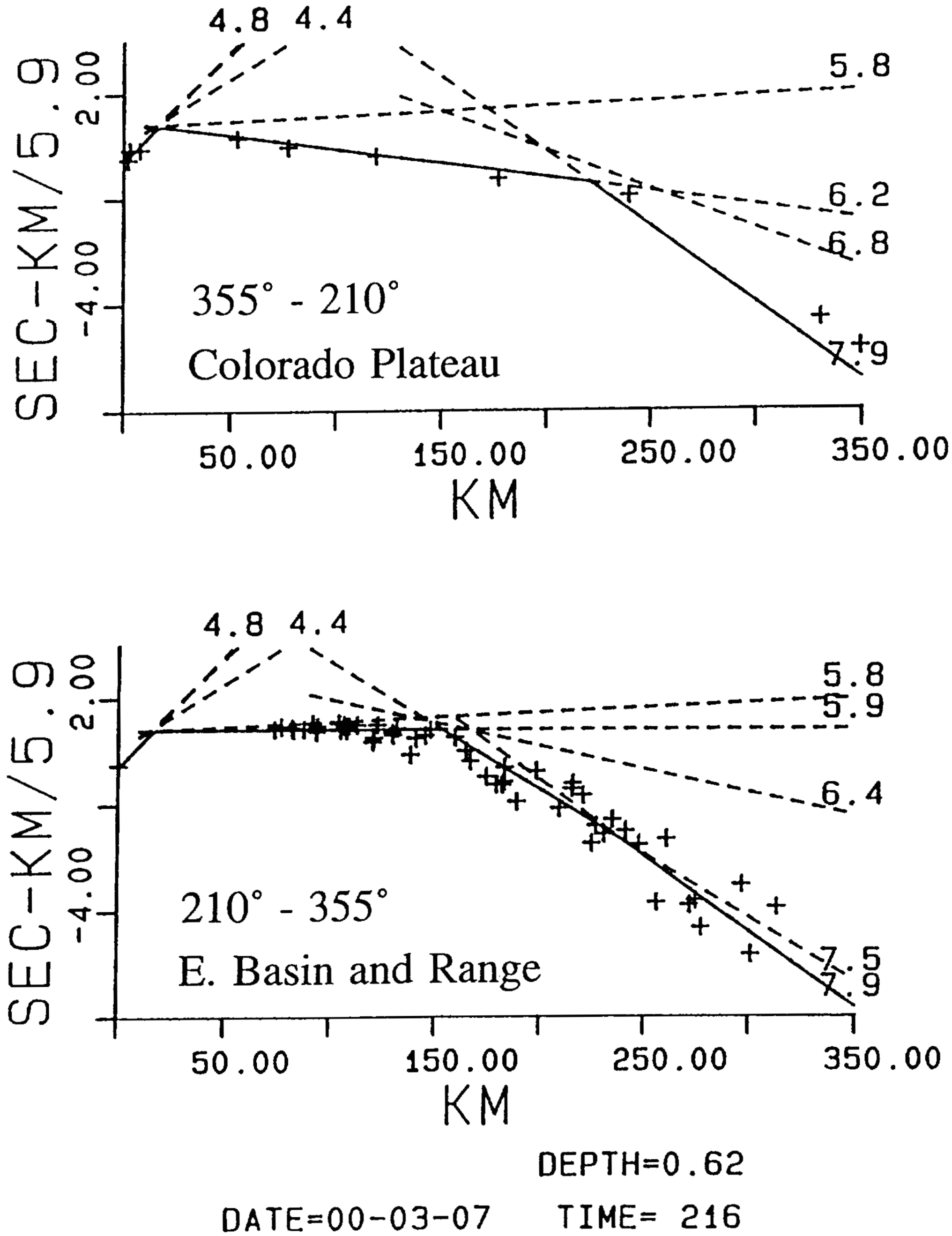

Figure 4-3. Plots of reduced travel time, time (sec) – distance (km)/5.9 km/sec, versus distance in km for the March 7, 2000, M_L 4.2 Willow Creek earthquake: (top) Colorado Plateau stations, (bottom) eastern Basin and Range stations. The crosses show observed travel times for the first arrivals. The solid lines indicate first arrival times calculated from the Willow Creek Composite velocity model (Table 4-2) for the two groups of stations. The numbers are P-wave velocities in km/sec.

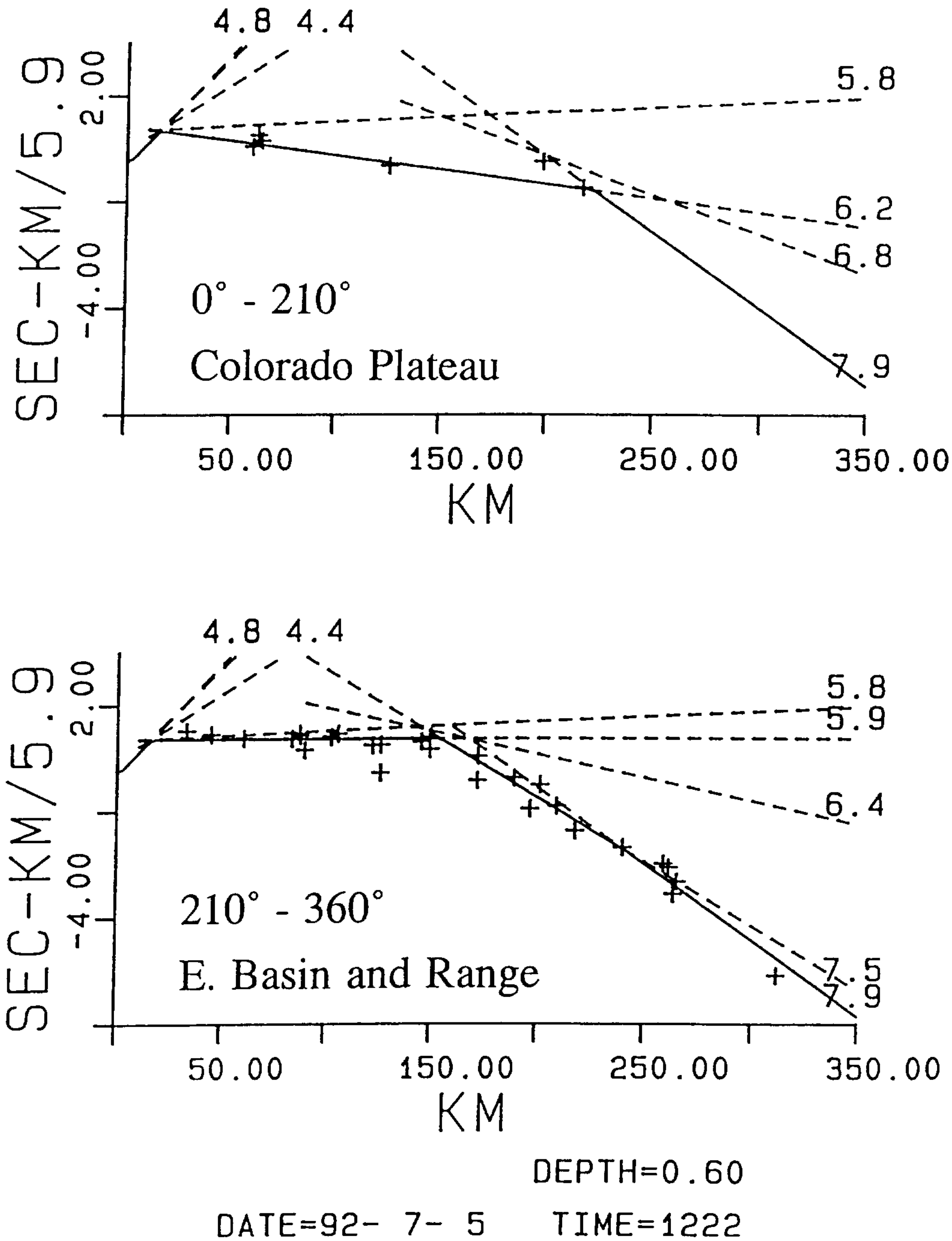

Figure 4-4. Plots of reduced travel time (reducing velocity is 5.9 km/sec) versus distance for the July 5, 1992, seismic event in the East Mountain area: (top) Colorado Plateau stations, (bottom) eastern Basin and Range stations. The solid lines indicate first arrival times calculated from the Trail Mountain Composite velocity model (Table 4-3) for these two groups of stations. See Figure 4-3 for further explanation.

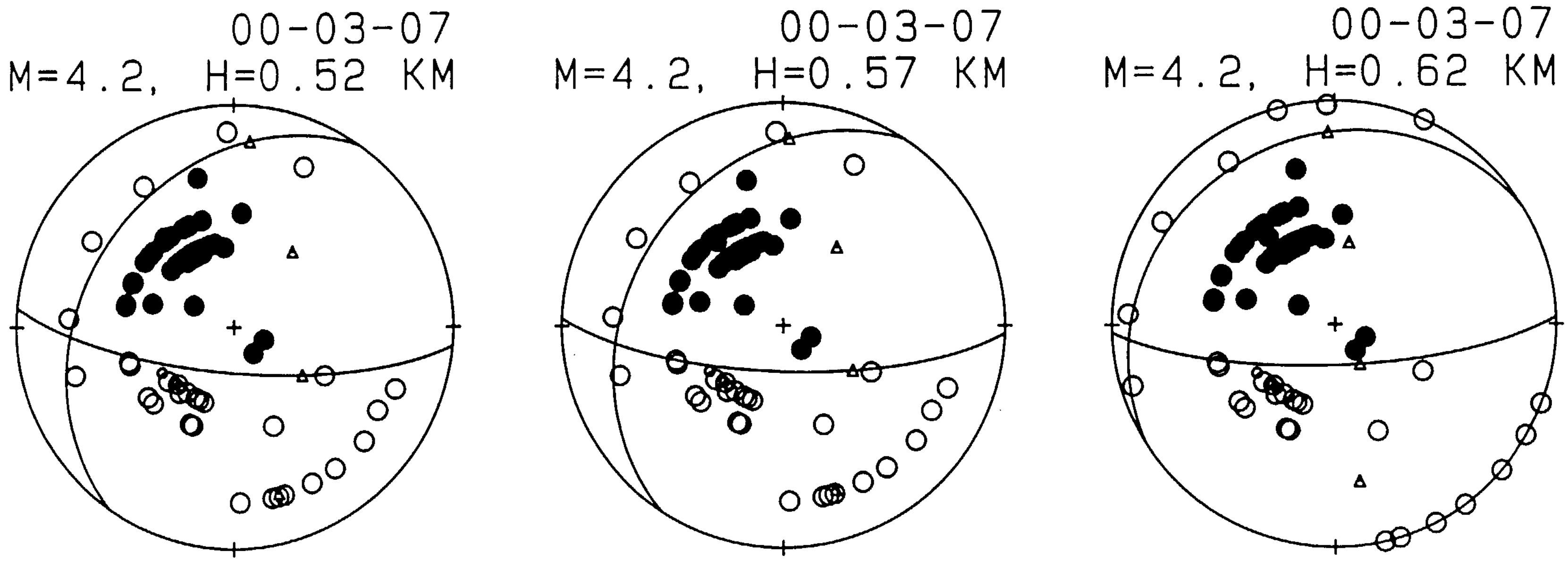

Figure 4-5. Focal mechanisms for the March 7, 2000, M_L 4.2 Willow Creek earthquake determined for three different focal depths, H, spanning the range of focal depth uncertainty: 0.57 ± .05 km. P-wave first motions are plotted on a lower-hemisphere projection, with compressions and dilatations shown as solid and open circles, respectively. Smaller circles indicate readings of lower confidence. The triangles show slip vectors and P and T axes. The best-fitting and therefore preferred mechanism is for the 0.62 km depth.

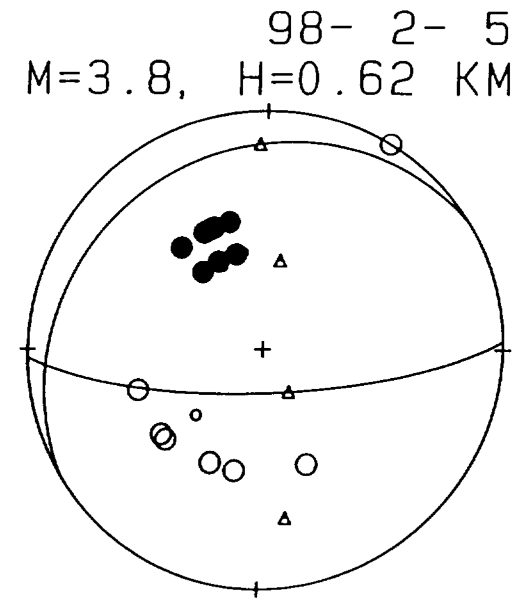

Figure 4-6. Focal mechanism for the February 5, 1998, M_L 3.8 Willow Creek earthquake determined for a fixed focal depth of 0.62 km—our preferred depth for the nearby March 7, 2000, event. The nodal planes shown are those determined for the 2000 event assuming this depth. These nodal planes fit the available first motion data, but many other sets of nodal planes would also fit. See Figure 4-5 for further explanation.

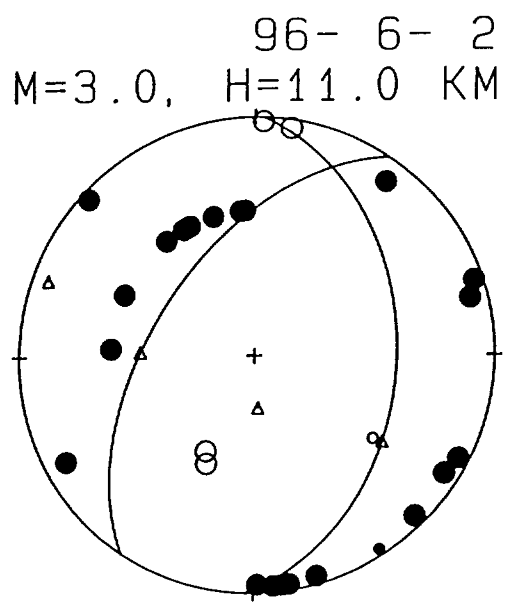

Figure 4-7. Focal mechanism for the June 2, 1996, M_L 3.0 earthquake in the northern Wasatch Plateau, computed for the well-constrained focal depth of 11.0 ± 1.5 km (95% confidence limits). See Figure 4-5 for further explanation.

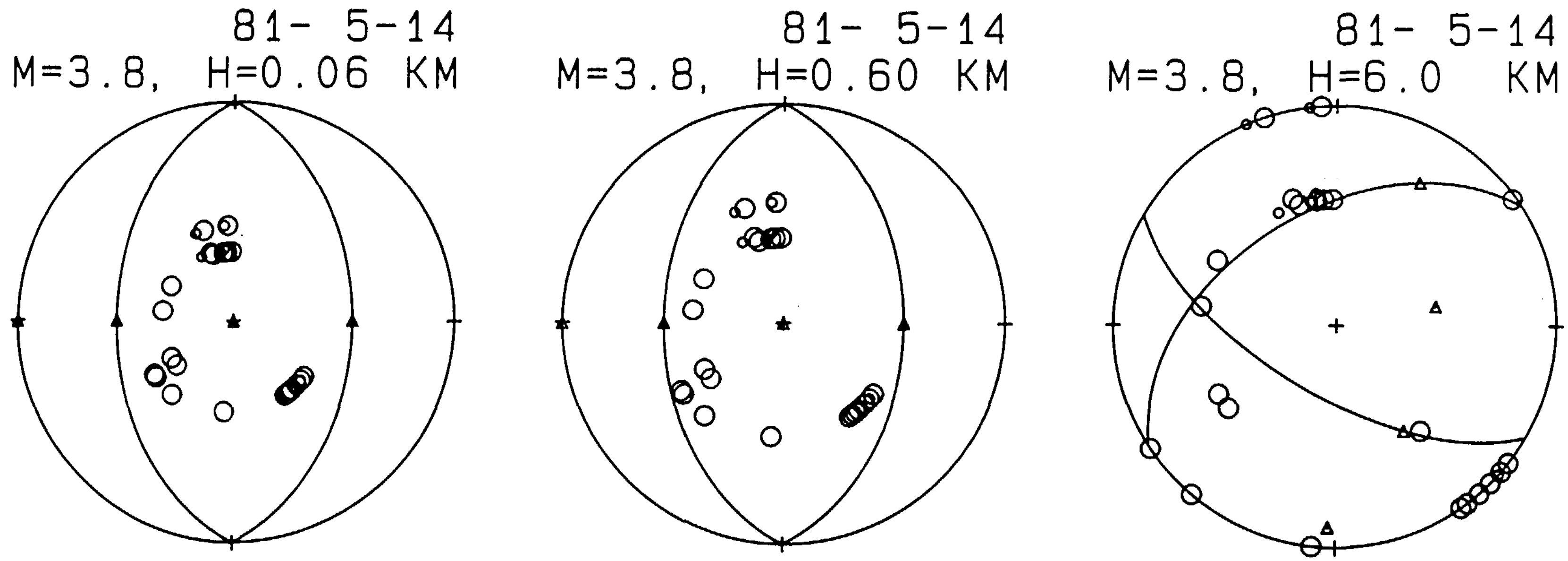

Figure 4-8. Focal mechanisms for the May 14, 1981, M_L' 3.8 earthquake in the Gentry Mountain area shown at three different focal depths, H, to illustrate the sensitivity of the focal mechanism to the poorly-constrained focal depth. The nodal planes shown on the first two plots, for focal depths of 0.06 and 0.6 km, illustrate just one of the many possible solutions which fit the first motion data. In contrast, the nodal planes on the 6.0 km focal depth plot are tightly constrained by the data. See Figure 4-5 for further explanation.

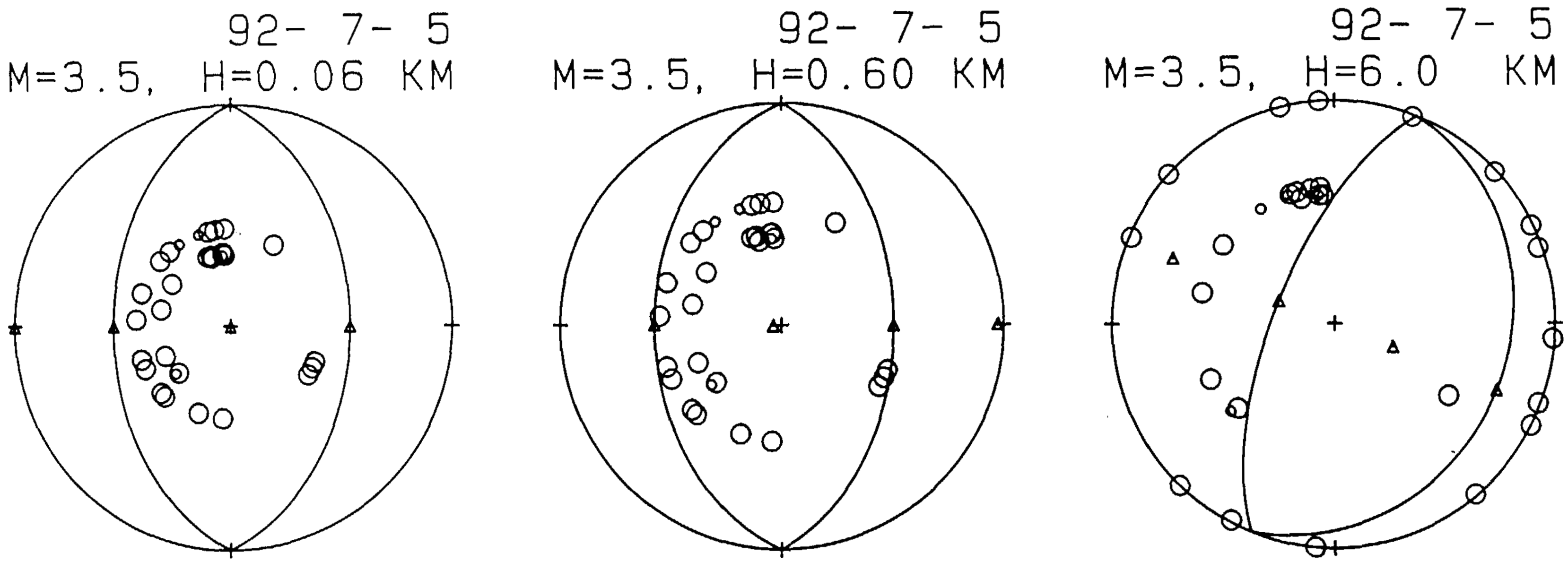

Figure 4-9. Focal mechanisms for the July 5, 1992, M_L' 3.5 earthquake in the East Mountain area shown at three different focal depths, H, to illustrate the sensitivity of the focal mechanism to the poorly-constrained focal depth. The nodal planes shown on the first two plots, for focal depths of 0.06 and 0.6 km, illustrate just one of the many possible solutions which fit the first motion data. The best-fit nodal planes shown on the 6.0 km focal depth plot do not fit the first motion data perfectly, but are reasonably well constrained. See Figure 4-5 for further explanation.

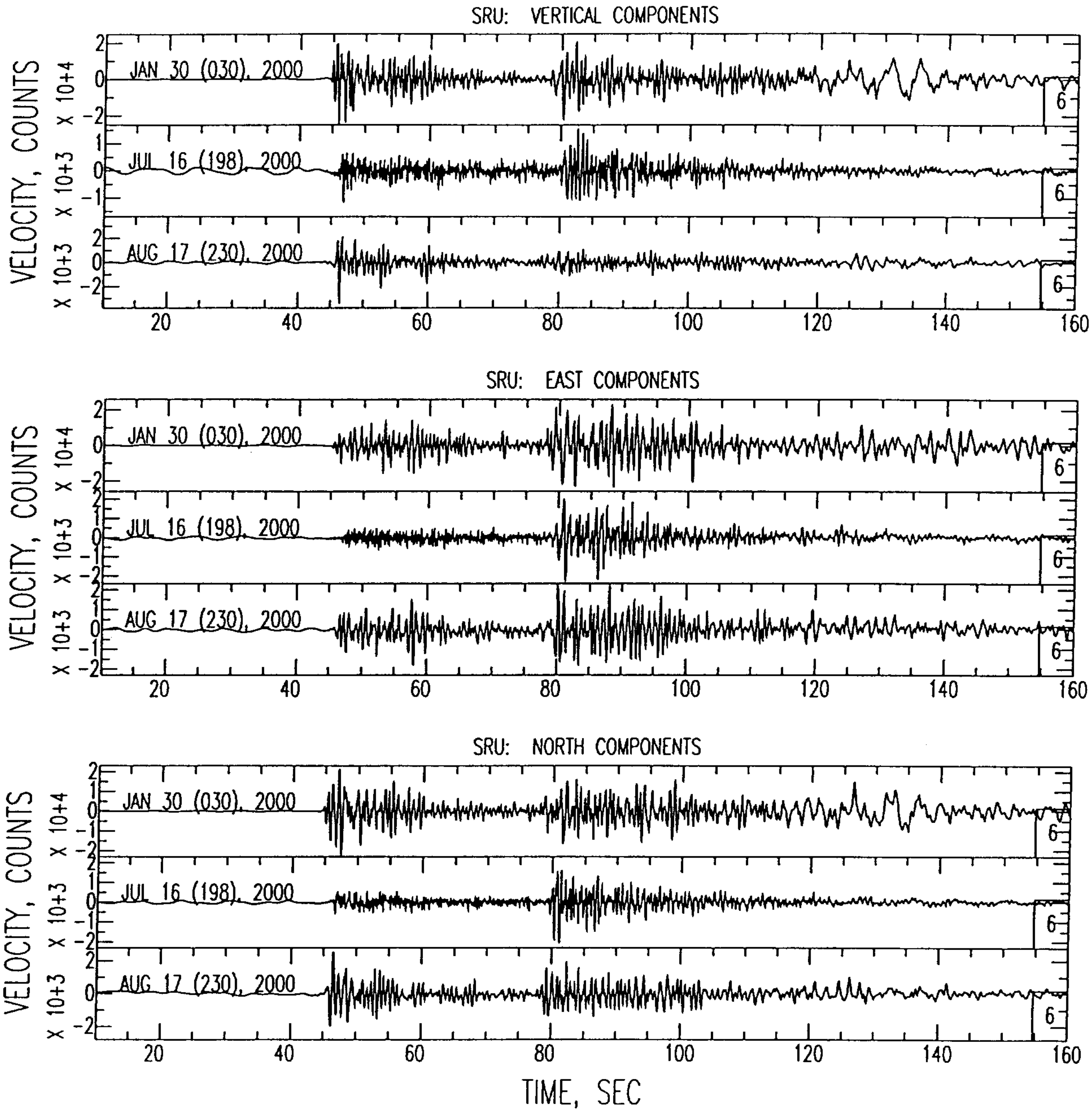

Figure 4-10. Comparison of SRU broadband recordings of the three seismic events in the trona mining area of southwestern Wyoming listed in Table 4-5. The first event is a collapse at the Solvay Mine. Note that the waveform characteristics of the first and third events are similar, but distinct from those of the second event.

5.0 REFERENCES

Arabasz, W. J. and D. R. Julander (1986). Geometry of seismically active faults and crustal deformation within the Basin and Range-Colorado Plateau transition, in *Cenozoic Tectonics of the Basin and Range Province: A Perspective on Processes and Kinematics of an Extensional Origin,* L. Mayer, Editor, *Geol. Soc. Am. Special Paper 208,* 43-74.

Arabasz, W. J. and M. K. McCarter (2000). Mine seismicity and the interface between mining engineers and seismologists (abstract), *Seismol. Res. Letters* **71** (1), 220.

Arabasz, W. J., S. J. Nava, and W. T. Phelps (1997). Mining seismicity in the Wasatch Plateau and Book Cliffs coal mining districts, Utah, USA, in *Rockbursts and Seismicity in Mines*, S. J. Gibowicz and S. Lasocki (eds.), Rotterdam: A. A. Balkema, 111-116.

Arabasz. W. J. and M. Wyss (1999). Spatially-varying b-values in coal-mining seismicity in Utah: Inferred influence of heterogeneity and stress differences on local mean magnitude (abstract), *Eos, Trans. Am. Geophys. Union* **80** (46), F651.

Bjarnason, I. T. (1987). Contemporary tectonics of the Wasatch front region, Utah, from earthquake focal mechanisms, *M.S. Thesis*, University of Utah, Salt Lake City, Utah, 79 pp.

Bjarnason, I. T. and J. C. Pechmann (1989). Contemporary tectonics of the Wasatch Front region, Utah, from earthquake focal mechanisms, *Bull. Seism. Soc. Am.* **79**, 731-755.

Boler, F. M., S. Billington, and R. K. Zipf (1997). Seismological and energy balance constraints on the mechanism of a catastrophic bump in the Book Cliffs Coal Mining District, Utah, U.S.A., *Int. J. Rock Mech. Min. Sci.* **34**, 27-43.

Brown, N. A. (1995). Union Pacific instrumental in developing Wyoming trona, *Mining Engineering*, February 1995, 135-141.

Committee on Seismic Signals from Mining Activity, National Research Council (1998). *Seismic Signals from Mining Operations and the Comprehensive Test Ban Treaty: Comments on a Draft Report by a Department of Energy Working Group*, National Academy Press, Washington, D.C., 68 pp., <http://stills.nap.edu/html/signals/index.html>.

Gearino, J. (2000). 1 injured in Solvay trona mine collapse, *Casper Star Tribune*, January 31, 2000.

Gibowicz, S. J. (1990). Keynote lecture: The mechanism of seismic events induced by mining, in *Rockbursts and Seismicity in Mines*, C. Fairhurst (ed.), Rotterdam: A. A. Balkema, 3-27.

Habermann, R. E. (1995). Opinion [on quality issues of seismicity catalogs], *Seism. Res. Letters* **66** (5), 3.

Hintze, L. F. (1988). *Geologic History of Utah,* Brigham Young University Geology Studies Special Publication 7, Department of Geology, Brigham Young University, Provo, Utah, 202 pp.

Jahanbani, F. R. (1999). *1998 Annual Review and Forecast of Utah Coal Production and*

Distribution, State of Utah Department of Natural Resources, Salt Lake City, Utah, 37 pp.

Johnson, C. E. and D. M. Hadley (1976). Tectonic implications of the Brawley earthquake swarm, Imperial Valley, California, January 1975, *Bull. Seism. Soc. Am.* **66,** 1133-1144.

Keller, G. R., R. B. Smith, and L. W. Braile (1975). Crustal structure along the Great Basin-Colorado Plateau transition from seismic refraction studies, *J. Geophys. Res.* **80,** 1093-1098.

Klein, F. W. (1978). Hypocenter location program HYPOINVERSE, *U.S. Geol. Surv., Open-File Rept. 78-694,* 113 pp.

Knoll, P. and W. Kuhnt (1990). Seismological and technical investigations of the mechanics of rockbursts, in *Rockbursts and Seismicity in Mines*, C. Fairhurst (ed.), Rotterdam: A. A. Balkema, 129-138.

Larsen, K. (1997). Cottonwood Canyon Tract lease-by-application no. 8 spring map, Energy West Mining Company, scale 1:24,000.

Loeb, D. T. (1986). The P-wave velocity structure of the crust-mantle boundary beneath Utah, *M.S. Thesis*, University of Utah, Salt Lake City, Utah, 126 pp.

Loeb, D. T. and J. C. Pechmann (1986). The P-wave velocity structure of the crust-mantle boundary beneath Utah from network travel-time measurements, *Earthquake Notes* **57** (1), 10.

Miller, L. (2000). 4.2 quake triggers rock slide on U.S. 6, *Salt Lake Tribune*, March 8, 2000.

Patton, H. J. and G. Zandt (1991). Seismic moment tensors of western U.S. earthquakes and implications for the tectonic stress field, *J. Geophys. Res.* **96,** 18,245-18,259.

Pechmann, J. C., S. J. Nava, and W. J. Arabasz (1999). Installation and calibration of five new broadband digital telemetry stations in Utah, *Seism. Res. Letters* **70**, 244.

Pechmann, J. C., W. R. Walter, S. J. Nava, and W. J. Arabasz (1995). The February 3, 1995, M_L 5.1 seismic event in the trona mining district of southwestern Wyoming, *Seism. Res. Letters* **66** (3), 25-34 [minor correction, including revision of the magnitude to M_L 5.2, added in **66,** no. 4, 28].

Phillips, W. S., D. C. Pearson, X. Yang, and B. W. Stump (1999). Aftershocks of an explosively induced mine collapse at White Pine, Michigan, *Bull. Seism. Soc. Am.* **89**, 1575-1590.

Richards, P. G. (1997). Seismological methods of verification and the International Monitoring System, in *The Comprehensive Test Ban Treaty: Issues and Answers,* M. Mckinzie (ed.), New York: Cornell University Peace Studies Program Occasional Paper No. 21, Ch. 7.

Richardson, A. M., L. J. Gilbride, J. Trackemas, and J. Mercier (1996). The influence of massive sandstones in the main roof on longwall support loading, in *Proceedings, 15th International*

Conference on Ground Control in Mining, L. Ozdemir, K. Hanna, K. Y. Haramy, and S. Peng (eds.), Colorado School of Mines, Golden, Colorado, 95-109.

Roller, R. C. (1965). Crustal structure in the eastern Colorado Plateaus province from seismic refraction measurements, *Bull. Seism. Soc. Am.* **55,** 107-119.

Taylor, S. T. (1994). False alarms and mine seismicity: An example from the Gentry Mountain mining region, Utah, *Bull. Seism. Soc. Am.* **84**, 350-358.

Swanson, P. L. and F. M. Boler (1995). The magnitude 5.3 seismic event and collapse of the Solvay Trona Mine: Analysis of pillar/floor failure stability, *U.S. Bureau of Mines Open File Rept. 86-9,* 82 pp.

Uhrhammer, R. A., W. Karavas, and B. Romanowicz (1998). Broadband seismic station installation guidelines, *Seism. Res. Lett.* **69,** 15-26.

Walter, W. R., S. L. Hunter, and L. A. Glen (1996). Preliminary report on LLNL mine seismicity deployment at the Twentymile Coal Mine, *Technical Report UCRL-ID-122800*, Lawrence Livermore National Laboratory, Livermore, California, 20 pp.

Walter, W. R., J. Swenson, W. Foxall, P. Vincent, A. J. Rodgers, and J. Bhattacharyya (2000). Complete regional waveform modeling for source and structure: A source example using the January 30, 2000 mine collapse in Wyoming, Abstract for Poster Presentation, 12th Annual IRIS Meeting, May 7-11, Rockport, Maine.

Wiemer, S. and M. Wyss (1994). Seismic quiescence before the Landers (M = 7.5) and Big Bear (M = 6.5) 1992 earthquakes, *Bull. Seism. Soc. Am.* **84,** 900-916.

Wiemer, S., R. Zuniga, and A. Allman (1995). ZMAP Version 2.1, May 1995 [interactive software program], Geophysical Institute, University of Alaska.

Williams, D. J. and W. J. Arabasz (1989). Mining-related and tectonic seismicity in the East Mountain area, Wasatch Plateau, Utah, *PAGEOPH* **129**, 345-368.

Wong, I. G. (1993). Tectonic stresses in mine seismicity: Are they significant?, in *Rockbursts and Seismicity in Mines* **93,** R. P. Youngs (ed.), Rotterdam: A. A. Balkema, 273-278.

Wong, I. G. and J. R. Humphrey (1989). Contemporary seismicity, faulting, and the state of stress in the Colorado Plateau, *Geol. Soc. Am. Bull* **101,** 1127-1146.

Wong, I. G., J. R. Humphrey, J. A. Adams, and W. J. Silva (1989). Observations of mine seismicity in the eastern Wasatch Plateau, U.S.A.: A possible case of implosional failure, *PAGEOPH* **129**, 369-405.

Wong, I. G. and A. McGarr (1990). Implosional failure in mining-induced seismicity: A critical review, in *Rockbursts and Seismicity in Mines*, C. Fairhurst (ed.), Rotterdam: A. A. Balkema, 45-51.

Woods, B. B., S. Kedar, and D. V. Helmberger (1993). M_L:M_0 as a regional seismic discriminant, *Bull. Seism. Soc. Am.* **83**, 1167-1183.

Yang, X., B. W. Stump, and W. S. Phillips (1998). Source mechanism of an explosively induced mine collapse, *Bull. Seism. Soc. Am.* **88**, 843-854.

Zuniga, R. and M. Wyss (1995). Inadvertent changes in magnitude reported in earthquake catalogs: Their evaluation through b-value estimates, *Bull. Seism. Soc. Am.* **85**, 1858-1866.

APPENDIX A

LIST OF MINING-RELATED SEISMIC EVENTS ≥ M 2.5 IN THE WASATCH PLATEAU-BOOK CLIFFS COAL MINING DISTRICTS JANUARY 1, 1978 TO JUNE 30, 2000

Summary and Data Explanation

This appendix contains a listing of seismic events of magnitude 2.5 and greater detected and located in the Wasatch Plateau and Book Cliffs coal mining districts by the University of Utah regional seismic network for the period January 1, 1978, to June 30, 2000. The geographic bounds of the sample area coincide with the two polygons shown in Figure 3-5: (1) an arcuate crescent encompassing the Wasatch Plateau and Book Cliffs coal fields and (2) an isolated area of mining in the southern Wasatch Plateau.

The computer program HYPOINVERSE (Klein, 1978) was used to process the earthquake data. For each earthquake, the following data are listed:

- Date and origin time in Universal Coordinated Time (UTC). Subtract seven hours to convert to Mountain Standard Time (MST) and six hours to convert to Mountain Daylight Time (MDT).

- Earthquake location coordinates in degrees and minutes of north latitude and west longitude, and depth in kilometers. Computed focal depths are unreliable because of poor focal-depth control (see section 3.23).

- MAG, the local magnitude (M_L) for each earthquake. "W" indicates peak amplitude measurements from Wood-Anderson seismograms were used; "h" indicates a weighted-average estimate of M_L, referred to in the main body of the report as M_L' (see section 3.21). Otherwise, the estimate is calculated from signal durations and is an empirical estimate of M_L referred to in the report as M_C' (also described in section 3.21).

- NO, the number of P and S readings used in the solution.

- GAP, the largest azimuthal separation in degrees between recording stations used in the solution.

- DMN, the epicentral distance in kilometers to the closest station.

- RMS, the root-mean-square of the travel-time residuals in seconds:

$$RMS = \left(\frac{\sum_i (W_i\ R_i)^2}{\sum_i (W_i)^2} \right)^{\frac{1}{2}}$$

where R_i is the observed minus the computed arrival time for the i-th P or S reading and W_i is the relative weight given to the i-th P or S arrival time (0.0 for no weight through 1.0 for full weight).

date	orig time	latitude	longitude	depth	mag	no	gap	dmn	rms
78 923	820 7.41	39°19.27′	111° 5.67′	7.0*	2.6	18	102	44	0.53
79 327	1711 56.32	39°35.63′	110°28.27′	7.0*	2.5	6	280	48	0.37
79 924	2226 12.93	39°19.57′	111° 7.38′	7.0*	2.5	6	139	47	0.33
791017	646 6.22	39°34.81′	110°26.39′	7.0*	2.5	8	236	48	0.37
791018	3 32.24	39°18.65′	111° 6.91′	7.0*	2.6	11	116	46	0.46
791018	653 35.61	39°18.55′	111° 7.15′	7.0*	2.5	11	136	46	0.54
791221	22 39.01	39°32.34′	110°21.02′	7.0*	2.5	12	240	47	0.60
80 301	1518 25.99	39°37.10′	110°42.90′	7.0*	2.7	10	233	93	0.62
80 815	1534 23.81	39°17.92′	111° 8.51′	7.0*	2.5	7	184	47	0.31
80 825	303 54.55	39°45.29′	110°43.48′	7.0*	2.6	6	247	65	0.40
80 910	556 4.86	39°47.22′	110°45.07′	7.7	2.6	9	202	21	0.18
801026	252 3.63	39°17.98′	111° 3.45′	7.0*	2.5	8	117	40	0.78
801227	628 3.79	39°27.00′	111° 7.90′	7.0*	2.6W	17	189	53	0.42
81 514	511 4.34	39°28.86′	111° 4.72′	0.7	3.8h	27	133	59	0.51
81 609	1912 19.35	39°30.76′	111°15.37′	1.1	2.8W	18	123	50	0.24
81 921	801 33.51	39°35.48′	110°25.47′	1.6	3.4h	15	229	50	0.38
81 922	503 59.43	39°35.35′	110°23.61′	7.5	3.3h	14	233	50	0.42
82 518	1051 21.90	39°42.82′	110°43.81′	0.2	2.8	20	192	23	0.32
821115	1659 59.23	39°30.26′	111° 4.24′	0.4	2.8	16	120	29	0.36
821125	127 59.82	39°20.09′	111° 7.42′	0.0	2.5	25	99	36	0.45
821209	1444 20.43	39°18.47′	111° 9.22′	4.5	2.7	22	93	33	0.45
83 209	2104 39.53	39°17.42′	111° 9.27′	0.5	2.5	15	91	33	0.45
83 212	1257 40.48	39°18.68′	111° 9.75′	0.5	2.6	10	92	32	0.38
83 322	1112 35.06	39°32.78′	110°25.32′	1.6	3.0h	21	239	45	0.43
83 628	2331 29.67	39°19.77′	111° 7.99′	0.6	2.5	25	97	47	0.40
84 321	1119 30.58	39°20.64′	111° 6.53′	0.1	3.0h	24	102	37	0.51
84 608	2152 21.61	39°43.96′	110°56.42′	1.4	2.5	23	169	5	0.30
84 829	909 30.57	39°19.22′	111° 9.69′	0.1	2.6	28	116	6	0.42
85 410	40 14.11	39°43.85′	110°56.18′	0.1	2.6W	24	196	5	0.40
85 505	530 56.68	39°36.48′	110°22.49′	0.4	2.5	17	243	53	0.39
85 508	324 46.64	39°36.51′	110°23.98′	0.1	2.6	17	240	52	0.43
85 627	1036 29.53	39°33.50′	110°23.74′	0.6	2.9	21	234	47	0.43
85 627	1850 23.48	39°36.00′	110°26.06′	1.1	2.5	25	219	50	0.41
85 717	1848 51.02	39°36.56′	110°23.82′	1.2	2.5	21	237	53	0.46
85 906	143 40.87	39°35.63′	110°25.19′	1.1	2.7	25	223	50	0.42
85 924	1811 2.87	39°35.30′	110°25.23′	0.6	2.5	14	163	114	0.41
851203	1755 36.17	39°42.09′	111°10.28′	1.3	2.6	22	73	17	0.34
86 211	2309 13.10	39°42.20′	110°33.88′	0.2	2.6	14	265	37	0.31
86 214	56 21.31	39°41.18′	110°31.50′	0.2	3.1h	14	239	41	0.38
86 312	617 24.67	39°19.54′	111° 5.96′	0.3	2.6W	19	177	38	0.40

date	orig time	latitude	longitude	depth	mag	no	gap	dmn	rms
86 807	2231 22.94	39°41.82′	110°44.18′	0.2	2.5W	14	254	23	0.32
86 927	734 14.80	39°33.64′	110°24.19′	0.2	2.8h	18	241	47	0.41
861030	5 42.79	39°44.11′	110°57.93′	5.6	3.0h	11	242	68	0.20
87 108	1459 2.77	39°43.95′	110°56.13′	7.5	2.6	14	175	68	0.18
87 121	1006 33.03	39°18.86′	111° 6.96′	7.5	2.5	13	115	46	0.26
87 204	2315 45.19	39°20.79′	111° 7.85′	6.8	2.6	13	118	48	0.20
87 205	1117 2.71	39°20.50′	111° 7.91′	7.1	2.7	13	118	47	0.16
87 225	1259 40.76	39°20.20′	111° 7.68′	9.1	2.8	12	117	48	0.20
87 603	1154 29.68	39°44.20′	110°55.43′	1.5	2.6W	16	110	13	0.20
87 608	29 19.90	39°34.41′	110°25.84′	8.9	2.6	8	236	42	0.18
87 715	1806 30.88	39°43.81′	110°50.47′	2.2	2.5W	13	149	10	0.21
87 803	605 52.94	39°43.70′	110°56.12′	2.9	2.5	12	109	14	0.18
87 909	1627 13.83	39°20.13′	111° 8.93′	4.9	2.7	12	114	34	0.28
87 909	1716 18.28	39°19.20′	111° 7.88′	7.0	2.5	10	200	35	0.25
87 914	725 32.83	39°41.57′	111° 7.12′	6.9	2.6	6	157	29	0.35
871216	1743 7.50	39°18.70′	111°12.92′	0.5	3.3h	26	78	28	0.44
88 125	1949 45.06	39°42.34′	110°37.95′	5.6	2.5	14	204	20	0.21
88 504	545 4.67	39°20.12′	111°10.26′	9.1	2.5	16	81	32	0.16
88 921	1758 25.89	39°18.39′	111° 9.97′	8.7	2.7	20	80	32	0.17
88 926	537 43.68	39°44.59′	110°53.65′	1.7	2.8W	22	119	10	0.20
881202	2144 10.21	39°44.30′	110°54.09′	1.1	2.7W	20	117	11	0.21
881218	443 10.77	39°41.79′	110°44.59′	2.9	2.5W	14	189	14	0.24
89 124	2337 53.54	39°20.16′	111° 9.89′	5.5	2.5	14	82	32	0.27
89 203	1808 21.24	39°44.61′	110°53.84′	0.4	2.7W	14	118	11	0.19
89 211	2037 57.29	39°20.66′	111° 9.71′	7.3	2.7	17	82	33	0.33
89 212	427 23.30	39°20.33′	111° 9.39′	0.2	2.6W	14	83	33	0.33
89 309	1433 15.42	39°42.28′	110°43.95′	0.9	2.5	12	201	14	0.37
89 713	1426 42.16	39°41.91′	110°44.09′	1.1	2.8h	11	198	15	0.12
89 804	1220 55.10	39°42.04′	110°44.91′	4.6	2.5	10	193	14	0.21
89 819	409 45.88	39°20.14′	111° 8.84′	12.2	2.5	15	84	46	0.23
891203	1734 53.29	39°42.40′	110°42.24′	1.6	2.8W	15	195	15	0.28
90 504	403 8.06	39°31.34′	111° 5.80′	3.3	2.6	15	97	40	0.25
90 901	1812 29.37	39°17.98′	111° 8.18′	8.0	2.9	10	81	35	0.21
90 927	1505 55.42	39°30.61′	111° 3.06′	8.0	2.8	13	101	39	0.27
901115	1408 28.79	39°31.40′	111° 5.77′	4.4	2.5	8	95	40	0.11
901121	1216 54.67	39°29.60′	111° 4.27′	3.5	2.9h	16	101	42	0.17
901224	632 8.27	39°29.45′	111° 3.74′	10.2	2.8h	12	102	42	0.22
91 206	1346 46.66	39°29.99′	111° 4.61′	4.3	3.1h	11	100	42	0.27
91 315	2033 14.72	39°21.05′	111°10.34′	8.5	2.8h	15	85	32	0.22
91 423	515 56.22	39°30.59′	111° 5.60′	7.9	2.5	11	97	41	0.16

date	orig time	latitude	longitude	depth	mag	no	gap	dmn	rms
91 523	736 1.81	39°17.52′	111° 9.69′	8.4	2.5	10	83	33	0.23
91 523	738 40.57	39°17.89′	111° 8.92′	12.4	3.1h	12	85	34	0.21
91 805	1730 47.07	39°17.96′	111° 9.66′	5.7	2.5	10	84	33	0.13
911029	2118 24.82	39°42.20′	110°43.38′	0.4	2.5	14	195	15	0.26
911123	1625 6.56	39°17.73′	111° 9.71′	9.1	2.6	12	83	33	0.12
92 203	711 28.03	39°42.49′	110°37.60′	7.4	2.5	7	206	20	0.20
92 501	2342 51.50	39°34.98′	110°23.23′	7.5	2.5	9	232	45	0.19
92 603	508 30.95	39°19.04′	111° 9.80′	0.6	3.2h	24	85	44	0.55
92 607	2016 29.54	39°19.15′	111° 9.10′	7.7	2.5	13	85	33	0.32
92 609	2330 18.57	39°18.13′	111° 9.57′	6.1	2.9h	16	84	33	0.30
92 705	1222 22.76	39°18.81′	111° 9.60′	5.6	3.5h	17	84	33	0.37
92 711	1323 7.62	39°18.52′	111° 8.94′	9.3	3.1h	19	85	34	0.33
92 818	1641 41.77	39°20.77′	111° 9.04′	3.0	2.9W	10	87	46	0.17
92 910	620 12.62	39°42.08′	110°37.95′	0.9	2.5W	25	162	20	0.40
921218	1050 48.13	39°43.75′	110°50.52′	1.2	2.9h	31	144	10	0.38
93 121	901 20.41	39°42.73′	110°37.26′	1.3	3.0h	26	159	20	0.32
93 123	1118 46.90	39°42.70′	110°37.58′	1.2	2.5W	22	196	20	0.35
93 714	2007 19.36	39°41.40′	111°15.33′	1.3	2.7W	11	70	40	0.28
93 927	1121 0.61	39°19.76′	111° 8.70′	0.3	2.6	22	88	34	0.43
94 216	57 7.23	39°42.11′	111°15.19′	5.0	2.5	9	74	40	0.14
94 601	48 17.69	39°42.05′	111°14.74′	0.8	2.5	7	109	39	0.49
941219	342 28.20	39°43.72′	110°49.79′	0.1	2.5	23	152	10	0.29
95 105	2123 28.93	39°42.15′	111°15.10′	4.2	2.5	12	74	39	0.16
95 315	2307 0.24	39°42.06′	111°15.21′	1.4	2.5	14	79	40	0.19
95 428	1139 1.80	39°41.81′	111°15.03′	1.7	2.5	21	71	39	0.23
95 513	1001 3.67	39°41.65′	110°39.80′	7.1	2.5	14	158	19	0.15
95 513	1413 4.67	39°42.05′	110°39.40′	5.0	2.5	11	202	19	0.24
95 519	731 30.11	39°33.18′	110°23.69′	1.3	2.5	16	173	46	0.39
95 525	512 58.16	39°41.17′	111°14.43′	1.2	2.7	9	133	39	0.05
95 528	2111 33.22	39°42.74′	110°38.89′	0.6	2.5	18	202	18	0.40
95 803	802 47.07	39°41.29′	111°14.17′	0.2	2.5	15	70	3	0.22
95 804	204 54.88	39°41.35′	111°13.97′	1.6	2.5	13	70	3	0.46
951009	2151 15.51	39°36.88′	111° 6.04′	7.4	2.7	20	90	13	0.14
951011	1336 0.49	39°37.67′	111° 6.11′	1.3	2.5	20	89	11	0.29
951108	732 52.75	39°31.20′	111° 7.58′	2.8	2.8	22	92	21	0.19
951206	741 6.10	39°41.77′	111°14.37′	0.5	2.5	13	74	3	0.28
951215	1243 22.22	39°42.37′	111°12.74′	0.2	2.5	17	80	2	0.32
951231	1823 13.22	39°41.93′	111°14.34′	0.1	2.5	23	72	3	0.31
96 202	211 14.55	39°28.00′	111°13.66′	1.2	2.8	27	81	25	0.30
96 318	724 15.42	39°41.35′	111°14.52′	1.6	2.5	15	76	3	0.30

date	orig time	latitude	longitude	depth	mag	no	gap	dmn	rms
96 429	252 19.24	39°42.11′	111°14.50′	0.3	2.7	25	70	3	0.25
96 602	809 10.02	39°37.55′	111°14.45′	5.5	3.0W	24	73	8	0.18
961018	2253 7.23	39°31.00′	111° 7.27′	2.2	2.6	11	138	21	0.09
961018	2255 17.96	39°30.86′	111° 7.43′	3.5	2.6	17	137	21	0.23
961024	2042 18.49	39°41.10′	110°40.22′	7.4	2.5	16	198	19	0.25
961025	1832 53.35	39°42.12′	110°39.24′	3.3	3.1W	20	194	19	0.21
961121	1415 46.10	39°42.47′	110°37.90′	4.1	2.5	17	203	20	0.25
961203	1120 57.33	38°59.23′	111°21.33′	0.4	2.8	14	98	24	0.31
961203	1144 59.14	38°59.49′	111°22.34′	1.3	2.6	10	96	24	0.23
961203	1255 52.56	38°59.75′	111°22.97′	0.8	2.5	14	95	24	0.20
961206	1353 13.42	39°42.38′	110°39.46′	1.1	2.8	21	200	18	0.21
961212	155 49.62	39°42.75′	110°45.45′	3.8	2.7	15	187	12	0.18
961224	1321 41.89	38°59.33′	111°22.40′	2.7	2.7	18	96	24	0.23
97 328	5 9.96	39°17.82′	111° 9.58′	5.1	2.8	15	84	33	0.24
97 404	2212 1.02	38°58.51′	111°22.19′	1.2	2.6	13	98	22	0.31
97 413	1750 47.87	39°43.09′	110°44.54′	2.8	2.6W	15	191	12	0.20
97 414	930 48.47	38°59.00′	111°22.09′	1.4	2.5	15	97	23	0.18
98 205	519 56.62	39°45.05′	110°50.73′	1.3	3.8W	17	139	8	0.23
98 504	1200 12.30	38°59.80′	111°21.92′	1.2	2.8W	19	96	25	0.18
98 509	36 25.11	38°59.25′	111°21.53′	0.7	2.5	14	97	24	0.18
98 926	1701 59.83	39°43.00′	110°45.35′	2.9	2.7	15	184	12	0.18
981108	416 39.53	39°44.91′	110°50.24′	1.5	2.6	14	145	8	0.24
981216	1918 50.13	39°43.03′	110°44.62′	2.3	2.5	13	193	12	0.23
99 206	625 44.20	39°43.15′	110°44.83′	1.0	2.6W	12	191	12	0.24
99 717	2000 18.91	38°59.23′	111°21.76′	2.5	2.5	14	97	24	0.10
0 225	402 3.10	39°45.97′	110°50.61′	0.0	2.7W	12	135	6	0.19
0 307	216 4.72	39°44.95′	110°50.19′	1.8	4.2W	24	145	8	0.18
0 420	1711 36.63	39°24.70′	111° 5.89′	4.4	2.6W	12	96	11	0.12

number of earthquakes = 148

* indicates fixed focal depth of 7.0km

APPENDIX B

QUARTERLY COAL MINE PRODUCTION FOR MINES IN THE WASATCH PLATEAU-BOOK CLIFFS COAL MINING DISTRICTS, 1995–1998

compiled by

Jefferson D. McKenzie
Department of Mining Engineering
University of Utah

University of Utah

State of Utah Coal Production by Quarter [1]

For the year: 1995

Company Name	Mine or Prep. Plant/Loadout	Clean Tons Produced 1st Qtr	2nd Qtr	3rd Qtr	4th Qtr	Total	County	Mine Fed ID #
ENERGY WEST MINING COMPANY	DEER CREEK MINE	1,103,344	1,088,679	958,461	989,540	4,140,024	EMERY	4200121
SOUTHERN UTAH FUEL COMPANY	SUFCO	695,951	1,122,361	893,910	1,084,291	3,796,513	SEVIER	4200089
UTAH FUEL COMPANY	SKYLINE MINE NO. 3	1,003,643	910,094	599,544	701,746	3,215,027	CARBON	4201566
CYPRUS PLATEAU MINING CORPORATION	STAR POINT #2	645,273	761,637	742,175	697,635	2,846,720	CARBON	4200171
ENERGY WEST MINING COMPANY	COTTONWOOD MINE	867,674	693,306	594,377	217,597	2,372,954	EMERY	4201944
GENWAL RESOURCES, INC.	CRANDALL CANYON MINE	398,173	419,894	665,445	596,379	2,079,891	EMERY	4201715
UTAH FUEL COMPANY	SKYLINE MINE NO. 1	92,443	422,371	589,867	625,717	1,730,398	CARBON	4201435
ANDALEX RESOURCES, INC.	PINNACLE	446,214	323,994	371,420	268,237	1,409,865	CARBON	4201474
ENERGY WEST MINING COMPANY	TRAIL MOUNTAIN MINE	129,001	195,667	205,310	612,218	1,142,196	EMERY	4201211
WHT OAK MINING & CONSTR CO., Inc.	WHITE OAK MINE #2	264,399	157,772	280,536	332,562	1,035,269	CARBON	4201280
ANDALEX RESOURCES, INC.	ABERDEEN	124,850	137,806	133,885	130,406	526,947	CARBON	4202028
SOLDIER CREEK COAL COMPANY	SOLDIER CANYON	163,116	149,223	78,649	89,907	480,895	CARBON	4200077
SAVAGE INDUSTRIES, INC.	[2] SUNNYSIDE FACILITY	96,500	37,162	117,375	119,118	370,155	CARBON	4202093
C.W. MINING COMPANY (CO-OP MINING)	BEAR CANYON NO. 2	0	0	90,131	131,435	221,566	SEVIER	4202095
C.W. MINING COMPANY (CO-OP MINING)	BEAR CANYON NO. 1	102,530	0	0	0	102,530	SEVIER	4201697
CONSOLIDATION COAL COMPANY	EMERY	0	0	0	0	0	EMERY	4200079
NEVADA ELECTRIC INVESTMENT CO.	WELLINGTON LOADOUT	0	0	0	0	0	CARBON	4200099
WHT OAK MINING & CONSTR CO., Inc.	WHITE OAK MINE #1	0	0	0	0	0	CARBON	4201279
SAVAGE INDUSTRIES INC.	SAVAGE COAL TERMINAL	0	0	0	0	0	CARBON	4201444
ANDALEX RESOURCES, INC.	APEX	0	0	0	0	0	CARBON	4201750
SOLDIER CREEK COAL COMPANY	BANNING TRAIN LOADOUT	0	0	0	0	0	CARBON	4201756
CONSOLIDATION COAL COMPANY	EMERY SURFACE MINE	0	0	0	0	0	EMERY	4201778
CONSOLIDATION COAL COMPANY	EMERY PREPARATIOM PLANT	0	0	0	0	0	EMERY	4201779
ANDALEX RESOURCES, INC.	WILDCAT LOADOUT	0	0	0	0	0	CARBON	4201864
ENERGY WEST MINING COMPANY	COTTONWOOD COAL BLENDING & PREP	0	0	0	0	0	EMERY	4202052
					Total for Year	25,470,950		

[1] Taken from US Dept. of Labor Mine Safety and Health Administration (MSHA) Statistics
"Mine Accident, Injury, Illness, Employment and Coal Production Statistics"
"Year 2000 Compliant Part 50 Data Self-extracting Files"
(Reporting required by law -- 30 U.S.C. Sec. 813; 30 C.F.R. Part 50)

25-Jul-00 : JDM

[2] Not new coal production, use of previously discarded coal washery tailings.

University of Utah

State of Utah Coal Production by Quarter [1]
For the year: 1996

		Clean Tons Produced						Mine
Company Name	Mine or Prep. Plant/Loadout	1st Qtr	2nd Qtr	3rd Qtr	4th Qtr	Total	County	Fed ID #
ENERGY WEST MINING COMPANY	DEER CREEK MINE	1,051,715	1,211,578	876,853	1,197,853	4,337,999	EMERY	4200121
CANYON FUEL COMPANY, LLC	SUFCO	1,243,593	1,066,659	886,987	1,005,240	4,202,479	SEVIER	4200089
ENERGY WEST MINING COMPANY	TRAIL MOUNTAIN MINE	943,823	977,625	932,063	972,135	3,825,646	EMERY	4201211
CANYON FUEL COMPANY, LLC	SKYLINE MINE NO. 3	750,269	760,215	911,484	737,758	3,159,726	CARBON	4201566
CYPRUS PLATEAU MINING CORPORAT	STAR POINT #2	791,972	836,105	703,181	702,483	3,033,741	CARBON	4200171
GENWAL RESOURCES, INC.	CRANDALL CANYON MINE	611,994	630,787	584,966	649,497	2,477,244	EMERY	4201715
ANDALEX RESOURCES, INC.	ABERDEEN	684,059	692,018	592,586	462,547	2,431,210	CARBON	4202028
CANYON FUEL COMPANY, LLC	SKYLINE MINE NO. 1	316,621	387,622	418,911	559,466	1,682,620	CARBON	4201435
WHITE OAK MINING & CONSTRUCTIO	WHITE OAK MINE #2	285,552	245,604	264,851	272,638	1,068,645	CARBON	4201280
CANYON FUEL COMPANY, LLC	SOLDIER CANYON	196,831	222,702	275,254	281,856	976,643	CARBON	4200077
C.W. MINING COMPANY (CO-OP MIN	BEAR CANYON NO. 2	142,049	154,439	115,336	168,713	580,537	SEVIER	4202095
SAVAGE INDUSTRIES, INC.	[2] SUNNYSIDE FACILITY	111,320	58,378	74,698	97,793	342,189	CARBON	4202093
CYPRUS PLATEAU MINING CORP.	WILLOW CREEK MINE	0	0	20,760	10,200	30,960	CARBON	4202113
CONSOLIDATION COAL COMPANY	EMERY	0	0	0	0	0	EMERY	4200079
NEVADA ELECTRIC INVESTMENT CO.	WELLINGTON LOADOUT	0	0	0	0	0	CARBON	4200099
WHT OAK MINING & CONSTR CO., I	WHITE OAK MINE #1	0	0	0	0	0	CARBON	4201279
SAVAGE INDUSTRIES INC.	SAVAGE COAL TERMINAL	0	0	0	0	0	CARBON	4201444
ANDALEX RESOURCES, INC.	PINNACLE	0	0	0	0	0	CARBON	4201474
C.W. MINING COMPANY (CO-OP MIN	BEAR CANYON NO. 1	0	0	0	0	0	SEVIER	4201697
ANDALEX RESOURCES, INC.	APEX	0	0	0	0	0	CARBON	4201750
CANYON FUEL COMPANY, LLC	BANNING TRAIN LOADOUT	0	0	0	0	0	CARBON	4201756
CONSOLIDATION COAL COMPANY	EMERY SURFACE MINE	0	0	0	0	0	EMERY	4201778
CONSOLIDATION COAL COMPANY	EMERY PREPARATIOM PLA	0	0	0	0	0	EMERY	4201779
ANDALEX RESOURCES, INC.	WILDCAT LOADOUT	0	0	0	0	0	CARBON	4201864
ENERGY WEST MINING COMPANY	COTTONWOOD MINE	0	0	0	0	0	EMERY	4201944
ENERGY WEST MINING COMPANY	COTTONWOOD COAL BLEND	0	0	0	0	0	EMERY	4202052
UNITED STATES FUEL COMPANY	KING MINE					0	CARBON	4202157
					Total for Year	28,149,639		

[1] Taken from US Dept. of Labor Mine Safety and Health Administration (MSHA) Statistics
"Mine Accident, Injury, Illness, Employment and Coal Production Statistics"
"Year 2000 Compliant Part 50 Data Self-extracting Files"
(Reporting required by law -- 30 U.S.C. Sec. 813; 30 C.F.R. Part 50)

25-Jul-00 : JDM

[2] Not new coal production, use of previously discarded coal washery tailings.

University of Utah
State of Utah Coal Production by Quarter [1]
For the year: 1997

		Clean Tons Produced						Mine
Company Name	Mine or Prep. Plant/Loadout	1st Qtr	2nd Qtr	3rd Qtr	4th Qtr	Total	County	Fed ID #
CANYON FUEL COMPANY, LLC	SUFCO	1,171,645	1,445,281	1,119,616	1,160,956	4,897,498	SEVIER	4200089
ENERGY WEST MINING COMPANY	DEER CREEK MINE	1,150,385	1,299,051	880,966	1,149,304	4,479,706	EMERY	4200121
ENERGY WEST MINING COMPANY	TRAIL MOUNTAIN MINE	789,606	1,168,912	782,895	1,186,166	3,927,579	EMERY	4201211
CANYON FUEL COMPANY, LLC	SKYLINE MINE NO. 3	960,226	152,299	882,834	910,975	2,906,334	CARBON	4201566
GENWAL RESOURCES, INC.	CRANDALL CANYON MINE	594,796	757,839	681,133	628,679	2,662,447	EMERY	4201715
ANDALEX RESOURCES, INC.	ABERDEEN	409,142	477,972	520,611	449,298	1,857,023	CARBON	4202028
CANYON FUEL COMPANY, LLC	SKYLINE MINE NO. 1	171,401	867,812	126,194	243,709	1,409,116	CARBON	4201435
CYPRUS PLATEAU MINING CORPORAT	STAR POINT NO.2	510,040	301,424	347,931	231,780	1,391,175	CARBON	4200171
CANYON FUEL COMPANY, LLC	SOLDIER CANYON	275,234	307,843	295,687	270,975	1,149,739	CARBON	4200077
WHITE OAK MINING & CONSTRUCTIO	WHITE OAK MINE #2	242,047	250,907	158,312	88,550	739,816	CARBON	4201280
C.W. MINING COMPANY (CO-OP MIN	BEAR CANYON NO. 2	188,552	194,996	95,197	91,315	570,060	SEVIER	4202095
SUNNYSIDE COGENERATION ASSOCIA	[2] SUNNYSIDE WASTE COAL SITE	107,702	99,360	88,992	111,813	407,867	CARBON	4202093
WHT OAK MINING & CONSTR CO., I	WILLOW CREEK MINE	27,579	34,854	178,558	91,808	332,799	CARBON	4202113
HORIZON MINING, LLC	WHITE OAK MINE #1	0	0	27,423	115,373	142,796	CARBON	4201279
CONSOLIDATION COAL COMPANY	HORIZON MINE	0	0	0	8,860	8,860	CARBON	4202074
COVOL TECHNOLOGIES, INC.	EMERY	0	0	0	0	0	EMERY	4200079
SAVAGE INDUSTRIES INC.	WELLINGTON, UT PREPARATION PLA	0	0	0	0	0	CARBON	4200099
ANDALEX RESOURCES, INC.	SAVAGE COAL TERMINAL	0	0	0	0	0	CARBON	4201444
C.W. MINING COMPANY (CO-OP MIN	PINNACLE	0	0	0	0	0	CARBON	4201474
ANDALEX RESOURCES, INC.	BEAR CANYON NO. 1	0	0	0	0	0	SEVIER	4201697
CANYON FUEL COMPANY, LLC	APEX	0	0	0	0	0	CARBON	4201750
CONSOLIDATION COAL COMPANY	BANNING TRAIN LOADOUT	0	0	0	0	0	CARBON	4201756
CONSOLIDATION COAL COMPANY	EMERY SURFACE MINE	0	0	0	0	0	EMERY	4201778
ANDALEX RESOURCES, INC.	EMERY PREPARATIOM PLANT	0	0	0	0	0	EMERY	4201779
CANYON FUEL COMPANY, LLC	WILDCAT LOADOUT	0	0	0	0	0	CARBON	4201864
ENERGY WEST MINING COMPANY	DUGOUT CANYON MINE					0	CARBON	4201890
ENERGY WEST MINING COMPANY	COTTONWOOD MINE	0	0	0	0	0	EMERY	4201944
CYPRUS PLATEAU MINING CORP.	COTTONWOOD COAL BLENDING & PRE	0	0	0	0	0	EMERY	4202052
UNITED STATES FUEL COMPANY	KING MINE	0	0	0	0	0	CARBON	4202157
					Total for Year	26,882,815		

[1] Taken from US Dept. of Labor Mine Safety and Health Administration (MSHA) Statistics
"Mine Accident, Injury, Illness, Employment and Coal Production Statistics"
"Year 2000 Compliant Part 50 Data Self-extracting Files"
(Reporting required by law -- 30 U.S.C. Sec. 813; 30 C.F.R. Part 50)

25-Jul-00 : JDM

[2] Not new coal production, use of previously discarded coal washery tailings.

University of Utah
State of Utah Coal Production by Quarter [1]
For the year: 1998

Company Name	Mine or Prep. Plant/Loadout	Clean Tons Produced 1st Qtr	2nd Qtr	3rd Qtr	4th Qtr	Total	County	Mine Fed ID #
CANYON FUEL COMPANY, LLC	SUFCO	918,490	1,608,734	1,555,167	1,636,780	5,719,171	SEVIER	4200089
ENERGY WEST MINING COMPANY	DEER CREEK MINE	1,074,312	1,001,318	791,749	919,919	3,787,298	EMERY	4200121
GENWAL RESOURCES, INC.	CRANDALL CANYON MINE	866,207	710,226	900,225	1,040,980	3,517,638	EMERY	4201715
ENERGY WEST MINING COMPANY	TRAIL MOUNTAIN MINE	990,214	735,914	590,318	1,102,233	3,418,679	EMERY	4201211
CANYON FUEL COMPANY, LLC	SKYLINE MINE NO. 3	347,459	619,367	897,070	1,051,878	2,915,774	CARBON	4201566
ANDALEX RESOURCES, INC.	ABERDEEN	350,624	462,132	507,918	433,087	1,753,761	CARBON	4202028
PLATEAU MINING CORP.	WILLOW CREEK MINE	144,582	170,908	488,123	503,360	1,306,973	CARBON	4202113
CANYON FUEL COMPANY, LLC	SKYLINE MINE NO. 1	706,937	312,101	116,622	0	1,135,660	CARBON	4201435
CYPRUS PLATEAU MINING CORPORAT	STAR POINT NO.2	206,364	227,068	282,400	242,862	958,694	CARBON	4200171
C.W. MINING COMPANY (CO-OP MIN	BEAR CANYON NO. 2	117,201	181,219	235,539	126,243	660,202	SEVIER	4202095
CANYON FUEL COMPANY, LLC	SOLDIER CANYON	300,937	153,582	106,951	12,131	573,601	CARBON	4200077
SUNNYSIDE COGENERATION ASSOCIA	[2] SUNNYSIDE WASTE COAL SITE	128,542	96,457	125,389	98,436	448,824	CARBON	4202093
LODESTAR ENERGY, INC.	WHITE OAK MINE #2	0	91,477	140,636	103,046	335,159	CARBON	4201280
LODESTAR ENERGY, INC.	WHITE OAK MINE #1	176,678	116,535	0	0	293,213	CARBON	4201279
CANYON FUEL COMPANY, LLC	DUGOUT CANYON MINE	0	0	34,410	134,068	168,478	CARBON	4201890
LODESTAR ENERGY, INC	HORIZON MINE	38,951	22,573	19,594	16,101	97,219	CARBON	4202074
CONSOLIDATION COAL COMPANY	EMERY	0	0	0	0	0	EMERY	4200079
COVOL TECHNOLOGIES, INC.	WELLINGTON, UT PREPARATION PLA	0	0	0	0	0	CARBON	4200099
SAVAGE INDUSTRIES INC.	SAVAGE COAL TERMINAL	0	0	0	0	0	CARBON	4201444
ANDALEX RESOURCES, INC.	PINNACLE	0	0	0	0	0	CARBON	4201474
C.W. MINING COMPANY (CO-OP MIN	BEAR CANYON NO. 1	0	0	0	0	0	SEVIER	4201697
ANDALEX RESOURCES, INC.	APEX	0	0	0	0	0	CARBON	4201750
CANYON FUEL COMPANY, LLC	BANNING TRAIN LOADOUT	0	0	0	0	0	CARBON	4201756
CONSOLIDATION COAL COMPANY	EMERY SURFACE MINE	0	0	0	0	0	EMERY	4201778
CONSOLIDATION COAL COMPANY	EMERY PREPARATIOM PLANT	0	0	0	0	0	EMERY	4201779
ANDALEX RESOURCES, INC.	WILDCAT LOADOUT	0	0	0	0	0	CARBON	4201864
ENERGY WEST MINING COMPANY	COTTONWOOD COAL BLENDING & PRE	0	0	0	0	0	EMERY	4202052
HIAWATHA COAL COMPANY	KING MINE	0	0	0	0	0	CARBON	4202157
WEST RIDGE RESOURCES, INC.	WEST RIDGE MINE					0	CARBON	4202233
COVOL TECHNOLOGIES, INC.	UTAH SYNFUELS					0	CARBON	4202238
					Total for Year	27,090,344		

[1] Taken from US Dept. of Labor Mine Safety and Health Administration (MSHA) Statistics
"Mine Accident, Injury, Illness, Employment and Coal Production Statistics"
"Year 2000 Compliant Part 50 Data Self-extracting Files"
(Reporting required by law – 30 U.S.C. Sec. 813; 30 C.F.R. Part 50)

25-Jul-00 : JDM

APPENDIX C

DOCUMENTATION OF GROUND TRUTH FOR SIGNIFICANT SEISMIC EVENTS RELATED TO UNDERGROUND MINING IN UTAH AND WYOMING

by

Michael K. McCarter
Department of Mining Engineering
University of Utah

DOCUMENTATION OF GROUND TRUTH FOR SIGNIFICANT SEISMIC EVENTS RELATED TO UNDERGROUND MINING IN UTAH AND WYOMING

by

Michael K. McCarter
Department of Mining Engineering
University of Utah

The purpose of this section is to present in a systematic way ground-truth information for eight seismic events (Table C-1) related either to underground coal mining (seven events) in the Wasatch Plateau-Book Cliffs coal mining region of east-central Utah or to underground trona mining (one event) in southwestern Wyoming. The rationale for this effort is described more fully in the main body of this report in sections 1.0, 1.1, and 3.4.

Figure 3-15 demonstrates a close spatial relationship between mining and seismic events in the Wasatch Plateau-Book Cliffs area. Table 3-3 lists 18 of these events of magnitude 3.0 or larger which occurred between January 1978 and June 2000. We set out to obtain as much information as possible concerning operations in underground mines closest to the epicenter at the time of each of these 18 events. The threshold magnitude of 3.0 was selected to reduce the total number of recorded events to a reasonable subset and to increase the prospect of recovering substantial data from mine records or living memory. It was likely that such information would be more readily available for the larger events than the more routine smaller disturbances.

As shown on Table C-1, data for seven of the 18 events listed in Table 3-3 have been successfully obtained. In addition, data have also been obtained for an event which occurred on January 30, 2000 related to a panel collapse in the Solvay mine in southwestern Wyoming. Details for the remaining events in Table 3-3 may yet be obtained, but additional work – beyond the scope of this project – is needed to link those events and specific underground observations.

An outline format in the form of a "Data Sheet"was selected to ensure consistent reporting of pertinent factors. Where possible, each outline is accompanied by a sketch, showing configurations of mine openings and type of mining being conducted at the time of the event. In some cases, such as a major roof fall, the cause (mining configurations) and the effect (seismic event) are strongly related. In other cases, the reported conditions underground may well be the effect rather than the cause. Relating cause and effect requires a hypothesis concerning the mechanism and accompanying energy yield which can be confirmed with field observations. Thus, part of the objective of documenting the field conditions is to assist, over time, with such analyses.

Each Data Sheet includes the following information fields:

Date and time - The date and time are referenced to UTC. Consequently, there can be an apparent inconsistency between times recorded on incident reports (local time) and UTC. Local Mountain Standard Time is seven hours earlier than the recorded UTC. Local Mountain Daylight Time is six hours earlier than the recorded UTC.

Magnitude - The magnitude M_L is the local magnitude from Table 3-3 of this report (see Arabasz, Nava and Phelps, 1997, and section 3.2).

Location - The location is reported by cluster as defined on Table 3-15 and the name of the USGS 7.5 minute quadrangle in which the underground workings are located. A more complete listing of mines that occur in each cluster is included on Table 3-4. In addition, the location field identifies the closest mine for reference purposes. In some instances there is more than one mine in a given cluster and some clusters are closely related spatially. Therefore, it is possible that the reported underground observations may be the effect of a nearby seismic event rather than the cause.

Computed epicenter location - The computed epicenter is the calculated location of the event in both latitude and longitude as well as state plane coordinates. In the case of events recorded in Utah, the state plane coordinates are defined by NAD27, Utah Central Lambert Conformal projection. For Wyoming, the system is the West Central Transverse Mercator projection defined according to NAD27. The latitude and longitude are also based on NAD27, these systems are easily identifiable on the USGS quadrangle maps identified under the heading "location."

Computed focal depth - These values are based on the best information available but most are not well constrained because of the geographic location of recording sites.

Location of affected workings - The geographic position of observed roof falls, panel collapse, pillar failure, and the like is given in latitude and longitude as well as state plane coordinates as defined above. The intention here is to provide locations which may be used to help verify the mechanism involved in generating the seismic event or assist in evaluating the velocity model used to calculate the epicenters. In addition, the geographic location of affected working may assist in determining the likely offset in epicenter location due to uncertainty in the velocity model. Each sketch includes marks with approximate state plane coordinate locations. This was done to assist future research where spatial relationships may be of importance.

Area affected - This data field was included to provide a quantitative measure of the area of underground workings involved. In some cases, this value may assist in calculating the available energy which could be released by movement of the associated volume through a vertical distance as identified as vertical displacement.

Vertical displacement - In the case of pillar failure or panel collapse, the roof and floor of the mine may converge. If measurements were recorded or if estimates could be made, the data were included under this entry.

Mean elevation of surface topography - Coordinating locations with the USGS quadrangles provides additional information, not only on mean elevation, but also on topographic configurations. In central Utah, many of the events correlate with mines that are beneath rugged terrain characterized by escarpments and deep canyons.

Elevation of mining horizon or depth of cover - Mine records and maps frequently record the depth of cover. When this information is not so designated, the elevation of the mining horizon and elevation of topography are given which allow calculation of the depth of mining. This information should help resolve questions concerning computed focal depth.

Geologic conditions - Geologic conditions of the overlying strata and attitude of the mining horizon (coal or trona seam) are presented. Factors which may be of particular interest include: presence of massive sandstone layers, relatively stiff floor or roof materials, and strength of seams relative to the roof and floor.

Underground observations attending event - Information concerning mining method and operational details were recorded under this heading.

Reference source - The individuals who provided information concerning underground conditions are identified here for purposes of documentation and attribution.

Mining Methods – The data sheets were prepared assuming the reader has some familiarity with mining methods used in western bedded deposits. However, to clarify terms used in the data sheets, the following brief descriptions are provided:

Mining of western underground bedded deposits (coal and trona) may be accomplished by either "room and pillar" or "longwall" mining. Both methods require similar preliminary development openings to access the deposit but differ primarily in the machinery used to harvest the deposit in the production phase. Longwall is the most common method for recovering coal in the western United States. Room and pillar is the most common method to recover trona; however, longwall mining is now being applied by some of the trona producers.

Development openings, referred to as entries, serve to connect the mine to the surface. The main entry is centrally located relative to the deposit and consists of three or more parallel openings. It is used for ventilation, materials handling and travel by personnel and equipment. The mains are interconnected by crosscuts which are necessary for equipment access and proper ventilation. After the mains are completed, the deposit is subdivided into rectangular-shaped production areas (panels) by panel entries and submains. Room entries may be used to create smaller production panels. If the development openings are extended to the limit of the permitted area, and production begins at this boundary and progresses toward the mains, the mine is operating on the retreat.

Longwall panels range up to 300 m in width and 2700 m in length. Nearly horizontal tabular deposits from 1 to 4.5 m thick are amenable to longwall mining. This mining technique employs a rotating toothed drum (shearer) which cuts the bedded deposit in parallel to the width of the panel. As the shearer advances, the broken coal or trona falls onto a face conveyor which transports it to a conventional conveyor belt located in the panel entry. This transfer point is known as the "headgate." The opposite end of the longwall system is known as the "tailgate." The face conveyor, shearer, and personnel are protected by a series of steel canopies which are supported by hydraulic props. The combination of canopy and prop is known as a shield. The shearer and face conveyor are supported by, and advance with the shields. As the shearer, face conveyor, and shields advance, the deposit is removed in a continuous extraction horizon. The strata are encouraged to cave behind the advancing shields. The broken material which accumulates behind the shields is referred to as the "gob." Collapse of material into the gob zone transfers the weight of the overlying strata to the coal or trona seam ahead of the face and laterally to the pillars near the headgate and tailgate.

Room and pillar mining is accomplished by driving successive openings (rooms) to create a checkerboard or herringbone pattern of pillars. The pillars may be square or rectangular. If surface subsidence is to be minimized, pillars may be left in place. To maximize recovery of the resource, pillars may be extracted on retreat. It they are extracted, caving is induced and stress is ultimately shifted to perimeter pillars in a fashion similar to a longwall panel. If the pillars are not extracted, the weight of overlying strata or other tectonic stresses may eventually crush the pillars.

Table C-1

Selected Mining-Related Seismic Events for Which Ground-Truth Information Was Compiled for This Study

ID*	Yr	Mo/Da (UTC)	Hr:Min (UTC)	Lat N	Long W	Mag. (ML)	Area
1	2000	03/07	02:16	39-44.95	110-50.19	4.2	Book Cliffs, Utah
n/a	2000	01/30	14:46	41-29.23	109-45.26	4.3	SW Wyoming
3	1998	02/05	05:19	39-45.05	110-50.73	3.8	Book Cliffs, Utah
14	1993	01/21	09:01	39-42.73	110-37.26	3.1	Book Cliffs, Utah
4	1992	07/05	12:22	39-18.81	111-09.60	3.5	Wasatch Plateau, Utah
8	1992	06/03	05:08	39-19.04	111-09.80	3.2	Wasatch Plateau, Utah
7	1987	12/16	17:43	39-18.70	111-12.92	3.3	Wasatch Plateau, Utah
2	1981	05/14	05:11	39-28.86	111-04.72	3.8	Wasatch Plateau, Utah

* Keyed to Table 3-3.

DATA SHEET - UNDERGROUND OBSERVATIONS ATTENDING SEISMIC EVENT

Date and time:	March 7, 2000	$2^h\ 16^m\ 04.72^s$
Magnitude:	4.2	
Location:	Cluster - Castle Gate	Quad. - Matts Summit, UT
	Nearest Mine - Willow Creek	
Computed epicenter location:	39° 44.95' N latitude y = 516,375 ft UCSPC	110° 50.19' W longitude x = 2,186,551 ft UCSPC
Computed focal depth:	1.84 km	
Location of affected workings:	39° 45.12' N latitude y = 517,400 ft UCSPC	110° 51.03' W longitude x = 2,182,650 ft UCSPC
Area affected:	Seven roof falls were reported at various locations in the bleeder entries to the southwest of the active longwall panel. Location of affected workings identified above is the center of the longwall face	
Vertical displacement:	Not applicable	
Mean elevation of surface topography:	Topography vertically above is a narrow ridge formed by two canyons. Maximum elevation is about 8000 ft (2438 m). Slopes dip steeply to the southeast and northwest.	
Elevation of mining horizon or depth of cover:	Elevation of mining horizon is approximately 5600 ft (1707 m). Maximum depth of cover 2400 ft (732 m).	
Geologic conditions:	Mining occurs in the "D" seam which dips about 11° northward. The Castlegate Sandstone, approximately 500 ft (152 m) thick occurs about 500 ft (152 m) above the seam.	
Underground observations attending event:	Exact cause of the event is undetermined. The roof fall is likely the result of the bounce and not the cause. The active longwall face had advanced to approximately the length of the previous panel which was sealed as a result of a fire, November 1998. The panel had progressed southward approximately 2500 feet (760 m). Width measures about 520 ft (158 m) and height 10 - 11 ft (3.3 m). Old workings are located approximately 3000 ft (914 m) to the south of the existing longwall and about 125 ft (381 m) lower in elevation.	
Reference sources:	Personal communications Tom Hurst, Chief Engineer, RAG, July 18, 2000 Incident report completed by Kerry Jensen 3/10/00	

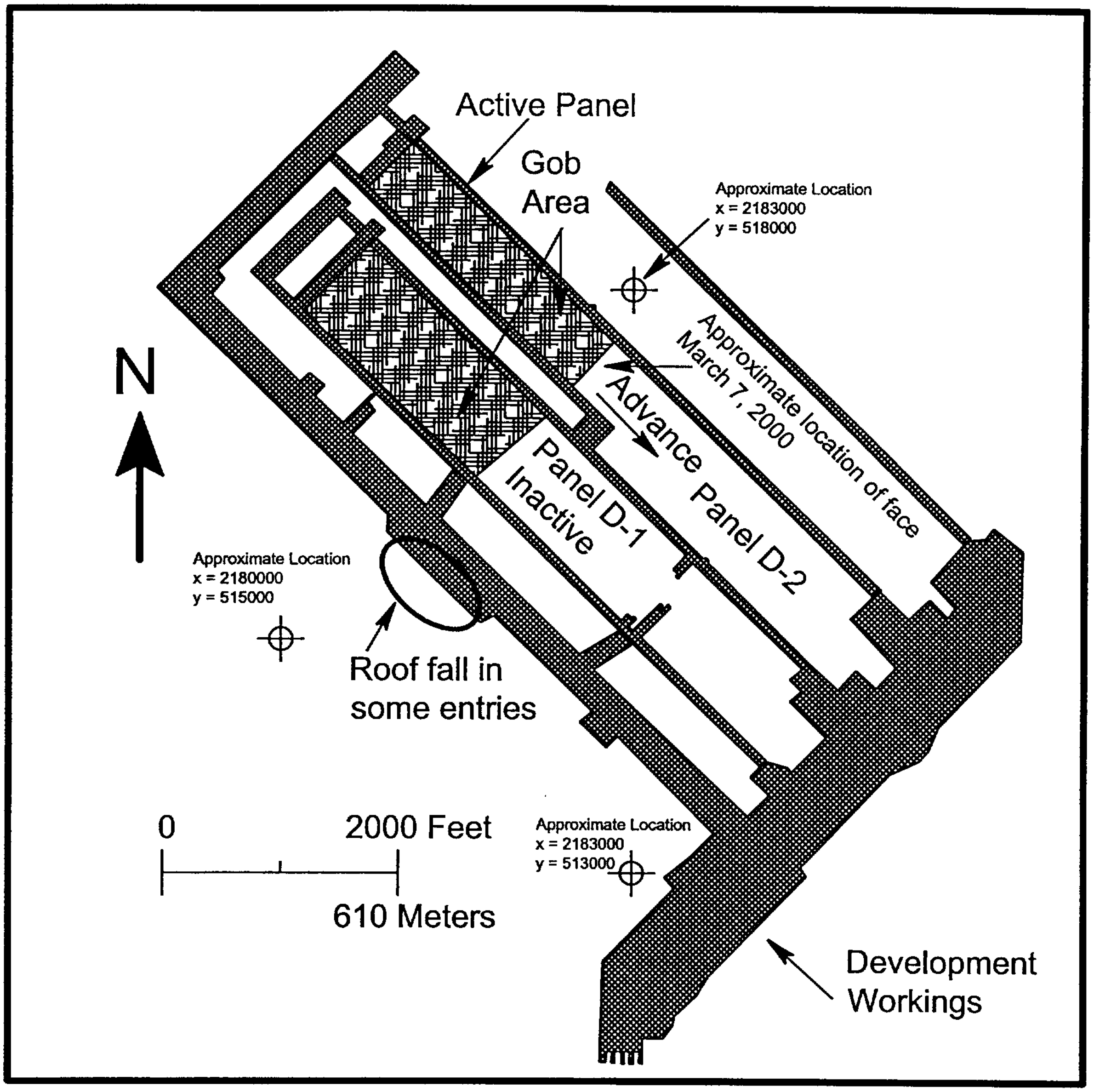

Figure C-1. Configuration of Underground Workings - March 7, 2000

DATA SHEET - UNDERGROUND OBSERVATIONS ATTENDING SEISMIC EVENT

Date and time:	January 30, 2000	$14^h\ 46^m\ 52.81^s$
Magnitude:	4.3	
Location:	Cluster - Little America	Quad. - Antelope Knoll NE, WY
	Nearest Mine - Solvay	
Computed epicenter location: (Computed relative to 1992, M_L 5.2 event.)	41° 29.23' N latitude y = 300528 Ft WWCSPC	109° 45.26' W longitude x = 224829 Ft WWCSPC
Computed focal depth:	4.00 km (fixed for computing epicentral location)	
Location of affected workings:	41° 29.48' N latitude y = 302000 Ft WWCSPC	109° 44.57' W longitude x = 228000 Ft WWCSPC
Area affected:	Uncertain. Max. area is approximately 7,000,000 ft^2 (650,000 m^2)	
Vertical displacement:	Unknown. Estimated at 4.5 ft (1.4 m)	
Mean elevation of surface topography:	Surface is relatively flat and at an elevation of 6310 ft (1923 m)	
Elevation of mining horizon or depth of cover:	Depth of cover approximately 1560 ft (475 m)	
Geologic conditions:	Mining operations are confined to Bed 17. Here, the trona formation is approximately 11 ft (3.4 m) thick. The immediate roof is shale measuring about 59 ft (18 m) thick. Two sandstone beds are located above the shale: the first is "D" sandstone 31 ft (9.4 m) thick. The Tower Sandstone is approximately 260 ft (79 m) thick and the two sandstone layers are separated by approximately 253 ft (77 m) of shale.	
Underground observations attending event:	The event was accompanied by a roof fall (collapse) involving three room and pillar sections. Pillar extraction in the lower two sections shown on the attached drawing had been completed and pillar extraction was being carried out in the northern section when the roof fall occurred. The retreat line was located at about the midline of the section advancing eastward. Mining height was approximately 9 ft (2.7 m) in these sections. Extraction was approximately 51% in the "reduced pillar recovery" areas and 65% in the "maximum pillar recovery" areas. The collapse was accompanied by surface subsidence roughly the shape of the affected sections. The maximum subsidence was 2.5 ft (0.8 m) near the center and about 0.5 ft (0.15 m) near the margins.	
Reference sources:	Personal communications Larry Refsdal, Mine Engineer, Solvay Minerals Inc., July 12, 2000 Salt Lake Tribune, Associated Press Article, Jan. 31, 2000	

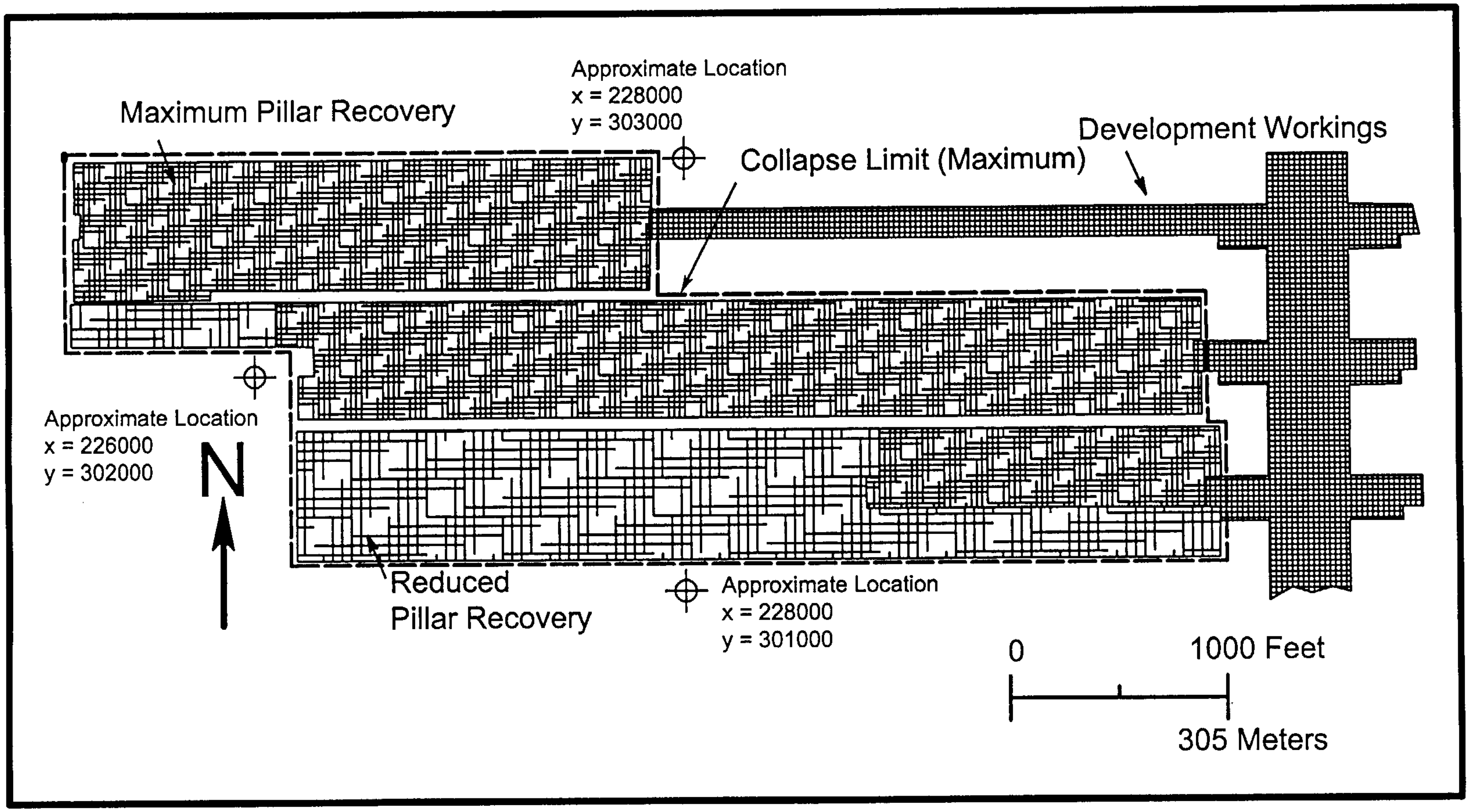

Figure C-2. Configuration of Underground Workings - January 30, 2000

DATA SHEET - UNDERGROUND OBSERVATIONS ATTENDING SEISMIC EVENT

Date and time:	February 5, 1998	5^h 19^m 56.62^s
Magnitude:	3.8	
Location:	Cluster - Castle Gate	Quad. - Matts Summit, UT
	Nearest Mine - Willow Creek	
Computed epicenter location:	39° 45.05' N latitude y = 516,963 ft UCSPC	110° 50.73' W longitude x = 2,184,016 ft UCSPC
Computed focal depth:	1.32 km	
Location of affected workings:	39° 44.98' N latitude y = 516,500 ft UCSPC	110° 51.00' W longitude x = 2,182,750 ft UCSPC
Area affected:	Approximately 264 ft^2 (25 m^2)	
Vertical displacement:	Not known	
Mean elevation of surface topography:	Topography vertically above is a narrow ridge formed by two canyons. Maximum elevation is about 8000 ft (2438 m). Slopes dip steeply to the southeast and northwest.	
Elevation of mining horizon or depth of cover:	Elevation of mining horizon is approximately 5600 ft (1707 m). Maximum depth of cover 2400 ft (732 m).	
Geologic conditions:	Mining occurs in the "D" seam which dips about 11° northward. The Castlegate Sandstone, approximately 500 ft (152 m) thick occurs about 500 ft (152 m) above the seam.	
Underground observations attending event:	Mining was limited to gate road development. Gate roads consist of two parallel entries 20 ft (6 m) wide by 8 - 9 ft (2.7 m) high separated by pillars 25 - 30 ft (9 m) wide. Cross cuts are driven on 125 - 200 ft (38 - 61 m) centers (see attached drawing). Damage was limited to pillar sluff for a distance of about 44 ft (13.5 m) by 6 ft (2 m) depth. Two bounces occurred separated by approximately 50 minutes. First bounce at 10:20 PM MST and the second at 11:08 PM MST. Rib sluff occurred on the second bounce.	
Reference sources:	Personal communications Tom Hurst, Chief Engineer, RAG, July 18, 2000 Incident report completed by Steve Rigby 2/13/98	

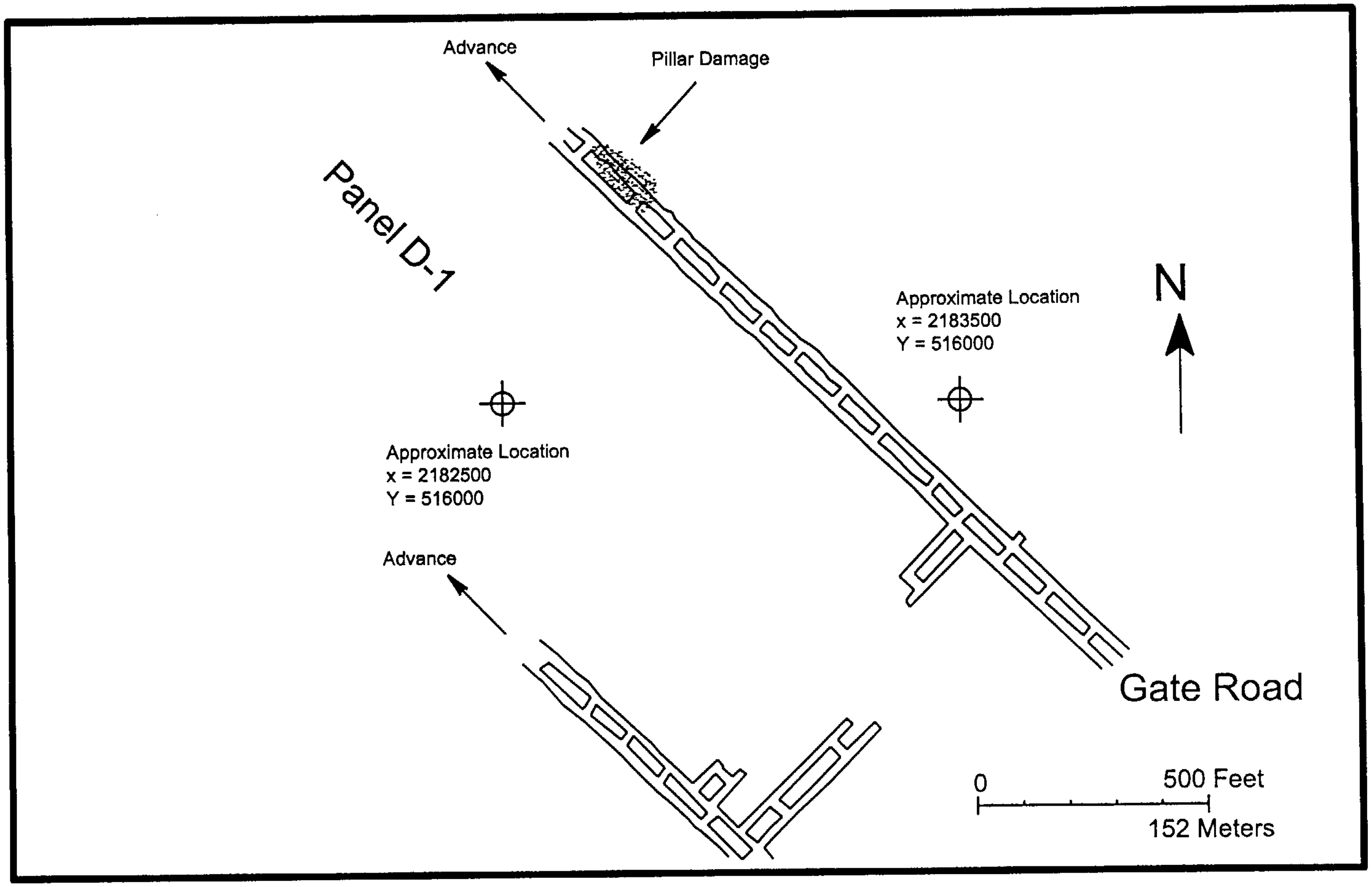

Figure C-3. Configuration of Underground Workings - February 5, 1998

DATA SHEET - UNDERGROUND OBSERVATIONS ATTENDING SEISMIC EVENT

Date and time:	January 21, 1993	$9^h\ 01^m\ 20.41^s$
Magnitude:	3.1	
Location:	Cluster - Central Book Cliffs	Quad. - Pine Canyon, UT
	Nearest Mine - Soldier Canyon	
Computed epicenter location:	39° 42.73' N latitude y = 503,422 ft UCSPC	110° 37.26' W longitude x = 2,247,272 ft UCSPC
Computed focal depth:	1.26 km	
Location of affected workings:	39° 42.73' N latitude y = 503,500 ft UCSPC	110° 36.00' W longitude x = 2,253,200 ft UCSPC
Area affected:	Twenty-four pillars, 160,00 ft2 (15,000 m2) failed completely with damage reported in adjacent pillars.	
Vertical displacement:	Net roof-to-floor convergence was estimated at about an inch (a few centimeters). In several places the floor heaved up 5 ft (1.5 m).	
Mean elevation of surface topography:	Ground surface 7600 ft (2316 m).	
Elevation of mining horizon or depth of cover:	Depth of cover ranged from 1000 ft (305 m) to 1500 ft (457 m) above the collapse area.	
Geologic conditions:	The coal seam measured 9 ft (2.7 m) thick The lower of two coal seams was being mined, interburden thickness measured 135 ft (41 m). The seams dip 8° - 9° to the northeast Two massive sandstone layers occur above the production seam. The first is 9-30 ft (3-10 m) above the seam and is 39 ft (12 m) thick. The second is 105 ft (32 m) above the roof and is 36 ft (11 m) thick. Coal strength = 31.7 MPa	
Underground observations attending event:	Retreat mining (pillar recovery) progresses from north to south (uphill). Upper seam was mined first. The upper workings extended approximately 60 meters beyond the perimeter of the collapse area. Mining height varied from 8.3 to 12 ft (2.5 to 3.7 m). Pillar recovery had been completed in two adjacent panels to the east. Panels were being mined successively from the east to the west. A previous bounce damaged three rows of pillars in the panel immediately to the east and at about the same north-south position as the area involved in the January 21 event. (See attached figure.) The event occurred after removing four rows of pillars into the panel. No contact remained between pillars and the roof. The roof remained substantially intact and suspended above the crushed pillars. Pillars - 60 x 60 ft (18.2 x 18.2 m) on 80 ft (24.2 m) centers.	
Reference sources:	Boler, F.M., S. Billington, and R. K. Zipf, 1997, "Seismological and Energy Balance Constraints on the Mechanism of a Catastrophic Bump in the Book Cliffs Coal Mining District, Utah," Int. J. Rock Mech. Min. Sci., Vol. 34, No. 1 pp. 27-43.	

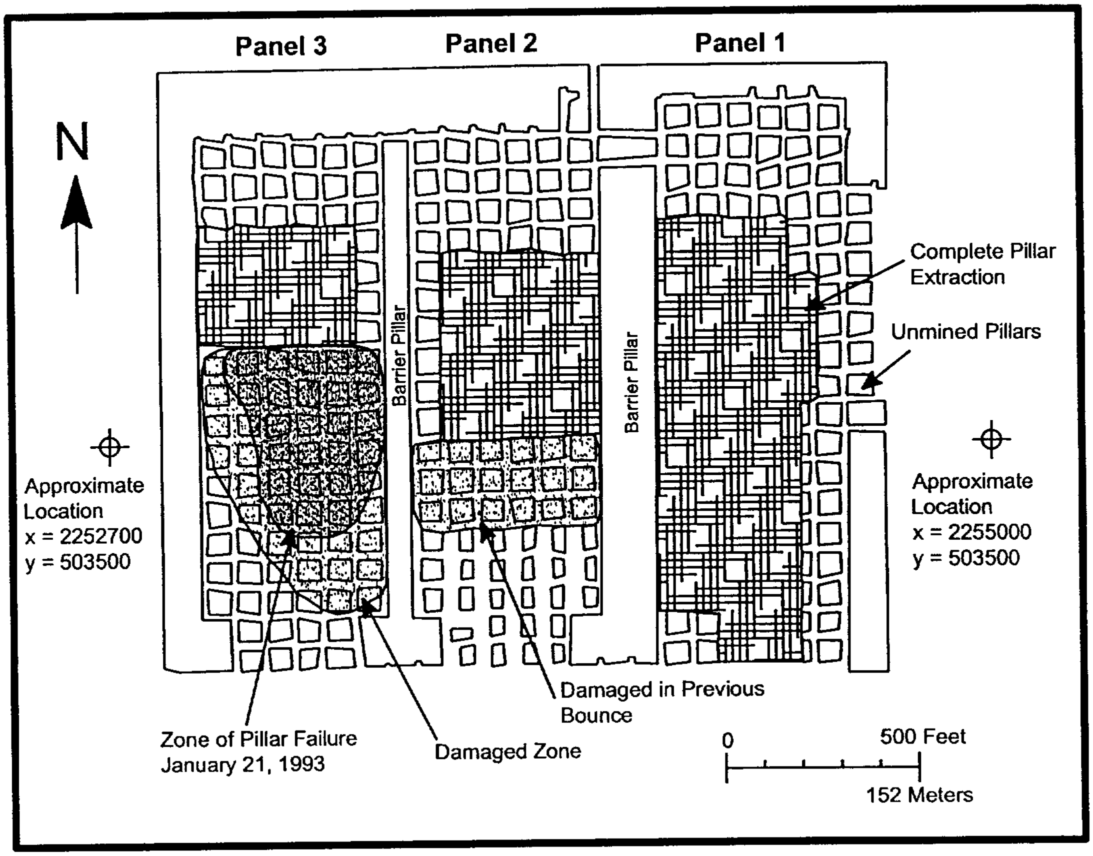

Figure C-4. Configuration of Underground Workings - January 21, 1993 (After F. M. Boler, S. Billington and R. K. Zipf, 1997)

DATA SHEET - UNDERGROUND OBSERVATIONS ATTENDING SEISMIC EVENT

Date and time:	July 5, 1992	$12^h 22^m 22.76^s$
Magnitude:	3.5	
Location:	Cluster - East Mountain	Quad. - Mahogany Point, UT
	Nearest Mine - Cottonwood	
Computed epicenter location:	39° 18.81' N latitude y = 357,188 ft UCSPC	111° 09.60' W longitude x = 2,096,199 ft UCSPC
Computed focal depth:	5.55 km	
Location of affected workings:	39° 19.07' N latitude y = 358,770 ft UCSPC	111° 08.47' W longitude x = 2,101,520 ft UCSPC
Area affected:	Approximately nine pillars and entries 100 x 900 ft (30 x 270 m), along the north and east sides of the panel	
Vertical displacement:	Pillars reduced in height about 1 ft (0.3 m)	
Mean elevation of surface topography:	9360 ft (2853 m) - Surface topography is in transition from steep side canyon to ridge top	
Elevation of mining horizon or depth of cover:	Depth of cover 1800 - 2000 ft (549 - 610 m)	
Geologic conditions:	Mining in Hiawatha seam 10 - 12 ft (3 - 3.7 m) thick, dip 2 - 3% to the northwest. Sand channel located approximately 1000 ft (300 m) to the north and running approximately east and west. Differential compaction along margins of sand channel evidenced by slickensides. The coal seam occurs on the top of the Star Point Sandstone. This unit is relative stiff compared to the strata above the seam.	
	Longwall panels (600 ft 180 m) wide were retreating from the south to the north, and the longwall face was advancing from west to east. The long dimension of the panel was oriented east and west. Panel development consisted of three entries on 100 ft (30 m) centers separated by 80 x 80 ft (24x24 m) pillars. Mining height was approximately 8.5 to 9 ft (2.6 to 2.7 m). Approximately nine pillars failed beginning at the headgate side, ahead of the longwall face. Six pillars in the panel entry and about three in the “second south” mains were affected. Most of the damage was confined to pillars immediately adjacent to the panel. Rib spall was ejected into the entries closest to the panel.	
Reference sources:	Personal communications with Rodger C. Fry, Exploration Administrator, Interwest Mining Co., July 31, 2000.	

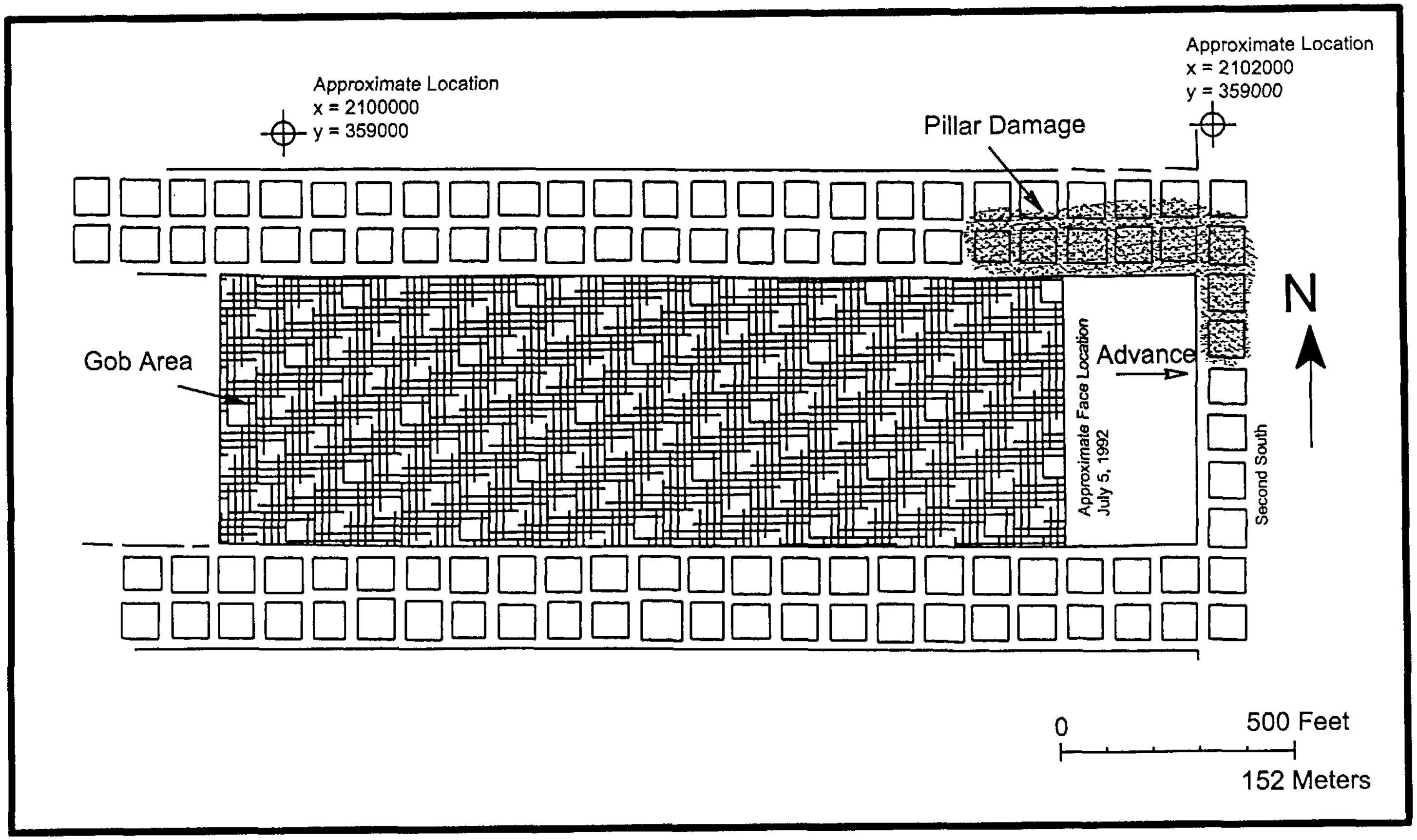

Figure C-5. Configuration of Underground Workings - July 5, 1992

DATA SHEET - UNDERGROUND OBSERVATIONS ATTENDING SEISMIC EVENT

Date and time:	June 3, 1992	$5^h\ 08^m\ 30.95^s$
Magnitude:	3.2	
Location:	Cluster - East Mountain	Quad. - Mahogany Point, UT
	Nearest Mine - Cottonwood	
Computed epicenter location:	39° 19.04' N latitude y = 358,580 ft UCSPC	111° 09.80' W longitude x = 2,095,251 ft UCSPC
Computed focal depth:	0.6 km	
Location of affected workings:	39° 19.07' N latitude y = 358,770 ft UCSPC	111° 08.72' W longitude x = 2,100,320 ft UCSPC
Area affected:	Approximately five pillars and entries 100 x 500 ft (30 x 150 m), long in an east-west direction	
Vertical displacement:	Pillars reduced in height about 1 ft (0.3 m)	
Mean elevation of surface topography:	9360 ft (2853 m) Surface topography is in transition from steep side canyon to ridge top	
Elevation of mining horizon or depth of cover:	Depth of cover 1800 - 2000 ft (549 - 610 m)	
Geologic conditions:	Mining in Hiawatha seam 10 - 12 ft (3.0 - 3.7 m) thick, dip 2 - 3% to the northwest. Sand channel located approximately 1000 ft (300 m) to the north and running approximately east and west. Differential compaction along margins of sand channel evidenced by slickensides. The coal seam occurs on the top of the Star Point Sandstone. This unit is relatively stiff compared to the strata above the seam.	
Underground observations attending event:	Mining was progressing from south to north in successive longwall panels (600 ft 180 m) wide. The longwall faces were advancing from west to east as shown on the attached figure. Panel development consisted of three entries on 100 ft (30 m) centers separated by 80 x 80 ft (24x24 m) pillars. Mining height was approximately 8.5 to 9 ft (2.6 to 2.7 m). Approximately five pillars failed on the headgate side immediately behind and ahead of the face position. Most of the pillar damage occurred between the first and second entries. Some damage was apparent in adjacent pillars.	
Reference sources:	Personal communications with Rodger C. Fry, Exploration Administrator, Interwest Mining Co., July 31, 2000.	

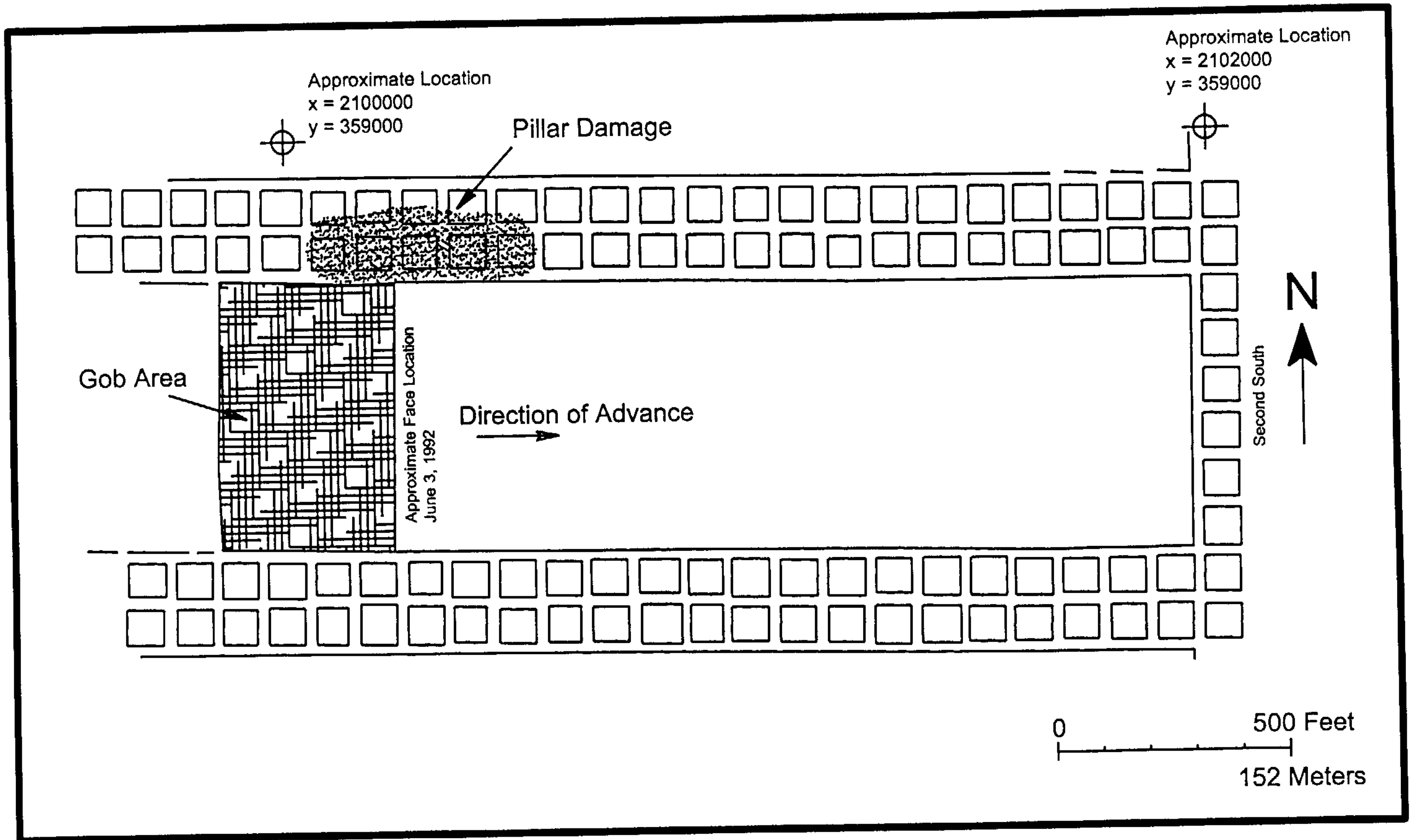

Figure C-6. Configuration of Underground Workings - June 3, 1992

DATA SHEET - UNDERGROUND OBSERVATIONS ATTENDING SEISMIC EVENT

Date and time:	December 16, 1987	$17^h 43^m 07.50^s$
Magnitude:	3.3	
Location:	Cluster - South Joes Valley	Quad. - Mahogany Point, UT
	Nearest Mine - Trail Mountain (ARCO)	
Computed epicenter location:	39° 18.70' N latitude y = 356,465 Utah Central SPC	111° 12.92' W longitude x = 2,080,545 Utah Central SPC
Computed focal depth:	0.5 km	
Location of affected workings:		
Area affected:		
Vertical displacement:		
Mean elevation of surface topography:		
Elevation of mining horizon or depth of cover:	Depth of cover ranges from 1200 ft (370 m) on the east to 1900 ft (580 m) on the west.	
Geologic conditions:		
Underground observations attending event:	Workings at the time of this event were typically room and pillar. Poor roof conditions were encountered in pillar extraction resulting in less than 30% recovery.[1]	
Reference sources:	[1]Personal communications with Rodger C. Fry, Exploration Administrator, Interwest Mining Co., July 31, 2000.	

DATA SHEET - UNDERGROUND OBSERVATIONS ATTENDING SEISMIC EVENT

Date and time:	May 14, 1981	$5^h\ 11^m\ 4.34^s$
Magnitude:	3.8	
Location:	Cluster - Gentry Mountain	Quad. - Hiawatha, UT
	Nearest Mine - King #4 ?	
Computed epicenter location:	39° 28.86' N latitude y = 418,291 ft UCSPC	111° 04.72' W longitude x = 2118924 ft UCSPC
Computed focal depth:	0.70 km	
Location of affected workings:	Not identified	
Area affected:	Estimate from company mining engineers indicate the area may have been as large as 500x500 ft^2 (150 x 150 m^2)	
Vertical displacement:	Not known	
Mean elevation of surface topography:		
Elevation of mining horizon or depth of cover:		
Geologic conditions:	Coal seam being mined was less than 13 ft (4 m) thick. Mining height was less than the full seam thickness.	
Underground observations attending event:	Panel layout is not available at this time. Mining operations involved pillar recovery involving irregular shaped and variable sized pillars.	
Reference sources:	Taylor, S. R., 1994, "False Alarms and Mine Seismicity: An Example from the Gentry mountain Mining Region, Utah", Bulletin of the Seismological Society of America, Vol. 84 No.2, April 1994, pp. 350-358.	